NOTICE

The quality of this microform is heavily dependent upon the quality of the original thesis submitted for microfilming. Every effort has been made to ensure the highest quality of reproduction possible.

If pages are missing, contact the university which granted the degree.

Some pages may have indistinct print especially if the original pages were typed with a poor typewriter ribbon or if the university sent us an inferior photocopy.

Reproduction in full or in part of this microform is governed by the Canadian Copyright Act, R.S.C. 1970, c. C-30, and subsequent amendments.

AVIS

La qualité de cette microforme dépend grandement de la qualité de la thèse soumise au microfilmage. Nous avons tout fait pour assurer une qualité supérieure de reproduction.

S'il manque des pages, veuillez communiquer avec l'université qui a conféré le grade.

La qualité d'impression de certaines pages peut laisser à désirer, surtout si les pages originales ont été dactylographiées à l'aide d'un ruban usé ou si l'université nous a fait parvenir une photocopie de qualité inférieure.

La reproduction, même partielle, de cette microforme est soumise à la Loi canadienne sur le droit d'auteur, SRC 1970, c. C-30, et ses amendements subséquents.

Canada

Fast and Efficient Carrier Synchronization for Burst-Mode Communications

Rocco Di Girolamo

A Thesis

in

The Department

of

Electrical and Computer Engineering

Presented in Partial Fulfillment of the Requirements

for the Degree of Master of Applied Science at

Concordia University

Montréal, Québec, Canada

October 1993

ISBN 0-315-90850-5

ABSTRACT

Fast and Efficient Carrier Synchronization for Burst-Mode Communications

Rocco Di Girolamo

Every coherent communication system requires some form of carrier phase and frequency synchronization. These synchronizers play an even greater role when transmission occurs in bursts, since the receivers must regularly reacquire lock. Since most of the synchronizers proposed in the literature possess some form of feedback, they tend to have high acquisition times, and are therefore inappropriate for burst-mode communications. Consequently, open-loop estimators are highly sought after.

At the foundation of most synchronizers is the Maximum Likelihood (ML) estimate, which leads to digital topologies. As it turns out, the estimate of the phase and the frequency are linked. Therefore, it is difficult to proceed with the independent optimization of either synchronizer. To circumvent this problem, non-linear open-loop estimators are used. Synchronizers developed from this technique are classified as a sub-category of ML-type synchronizers. The Viterbi and Viterbi phase synchronizer is an example of a nonlinear estimator. However, it has the drawback of being greatly influenced by frequency errors (difference in frequency between the transmitter and receiver oscillators). By contrast, the nonlinear phase estimator with modulation and frequency error removal (a new synchronizer) operates independently of this parameter. Furthermore, if frequency error is zero and all other factors are the same, the two phase estimators offer comparable performance in terms of variance, phase ambiguity resolution, and cycle skipping.

For frequency estimation, the ML estimate reduces to a least squares frequency estimator, under very restrictive conditions. In fact, these conditions are violated for most typical transmission channels, and the estimate becomes biased. Fortunately, nonlinear estimation can be applied to frequency This new synchronizer produces estimates which are unbiased, but whose variance does not approach the Cramer Rao lower bound.

ACKNOWLEDGEMENTS

It is with the utmost sincerity that I express my thanks to my thesis supervisor, Dr. Tho Le-Ngoc, for originally proposing the research area and subsequently guiding me through the various stages of the thesis development.

I am also grateful for the constant support provided by my family and friends. Although intangible their contribution can not be ignored.

TABLE OF CONTENTS

LIST OF FIGURES

LIST OF TABLES

LIST OF SYMBOLS

$\boldsymbol{A}$	All unknowns of the transmitted signal
$\widetilde{\boldsymbol{A}}$	Trial values of unknowns
$\boldsymbol{A}'$	Vector denoting parameters to be estimated
E_S	Energy per symbol
f_o	Nominal value of carrier frequency
G_k	Random transmitted k'th symbol
g_k	Sample value of G_k
K	Number of symbols in observation window; taken to be odd
$\boldsymbol{J}$	Fisher's Information Matrix
L	Length of unique word preamble for ambiguity resolution
$L(\widetilde{\boldsymbol{A}})$	Likelihood function
$\Lambda(\widetilde{\boldsymbol{A}})$	Log-likelihood function
$L_1(\widetilde{\boldsymbol{A}}')$	NDA likelihood function
$\Lambda_1(\widetilde{\boldsymbol{A}}')$	NDA log-likelihood function
M	Number of signalling elements for MPSK
$N(t)$	Random process representing AWGN
n_e	Number of symbols in observation window with $-\pi/M \leq \epsilon_k < \pi/M$
n_{e1}	Number of symbols in observation window with $\pi/M \leq \epsilon_k < 3\pi/M$
n_{e2}	Number of symbols in observation window with $-3\pi/M \leq \epsilon_k < -\pi/M$
N_k^i	Random variable denoting noise of X_k
n_k^i	Sample value of N_k^i
N_k^q	Random variable denoting noise of Y_k
n_k^q	Sample value of N_k^q
P_{ARE}	Probability of ambiguity resolution error
P_{CS}	Probability of cycle skipping
P_E	Probability of incorrectly determining state of m

p_r	Probability of a specific region error
$p(t)$	Pulse shaping function
$s(t, \boldsymbol{A})$	Transmitted waveform
T_A	Processing time required for a real addition
T_B	Duration of burst
T_F	Duration of frame
T_{LU}	Processing time required for a ROM look-up
T_M	Processing time required for a real multiplication
T_{obs}	Duration of observation window, during which Δf and $\Delta\theta$ are constant
T_P	Total processing time required for the estimators
$1/T_S$	Symbol rate
$R(T_{obs}, \widetilde{\boldsymbol{A}})$	Correlation between $r(t)$ and $s(t, \widetilde{\boldsymbol{A}})$
$r(t)$	Received sample process
$\mathcal{X}$	Complex sample used by the NPE/$\bar{\text{M}}$
$\mathcal{X}'$	Complex sample used by the NPE/$\bar{\text{M}}\bar{\text{F}}$
$\mathcal{X}''$	Complex sample used by the NFE
X_k	Random variable denoting in-phase component of I & D filter; sample value is x_k
Y_k	Random variable denoting quadrature-phase component of I & D filter; sample value is y_k
z_k	$x_k + jy_k$
(α_k, β_k)	Mean of random variables X_k and Y_k, respectively (given the modulation)
δ	Random variable (or sample value) denoting degradation of all three nonlinear estimators
Δf	Unknown frequency error

$\widetilde{\Delta f}$	Trial value of frequency error
$\widehat{\Delta F}$	Random estimate of frequency error; particular sample value denoted by $\widehat{\Delta f}$
$\Delta\theta$	Unknown phase error
$\widetilde{\Delta\theta}$	Trial value of phase error
$\widehat{\Delta\Theta}$	Random estimate of phase error, with particular sample value denoted by $\widehat{\Delta\theta}$
$\Delta\theta'$	Redefined phase error per window (to make symmetric)
$\widehat{\Delta\Theta'}$	Random estimate of redefined phase error; particular sample value denoted by $\widehat{\Delta\theta'}$
γ	Measure of signal-to-noise ratio ($= 2E_S/N_o$)
(ρ_k, ϵ_k)	Random variables (or sample values) denoting the magnitude and noise induced phase of $(X_k + jYk)$
η	Denominator of the arctangent function for all three nonlinear estimators
ξ	Numerator of the arctangent function for all three nonlinear estimators
ψ_k	Argument of z_k
ψ'_k	$(M\psi_k)\text{mod}(2\pi)$
θ_o	Nominal value of carrier phase
COV$[XY]$	Covariance of random variables X and Y
E$[X]$	Expected value of random variable X
$\Im[X]$	Imaginary part of complex quantity X
$\Re[X]$	Real part of complex quantity X
VAR$[X]$	Variance of random variable X
$\stackrel{def}{=}$	Read as 'equal by definition'

Chapter 1

Introduction

1.1 Background

Communication systems are characterized by the transmission of information from one user to another, over a link. Since most links have a passband channel, the transmitters are required to modulate the information bearing baseband signal onto a sinusoidal carrier. This would convert the original baseband signal to a passband signal, which could then be transmitted over the link. At the receiver, the effects of the carrier signal must be removed by carrier demodulation, which reconverts the signal back to baseband. These two processes are achieved by means of oscillators operating at a certain frequency and initial phase. Ideally, the two oscillators are completely synchronized (in terms of phase and frequency) and therefore their presence does not degrade the end-to-end performance. In practice, however, two oscillators in different locations cannot be identical. Consequently, the received signal is a function of the transmitted information, the noise introduced by the link, and some unknown parameters which arise owing to the discrepancies between the oscillators. This latter term introduces a performance degradation which we wish to reduce by synchronization. Essentially, synchronization involves the estimation of the unknown and unwanted parameters from the received signal. These estimated

parameters are then used by the receiver to improve performance.

The purpose of this thesis is to propose and analyze some of these carrier synchronization strategies. The transmission system considered involves communication between U users, via a central receiving station. In addition, transmission is over an additive white Gaussian noise (AWGN) channel, using a time-division multiple access (TDMA) scheme. In such an accessing scheme, each user transmits a burst of data in his assigned slot of the TDMA frame. Consider three user stations i, j, and k, all transmitting information in consecutive slots, as shown in Figure 1.1. Since these stations are dispersed geographically, it is improbable that their oscillators have the same carrier frequency ($f_{o,i} \neq f_{o,j} \neq f_{o,k}$), or initial phase ($\theta_{o,i} \neq \theta_{o,j} \neq \theta_{o,k}$). Consequently, with respect to the receiving station oscillator, each transmitted burst is corrupted by a phase and frequency error (Δf and $\Delta\theta$ respectively), resulting in a degradation in performance for every received burst. This implies that the quantities Δf and $\Delta\theta$ are different from one transmitted burst to another, as shown in Figure 1.2.

It will further be assumed that these quantities are slowly varying, possibly as a result of Doppler shifts. This occurs when the transmitter or the receiver are moving with respect to each other, as for example in satellite channels. Estimation of unwanted parameters is thus required multiple times per burst. Generally, before proper detection can proceed, symbol timing must also be estimated at the receiver. However, since this thesis focuses solely on carrier synchronization, it will be assumed that symbol timing is known exactly. This assumption is valid if any timing offset is removed prior to carrier frequency and phase synchronization. For instance, this can be accomplished by using the Gardner algorithm [1].

In the past, most synchronization techniques had as input the received analog signals. These original techniques could be categorized under two broad headings: waveform regenerators and analog trackers. The waveform regenerators passed the received random waveform through a nonlinear operation, producing a deterministic

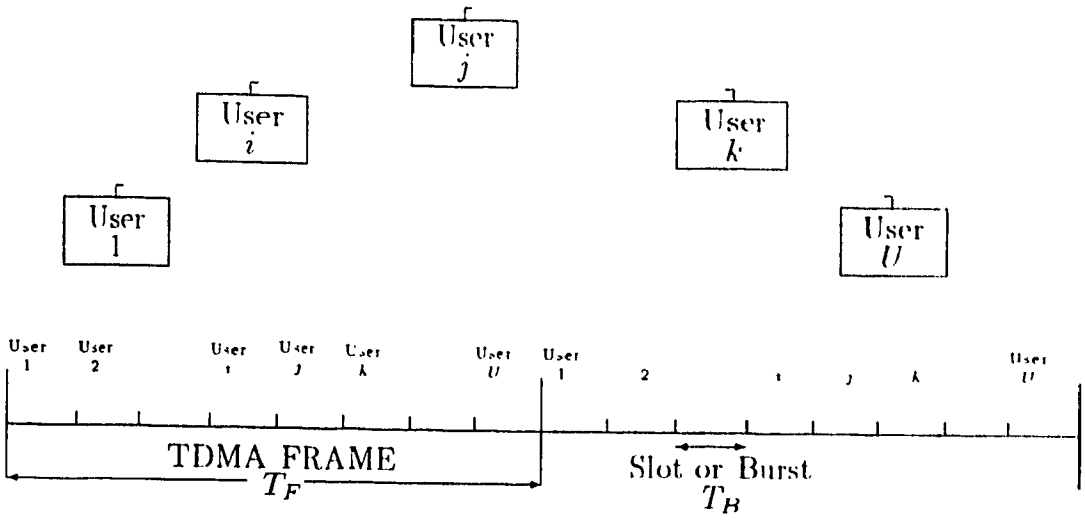

Figure 1.1: TDMA System Block Diagram

signal at the carrier frequency, or one of its harmonics. A bandpass filter or phase locked loop (PLL) could then be used to track this deterministic signal. The most common example of such a synchronizer is the X-M (times M) analog multiplier, applicable to M-ary phase shift keying (MPSK). Most other synchronizers went under the heading of analog trackers. These were devices which inherently involved PLL's, and attempted to track the carrier phase by forcing an error signal to zero. The most common of these synchronizers include the remodulator and the Costas loop. A thorough analysis of the three techniques just mentioned can be found in numerous texts, notably [2, 3]. It soon became apparent that these original ad hoc techniques could not be applied to all signalling formats. Furthermore, no general method of finding synchronizers for new formats had been found. To this end, Franks applied the Maximum Likelihood (ML) estimation procedure to the problem

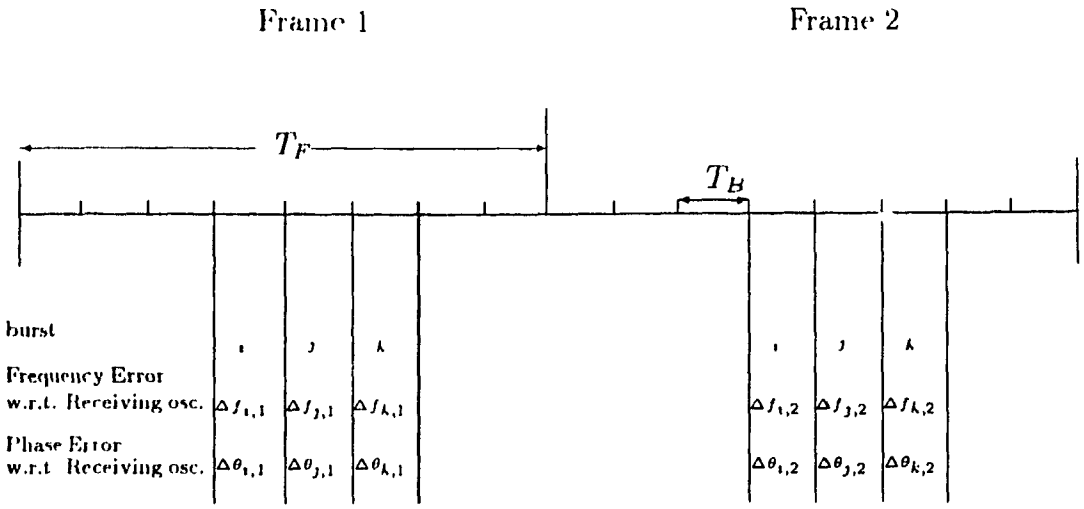

Figure 1.2: Phase and Frequency Errors from Burst to Burst

of carrier phase and found that the original ad hoc techniques were approximations of the ML estimate [4] . Thereafter, Booth, Del Re, and Fantacci found analog synchronizers of carrier phase which did not arise from simplification of the ML estimate [5, 6].

The one unifying drawback of all the techniques mentioned thus far is that they are all closed-loop feedback structures, and thus they all require some sort of voltage controlled oscillator (VCO). Consequently, all these techniques suffer from a phenomenon dubbed hang-up, resulting in possible high acquisition times (the time to acquire the estimate)[7]. To counter the effects of hang-up, open loop analog topologies were developed, such as the feedforward tracking filter (FTF) [8, 9].

With the advances in digital signal processing, the current trend is towards digital synchronizers. There are a host of factors which have led to the gain in

significance of digital versus analog st ategies. A few are listed below.

- Originally, processing speed was slow and digital synchronization techniques could not keep up with the incoming signal. This is no longer a problem in today's systems. In fact, digital signal processing allows implementation of strategies which would be too complicated to be implemented in an analog form.

- With the importance of digital communications, both in satellite and in modem channels, one can envisage receivers with greatly reduced complexity, owing to the sharing of operations between the synchronization, equalization, and decoding processes.

- Whereas storage and memory pose a very serious problem in analog strategies, they are easily implemented digitally.

- Certain synchronizers require the received signal path to be delayed. These dalays are much easier to implement for digital synchronizers.

- As will be shown in Chapter 2, there may be an advantage in using digital sampled techniques versus analog time continuous ones. In fact, it will be shown that the ML estimate results inherently in sampled topologies.

It is hoped that the above factors convincingly show the reason for analyzing digital synchronization techniques in this thesis.

1.2 Scope of Thesis

This chapter shows the importance of synchronization in communication systems, as well as the evolution of synchronization strategies, leading to the ones analyzed in Chapters 3 and 4. Chapter 2 focuses on the Maximum Likelihood estimate of phase and frequency error ($\Delta\theta$ and Δf), and finds the Cramer-Rao lower bound

(CRLB) for the variance of these estimates. This chapter also includes a classification of current digital estimators into categories. It further highlights which of these structures are best suited for the TDMA transmission scheme being considered. Moreover, a new class of estimator is identified (nonlinear estimator) which results in synchronizers whose performance is quite good.

The thesis presents an analysis of four open-loop digital estimators – two for phase error and two for frequency error. Chapter three deals specifically with phase estimation. One of the estimators studied is the Viterbi & Viterbi phase estimator, which we refer to as the nonlinear phase estimator with modulation removal (NPE/M). The justification for this new name will be given in Chapter 2. The drawbacks of this technique are presented, and a modified version is proposed. These two estimators are subsequently compared on the basis of three criteria, including variance, phase ambiguity resolution, and cycle skipping. Chapter four presents a similar analysis for frequency error estimation. A novel estimator, referred to as a nonlinear frequency estimator (NFE), is compared to the least-squares frequency estimator. Conclusions and suggestions for further research are given in Chapter 5.

Numerical results for QPSK are given as an illustrative example.

1.3 Contributions of Thesis

The major objective of this work is to present both a phase error and frequency error estimator for rapid and efficient synchronization in an AWGN environment, and for burst-mode MPSK modulation. Existing techniques suitable for such a transmission system are compared to two novel techniques. This results in the proposal and study of a new digital phase estimator and a new digital frequency estimator. In addition to the above research, other contributions include

- a systematic review of the Maximum Likelihood (ML) estimation procedure.Up until recently, the information concerning digital synchronization techniques

was not unified and was scattered throughout the literature. Thanks to the work of Gardner, Moeneclaey, Jesupret, and Ascheid [10, 11], a foundation upon which most of the techniques are based, was found - namely the ML estimate.

- a method of variance analysis applicable to the Viterbi & Viterbi phase estimator (NPE/$\bar{M}$), as well as to the new phase and frequency estimators. This method seems to be more generally applicable than the approximate analysis presented in the paper by Viterbi and Viterbi [12].

- an analysis of phase ambiguity resolution by unique word preambles. This analysis does not seem to be in any of the literature.

- a proof showing that the least-squares frequency estimator is in fact the ML estimate of frequency error.

Chapter 2

General Estimator Properties

In this chapter we will determine the Maximum Likelihood estimate for the carrier phase error ($\Delta\theta$) and the carrier frequency error (Δf), as well as the Cramer-Rao lower bound on the variance of these estimates. It will be shown that many of the common digital estimators have the ML estimate at their origin. To reduce the complexity of the analysis, the channel will be assumed to have infinite bandwidth, thus allowing the transmitters to use rectangular pulse shaping. More importantly, this implies that there is no intersymbol or interburst interference. Further, we will assume that there is no fading. As a result, only a single burst need be considered, say from the i'th user. The MPSK signal transmitted for the entire burst is of the form

$$s(t, \Delta f, \Delta\theta, \{g_k\}) = \sqrt{2E_S} \sum_{k=s}^{s+R-1} \sin\left(2\pi(fo + \Delta f)t + g_k 2\pi/M + \theta_o + \Delta\theta\right) p(t - kT_S) \qquad (2.1)$$

where accurate timing is assumed, and so the burst extends from $(s - 1/2)T_S < t < (s + R - 1/2)T_S$, and where

$$\begin{aligned} E_S &= \text{energy per symbol} \\ R &= \text{number of symbols per burst } (R >> 1) \\ f_o &= \text{nominal value of carrier frequency; known at receiver} \\ \Delta f &= \text{unknown frequency error} \\ \theta_o &= \text{nominal value of carrier phase; known at receiver} \end{aligned}$$

$$
\begin{aligned}
\Delta\theta &= \text{unknown phase error} \\
g_k &= \text{transmitted symbol for the } k\text{'th interval} \\
&= 0, 1, 2, ..., M-1 \qquad (M = \#\text{ of signalling elements}) \\
\{g_k\} &= \text{sequence of transmitted symbols} \\
1/T_S &= \text{symbol rate} \\
p(t - kT_S) &= \text{pulse shaping function of unit energy} \\
&= \begin{cases} 1/\sqrt{T_S} & -T_S/2 < t - kT_S < T_S/2 \\ 0 & \text{elsewhere} \end{cases}
\end{aligned}
$$

For proper coherent detection, the values of $\Delta\theta$ and Δf must be estimated by a synchronization device (or synchronizer) to produce estimates $\widehat{\Delta\theta}$ and $\widehat{\Delta f}$, respectively. Since the parameters to be estimated have been assumed to be slowly varying within a burst, they may be regarded as constant for small windows of duration T_{obs}, encompassing K symbols from say, $k = l$ to $k = l + K - 1$. Hence, a single estimate for Δf and $\Delta\theta$ is required for each window, providing a form of tracking (See Figure 2.1). Since the estimates from window to window are independent, we need only focus on one particular observation window (say the one beginning with symbol l). Note that it is assumed that Δf and $\Delta\theta$ are unknown, but nonrandom. Random parameter estimation uses a Maximum A Posteriori (MAP) procedure to determine estimates. It is shown in [13] that if the parameters to be estimated are uniformly distributed, then the MAP and ML estimates are identical.

2.1 Maximum Likelihood Estimation

There are generally two reasons for studying the ML estimation procedure for nonrandom unknown parameters [13, 14]. Firstly, if an efficient estimator for a parameter exists, then the ML estimate is efficient. This property ensures that the variance of the estimate is equal to the CRLB. Moreover, if an efficient estimate does not exist, the ML estimate is assured to be at least asymptotically efficient (i.e. for large

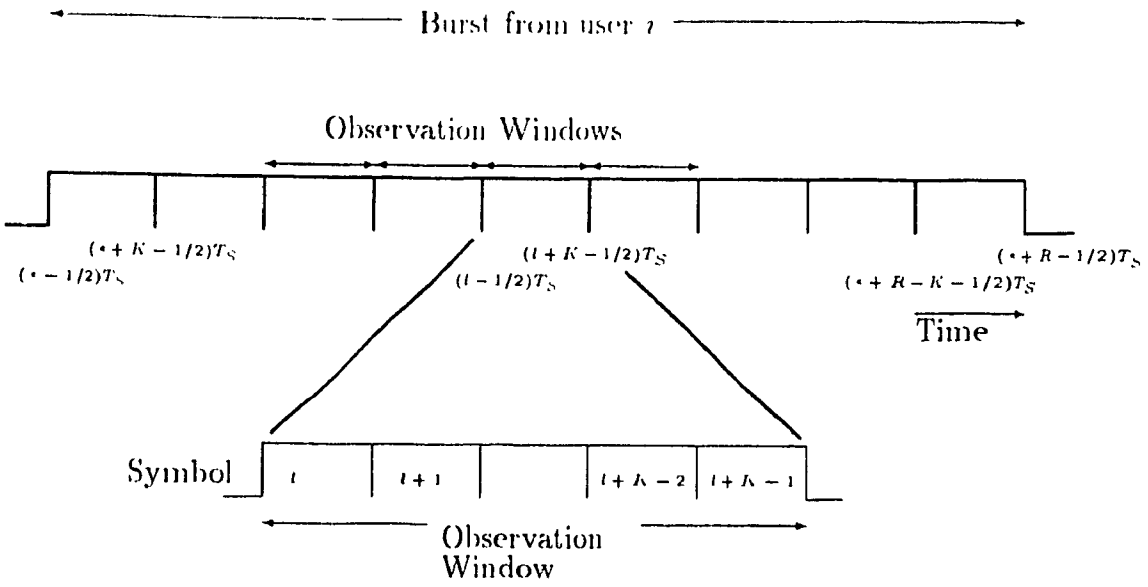

Figure 2.1: Description of Observation Windows in Single Burst from User i

observation window size K). The second important feature of the ML estimate is that it is consistent. This implies that the ML estimate converges, in probability, to the correct value of the unknown parameter, for K large. For instance, the phase estimate is such that

$$\lim_{K\to\infty} \Pr[|\widehat{\Delta\Theta} - \Delta\theta| < \epsilon] = 1$$

for some constant ϵ.

Before proceeding, we first define the vector $\boldsymbol{A}^*$, which consists of all the unknown parameters at the receiver - $\Delta\theta$, Δf, and $\{g_k\}$. If this vector were known, the signal $s(t, \boldsymbol{A})$ would be completely defined. However, the received signal is not only a function of the unknown $\boldsymbol{A}$, but it is also corrupted by an AWGN process $(N(t))^\dagger$ with two sided power spectral density of $N_o/2$. Therefore, the received signal

*Bolded symbols represent vectors.

†Random processes and random variables will be generally denoted by upper case symbols, with the specific sample functions denoted by the corresponding lower case version. In cases where no convenient upper case symbol exists, the same character will be used to designate both. The context should specify whether the symbol denotes a specific sample or a random variable.

is given by

$$r(t) = s(t, \boldsymbol{A}) + n(t) \quad \text{for } t \text{ in the observation window.} \tag{2.2}$$

Trial values of the vector $\boldsymbol{A}$, denoted $\widetilde{\boldsymbol{A}}$, make $s(t, \boldsymbol{A})$ deterministic.

Estimates of $\Delta\theta$ and Δf are obtained after the signal is observed for the entire observation window. In addition, keep in mind that the g_k are sample values of *discrete* random variables. Therefore, even though we refer to the estimate of the g_k, the problem of determining $\widehat{g_k}$ is really a problem in decision theory, and not estimation theory. As is shown in Appendix A, the ML estimate of $\boldsymbol{A}$, is that value of $\widetilde{\boldsymbol{A}}$ which maximizes the likelihood function

$$\mathrm{L}(\widetilde{\boldsymbol{A}}) = \exp\left[-\frac{1}{N_o}\int_{T_{obs}} |r(t) - s(t, \widetilde{\boldsymbol{A}})|^2 dt\right]. \tag{2.3}$$

If we expand the integrand, we obtain the sum of three terms. That is,

$$\begin{aligned} |r(t) - s(t, \widetilde{\boldsymbol{A}})|^2 &= (r(t) - s(t, \widetilde{\boldsymbol{A}}))(r(t) - s(t, \widetilde{\boldsymbol{A}}))^* \\ &= r(t)r^*(t) + s(t, \widetilde{\boldsymbol{A}})s^*(t, \widetilde{\boldsymbol{A}}) - r(t)s^*(t, \widetilde{\boldsymbol{A}}) - r^*(t)s(t, \widetilde{\boldsymbol{A}}) \\ &= |r(t)|^2 + |s(t, \widetilde{\boldsymbol{A}})|^2 - 2\Re[r(t)s^*(t, \widetilde{\boldsymbol{A}})] \end{aligned}$$

where $\Re[X]$ denotes the real part of complex quantity X. Using this result in equation (2.3),

$$\mathrm{L}(\widetilde{\boldsymbol{A}}) = \exp\left[-\frac{1}{N_o}\int_{T_{obs}} |r(t)|^2 dt - \frac{1}{N_o}\int_{T_{obs}} |s(t, \widetilde{\boldsymbol{A}})|^2 dt + \frac{2}{N_o}\int_{T_{obs}} \Re[r(t)s^*(t, \widetilde{\boldsymbol{A}})] dt\right]. \tag{2.4}$$

Each of the terms in the exponent of equation (2.4) can be treated separately. The first term represents the energy of the received signal in the observation window, and so is independent of the trial value $\widetilde{\boldsymbol{A}}$. The second term represents the energy of the transmitted waveform, with the unknown parameters fixed at $\widetilde{\boldsymbol{A}}$. If symbol timing is accurately known and modulation is MPSK, it is shown that this term is also a constant.

$$\int_{T_{obs}} |s(t, \widetilde{\boldsymbol{A}})|^2 dt = \int_{(l-1/2)T_s}^{(l+K-1/2)T_s} s(t, \widetilde{\boldsymbol{A}})s^*(t, \widetilde{\boldsymbol{A}}) dt$$

$$= \int_{(l-1/2)T_S}^{(l+K-1/2)T_S} \sqrt{2E_S} \sum_{k=l}^{l+K-1} \sin(2\pi(f_o + \widetilde{\Delta f})t + \widetilde{g_k}2\pi/M + \widetilde{\Delta\theta} + \theta_o)p(t - kT_S) \bullet$$

$$\sqrt{2E_S} \sum_{j=l}^{l+K-1} \sin(2\pi(f_o + \widetilde{\Delta f})t + \widetilde{g_j}2\pi/M + \widetilde{\Delta\theta} + \theta_o)p(t - jT_S)dt$$

$$= \int_{(l-1/2)T_S}^{(l+K-1/2)T_S} 2E_S \sum_{k=l}^{l+K-1} \sum_{j=l}^{l+K-1} \sin(2\pi(f_o + \widetilde{\Delta f})t + \widetilde{g_k}2\pi/M + \widetilde{\Delta\theta} + \theta_o) \bullet$$

$$\sin(2\pi(f_o + \widetilde{\Delta f})t + \widetilde{g_j}2\pi/M + \widetilde{\Delta\theta} + \theta_o)p(t - kT_S)p(t - jT_S)dt$$

$$= 2E_S \sum_{k=l}^{l+K-1} \int_{(l-1/2)T_S}^{(l+K-1/2)T_S} \sin^2(2\pi(f_o + \widetilde{\Delta f})t + \widetilde{g_k}2\pi/M + \widetilde{\Delta\theta} + \theta_o)p^2(t - kT_S)dt$$

$$= KE_S \qquad \text{(for } f_o \text{ large)}.$$

Combining these two integrals into a single constant, we can rewrite equation (2.4) as

$$\mathrm{L}(\widetilde{\boldsymbol{A}}) = C_1 \exp\left[\frac{2}{N_o}\int_{T_{obs}} \Re[r(t)s^*(t,\widetilde{\boldsymbol{A}})]dt\right] \tag{2.5}$$

where C_1 is independent of $\widetilde{\boldsymbol{A}}$. Maximizing the likelihood function given in equation (2.5) is equivalent to maximizing the log-likelihood function $\Lambda(\widetilde{\boldsymbol{A}})$ of (2.6), which is further equivalent to maximizing $R(T_{obs}, \widetilde{\boldsymbol{A}})$ given below.

$$\begin{aligned}\Lambda(\widetilde{\boldsymbol{A}}) &= \ln C_1 + \frac{2}{N_o}\int_{T_{obs}} \Re[r(t)s^*(t,\widetilde{\boldsymbol{A}})]dt \\ &= \ln C_1 + \frac{2}{N_o}R(T_{obs},\widetilde{\boldsymbol{A}})\end{aligned} \tag{2.6}$$

where

$$R(T_{obs},\widetilde{\boldsymbol{A}}) = \int_{T_{obs}} \Re[r(t)s^*(t,\widetilde{\boldsymbol{A}})]dt.$$

For the specific case of MPSK,

$$s(t,\widetilde{\boldsymbol{A}}) = \sqrt{2E_S}\sum_{k=l}^{l+K-1} \sin(2\pi(f_o + \widetilde{\Delta f})t + \widetilde{g_k}2\pi/M + \theta_o + \widetilde{\Delta\theta})p(t - kT_S)$$

and therefore

$$R(T_{obs},\widetilde{\boldsymbol{A}}) = \int_{T_{obs}} r(t)\sqrt{2E_S}\sum_{k=l}^{l+K-1} \sin(2\pi(f_o + \widetilde{\Delta f})t + \widetilde{g_k}2\pi/M + \theta_o + \widetilde{\Delta\theta})p(t - kT_S)dt$$

$$= \sum_{k=l}^{l+K-1} \sqrt{2E_S}\left[\int_{T_{obs}} r(t)\sin(2\pi f_o t + \theta_o)\cos(2\pi\widetilde{\Delta f}t + \widetilde{g_k}2\pi/M + \widetilde{\Delta\theta})p(t - kT_S)dt +\right.$$

$$\int_{T_{obs}} r(t)\cos(2\pi f_o t+\theta_o)\sin(2\pi\widetilde{\Delta f}t+\widetilde{g_k}2\pi/M+\widetilde{\Delta\theta})p(t-kT_S)dt\Big]$$

$$=\sum_{k=l}^{l+K-1}\frac{\sqrt{2E_S}}{\sqrt{T_S}}\left[\int_{(k-1/2)T_S}^{(k+1/2)T_S} r(t)\sin(2\pi f_o t+\theta_o)\cos(2\pi\widetilde{\Delta f}t+\widetilde{g_k}2\pi/M+\widetilde{\Delta\theta})dt+\right.$$

$$\left.\int_{(k-1/2)T_S}^{(k+1/2)T_S} r(t)\cos(2\pi f_o t+\theta_o)\sin(2\pi\widetilde{\Delta f}t+\widetilde{g_k}2\pi/M+\widetilde{\Delta\theta})dt\right].$$

If we assume that Δf is a small fraction of the symbol rate $(1/T_S)$, then the terms $\cos(2\pi\widetilde{\Delta f}t+\widetilde{g_k}2\pi/M+\widetilde{\Delta\theta})$ and $\sin(2\pi\widetilde{\Delta f}t+\widetilde{g_k}2\pi/M+\widetilde{\Delta\theta})$ are almost constant over the region of integration. Conditions under which this approximation is justified are given in Section 2.2. Therefore,

$$R(T_{obs},\widetilde{\boldsymbol{A}})\approx$$

$$\sum_{k=l}^{l+K-1}\left[\frac{\sqrt{2E_S}}{\sqrt{T_S}}\cos(2\pi\widetilde{\Delta f}kT_S+\widetilde{g_k}2\pi/M+\widetilde{\Delta\theta})\int_{(k-1/2)T_S}^{(k+1/2)T_S} r(t)\sin(2\pi f_o t+\theta_o)dt\right.$$

$$\left.+\frac{\sqrt{2E_S}}{\sqrt{T_S}}\sin(2\pi\widetilde{\Delta f}kT_S+\widetilde{g_k}2\pi/M+\widetilde{\Delta\theta})\int_{(k-1/2)T_S}^{(k+1/2)T_S} r(t)\cos(2\pi f_o t+\theta_o)dt\right].$$

The reader should note the similarity between the integrals above and the integrate-and-dump (I & D) samples of a regular MPSK receiver. Redefining these as x_k and y_k, where

$$x_k \stackrel{def}{=} \int_{(k-1/2)T_S}^{(k+1/2)T_S}\frac{\sqrt{2}}{\sqrt{T_S}}r(t)\sin(2\pi f_o t+\theta_o)dt$$

$$y_k \stackrel{def}{=} \int_{(k-1/2)T_S}^{(k+1/2)T_S}\frac{\sqrt{2}}{\sqrt{T_S}}r(t)\cos(2\pi f_o t+\theta_o)dt$$

yields

$$R(T_{obs},\widetilde{\boldsymbol{A}}) = \sum_{k=l}^{l+K-1}\sqrt{E_S}\left(\cos(2\pi\widetilde{\Delta f}kT_S+\widetilde{g_k}2\pi/M+\widetilde{\Delta\theta})x_k+\right.$$

$$\left.\sin(2\pi\widetilde{\Delta f}kT_S+\widetilde{g_k}2\pi/M+\widetilde{\Delta\theta})y_k\right) \qquad (2.7)$$

$$= \sum_{k=l}^{l+K-1}\sqrt{E_S}\Re[e^{-j\widetilde{\Delta\theta}}e^{-j2\pi\widetilde{\Delta f}kT_S}e^{-j\widetilde{g_k}2\pi/M}z_k] \qquad (2.8)$$

where $z_k \stackrel{def}{=} x_k+jy_k$.

Four interesting properties are noted from equation (2.8). First, the received signal $(r(t))$ enters the maximization procedure only in a sampled form. That is,

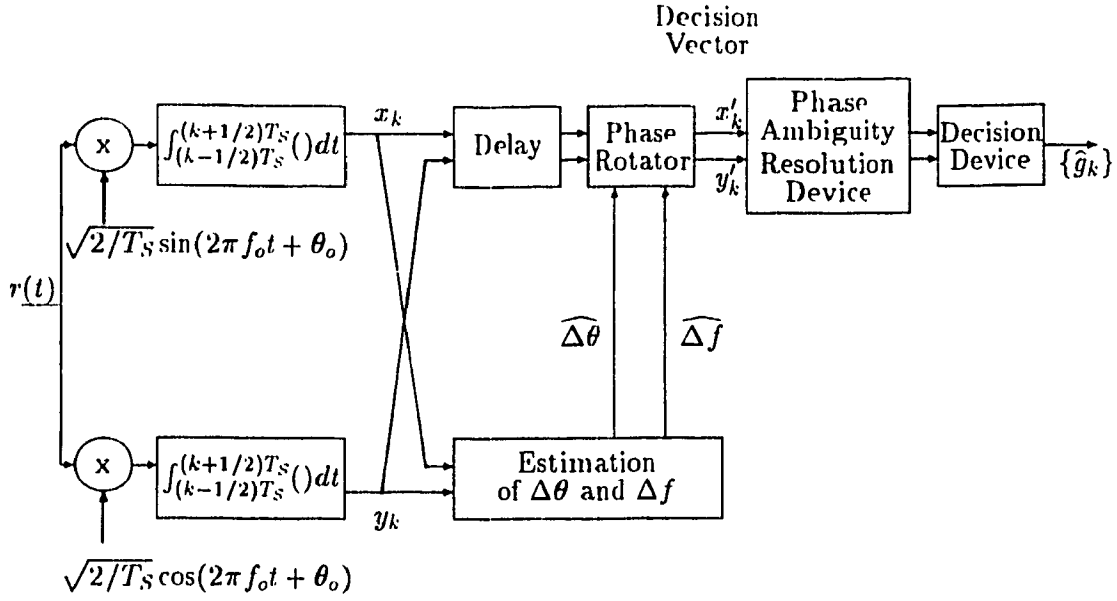

Figure 2.2: Typical Receiver

only the integrate-and-dump samples are required for ML estimation. Although it has long been established that I & D samples are sufficient for symbol detection, Gardner was the first to point out that they were also sufficient for ML estimation [2]. This statement has very important consequences. Essentially, it implies that no matter how good the original analog synchronization techniques were, they could never outperform the best digital ML based techniques. Therefore, the tendency towards transforming analog techniques to equivalent digital versions likely leads to suboptimum estimators. In fact, equation (2.8) suggests that it would be better to find digital estimators, and then convert these to analog, rather than the other way around.

Secondly, since ML estimators require only the I & D samples, it can be concluded that certain aspects of detection and synchronization can be combined. This reduces the overall receiver hardware, leading to a structure as shown in Figure 2.2. The only inputs to the synchronizer are the integrate-and-dump samples.

Equation (2.8) further suggests that the estimates of Δf and $\Delta\theta$ are intertwined, leading to joint estimation strategies. That is, maximization of (2.8) involves the simultaneous maximization with respect to both parameters, where $\Delta\theta$

is restricted to be between $-\pi$ and π, and where Δf must be a small fraction of the symbol rate ($1/T_S$). In Section 2.2, it is shown that Δf must be such that $-0.1/T_S \leq \Delta f \leq 0.1/T_S$. On the other hand, independent estimation produces isolated structures which estimate one parameter independently of the other. In these independent estimators, this *other* parameter becomes an unknown, and will generally result in a degradation in the estimator performance. Therefore, unless an efficient method of removing the effects of this *other* parameter is found, these independent estimators cannot be optimum. The resulting synchronizers can be thought of as using a pseudo-ML technique, and are classified as nonlinear estimators. This name is chosen to reflect the fact that in most cases, a nonlinear operation is used to deal with the unknown parameter. Note that the identification of the nonlinear estimator as a separate sub-class of the ML estimator, seems to be novel. Since this thesis will deal only with independent estimation, a great deal of effort will be devoted to finding the methods of eliminating this *other* parameter.

Lastly, $R(T_{obs}, \widetilde{\boldsymbol{A}})$ is a function of all the transmitted symbols $\{g_k\}$ in the observation window. As a result, the following question arises. How do we maximize $R(T_{obs}, \widetilde{\boldsymbol{A}})$ when we don't know the values of $\{g_k\}$? After all, the whole purpose of maximizing $R(T_{obs}, \widetilde{A})$ is to determine Δf and $\Delta\theta$, which could then be used to find $\{g_k\}$ (See Figure 2.2)! This problem is resolved by one of three methods, resulting in one of the estimation strategies discussed below.

Data-Aided (DA) Estimation: This method requires the use of a preamble. At the receiver this preamble is known and so the effects of the modulation ($\{g_k\}$) can be removed. The problem with this method is that the preamble uses up valuable data symbols in the TDMA frame (since a preamble would be required for every observation window within every burst) reducing TDMA efficiency.

Decision-Directed (DD) Estimation: Rather than using known values of $\{g_k\}$, the estimators employing this strategy use the decoded values, denoted $\{\widehat{g_k}\}$. Obviously this method requires some starting values for $\widehat{\Delta\theta}$ and $\widehat{\Delta f}$. Generally, the performance of these estimators approaches that for the DA versions, particularly when signal-to-noise ratio (SNR) is high. This result is expected since decision errors should be rare at high SNR.

Non Data-Aided (NDA) Estimation: This method resolves the problem by averaging out the effects of G_k from the likelihood function $\mathrm{L}(\widetilde{\boldsymbol{A}})$ (the likelihood function is taken to be a function of $\widetilde{\Delta f}$ $\widetilde{\Delta\theta}$, and modulation g_k). This results in an NDA likelihood function $\mathrm{L}_1(\widetilde{\boldsymbol{A}}')$, where $\mathrm{L}_1(\widetilde{\boldsymbol{A}}') = \mathrm{E}_{\{G_k\}}[\mathrm{L}(\widetilde{\boldsymbol{A}})]$, and where $\widetilde{\boldsymbol{A}}'$ is vector denoting the two unknowns $\widetilde{\Delta\theta}$ and $\widetilde{\Delta f}$.

Since our communication system is such that an estimate is needed for every observation window, the synchronizers are required to have short acquisition times. In addition, a large preamble devoted strictly for estimation is to be avoided in TDMA systems. This latter criteria eliminates any DA estimation method from further study. Moreover, since the DD methods have decision feedback, they suffer from a phenomenon resembling hang-up. Hence, the NDA estimation strategy is the only method which can satisfy the two objectives stated above. Therefore, in the remainder of this chapter the log-likelihood function $\Lambda_1(\widetilde{\boldsymbol{A}}')$ will be solved, in order to find NDA open-loop estimators. First, we recall that $\mathrm{L}(\widetilde{\boldsymbol{A}})$ is given by

$$\begin{aligned}
\mathrm{L}(\widetilde{\boldsymbol{A}}) &= C_1 \exp\left[\frac{2}{N_o} R(T_{obs}, \widetilde{\boldsymbol{A}})\right] \\
&= C_1 \exp\left[\frac{2C_2}{N_o} \sum_{k=l}^{l+K-1} \Re[e^{-j\widetilde{\Delta\theta}} e^{-j2\pi\widetilde{\Delta f}kT_s} e^{-jg_k 2\pi/M} z_k]\right] \\
&= C_1 \prod_{k=l}^{l+K-1} \exp\left[\frac{2C_2}{N_o} \Re[e^{-j\widetilde{\Delta\theta}} e^{-j2\pi\widetilde{\Delta f}kT_s} e^{-jg_k 2\pi/M} z_k]\right] \qquad (2.9)
\end{aligned}$$

where we notice that C_2 absorbs the energy, and that the equation is a function of the sample values g_k. This likelihood function must be made independent of $\{g_k\}$. To accomplish this, we average over all possible G_k in the observation window (for

$l \le k \le l+K-1$). The symbols g_k are samples from uniform, independent, and identically distributed random variables. To find $\mathrm{L}_1(\widetilde{\boldsymbol{A}}')$ we proceed as follows,

$$\begin{aligned}
\mathrm{L}_1(\widetilde{\boldsymbol{A}}') &= \mathrm{E}_{\{G_k\}}[\mathrm{L}(\widetilde{\boldsymbol{A}})] \\
&= \sum_{g_l=0}^{M-1}\sum_{g_{l+1}=0}^{M-1}\cdots\sum_{g_{l+K-1}=0}^{M-1}\Pr[G_l=g_l]\cdots\Pr[G_{l+K-1}=g_{l+K-1}]\mathrm{L}(\widetilde{\boldsymbol{A}}) \\
&= \prod_{k=l}^{l+K-1}\sum_{u=0}^{M-1} C_1 \exp\left[\frac{2C_2}{N_o}\Re[e^{-j\widetilde{\Delta\theta}}e^{-j2\pi\widetilde{\Delta f}kT_s}e^{-jg_k2\pi/M}z_k]\right]_{g_k=u}\Pr[G_k=u] \\
&= C_3\prod_{k=l}^{l+K-1}\sum_{u=0}^{M-1}\exp\left[\frac{2C_2}{N_o}\Re[e^{-j\widetilde{\Delta\theta}}e^{-j2\pi\widetilde{\Delta f}kT_s}e^{-ju2\pi/M}z_k]\right].
\end{aligned}$$

For MPSK, $e^{-ju2\pi/M} = -e^{-j(u+M/2)2\pi/M}$, and so

$$\begin{aligned}
\mathrm{L}_1(\widetilde{\boldsymbol{A}}') &= C_3\prod_{k=l}^{l+K-1}\sum_{u=0}^{M/2-1}\left(\exp\left[\frac{2C_2}{N_o}\Re[e^{-j\widetilde{\Delta\theta}}e^{-j2\pi\widetilde{\Delta f}kT_s}e^{-ju2\pi/M}z_k]\right]\right. \\
&\quad \left. + \exp\left[-\frac{2C_2}{N_o}\Re[e^{-j\widetilde{\Delta\theta}}e^{-j2\pi\widetilde{\Delta f}kT_s}e^{-ju2\pi/M}z_k]\right]\right) \\
&= C_4\prod_{k=l}^{l+K-1}\sum_{u=0}^{M/2-1}\cosh\left[\frac{2C_2}{N_o}\Re[e^{-j\widetilde{\Delta\theta}}e^{-j2\pi\widetilde{\Delta f}kT_s}e^{-ju2\pi/M}z_k]\right]. \quad (2.10)
\end{aligned}$$

In some cases, the log-likelihood function given below is more useful

$$\Lambda_1(\widetilde{\boldsymbol{A}}') = \ln C_4 + \sum_{k=l}^{l+K-1}\ln\left(\sum_{u=0}^{M/2-1}\cosh\left[\frac{2C_2}{N_o}\Re[e^{-j\widetilde{\Delta\theta}}e^{-j2\pi\widetilde{\Delta f}kT_s}e^{-ju2\pi/M}z_k]\right]\right) \quad (2.11)$$

At this point, it is possible to draw a tree showing the relative placement of all the ML estimation techniques mentioned (See Figure 2.3).

2.1.1 ML Phase Error Estimation

For the purpose of finding the ML estimate of $\Delta\theta$, the unknown $\widetilde{\Delta f}$ will be assumed to be zero. Substituting $\widetilde{\Delta f} = 0$ in equation (2.11),

$$\begin{aligned}
\Lambda_1(\widetilde{\boldsymbol{A}}') &= \ln C_4 + \sum_{k=l}^{l+K-1}\ln\left(\sum_{u=0}^{M/2-1}\cosh\left[\frac{2C_2}{N_o}\Re[e^{-j\widetilde{\Delta\theta}}e^{-ju2\pi/M}z_k]\right]\right). \quad (2.12) \\
&= \Lambda_1(\widetilde{\Delta\theta}).
\end{aligned}$$

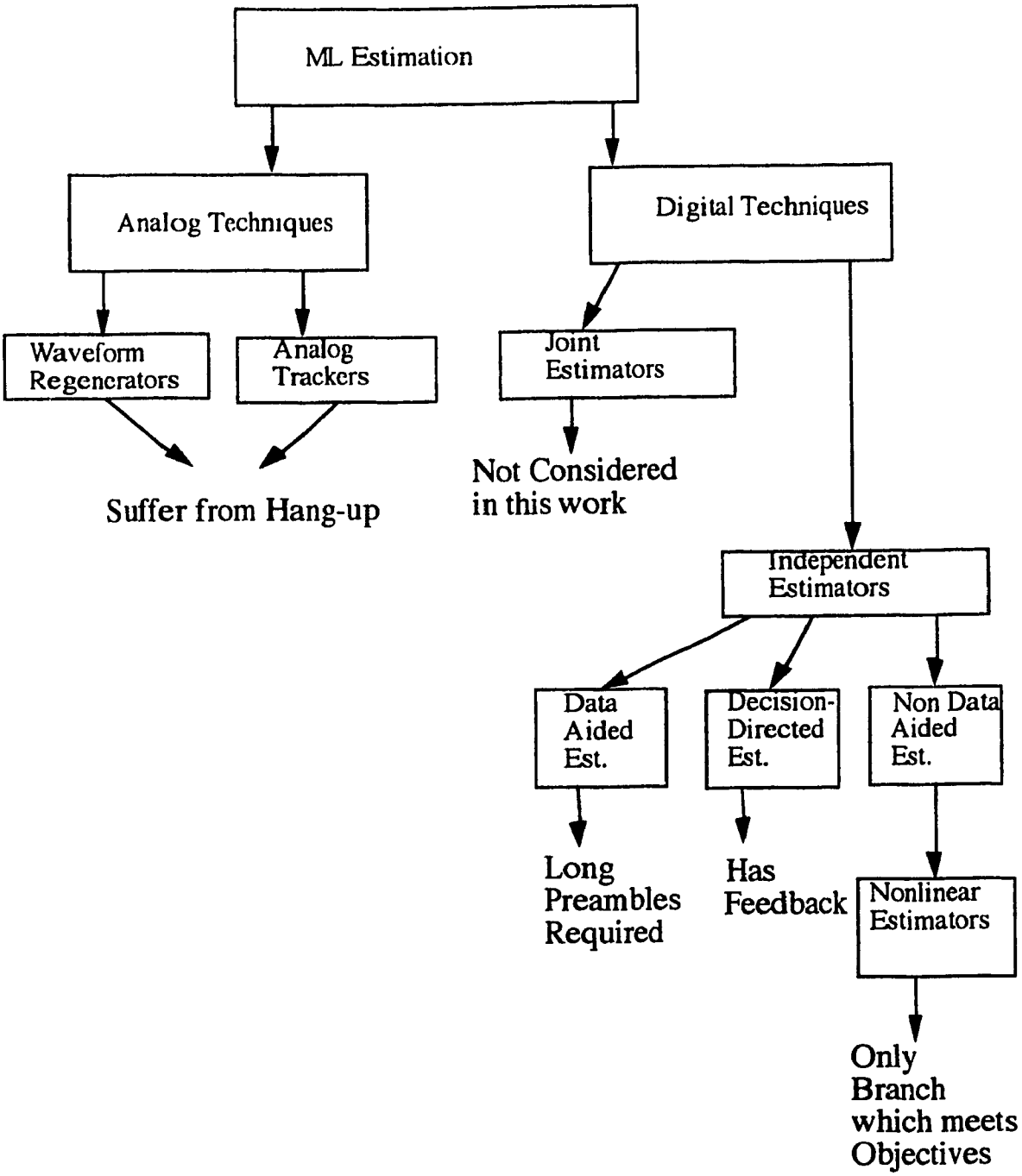

Figure 2.3: ML Estimation Tree

As noted by Gardner, there are three strategies to finding the maximum of (2.12) with respect to $\widetilde{\Delta\theta}$. The first of these is by a brute force search technique. Values over the entire space of $\widetilde{\Delta\theta}$ are substituted into $\Lambda_1(\widetilde{\Delta\theta})$, and $\widehat{\Delta\theta}$ is selected as the $\widetilde{\Delta\theta}$ which produces the maximum. One can foresee that this technique has very long acquisition times, owing to the number of computations which may be required to find the absolute maximum. Presentation and analysis of this technique is given in [15].

The second method of maximization actually reduces to a tracker. At the maximum, the derivative of the log-likelihood function (with respect to $\widetilde{\Delta\theta}$) reduces to zero. Therefore, we can set $d\Lambda_1(\widetilde{\Delta\theta})/d\widetilde{\Delta\theta} = 0$ and use this as an error signal, resulting in a digital closed-loop tracker. However, since this estimator would have feedback, it is unlikely to meet the speed requirements of our TDMA system. Interestingly, some authors do not consider the resulting synchronizer a *true* ML estimator [16].

The last method of maximization is by direct computation. This method involves setting $d\Lambda_1(\widetilde{\Delta\theta})/d\widetilde{\Delta\theta}$ to zero, making some simplifying assumption, and directly solving for $\widetilde{\Delta\theta}$. The result of this differentiation is shown below:

$$\frac{d\Lambda_1(\widetilde{\Delta\theta})}{d\widetilde{\Delta\theta}} = \sum_{k=l}^{l+K-1} \frac{\sum_{u=0}^{M/2-1} \sinh\left[\frac{2C_2}{N_o}\Re[e^{-j\widetilde{\Delta\theta}}e^{-ju2\pi/M}z_k]\right]\left[\frac{2C_2}{N_o}\Im[e^{-j\widetilde{\Delta\theta}}e^{-ju2\pi/M}z_k]\right]}{\sum_{u=0}^{M/2-1}\cosh\left[\frac{2C_2}{N_o}\Re[e^{-j\widetilde{\Delta\theta}}e^{-ju2\pi/M}z_k]\right]} \tag{2.13}$$

where $\Im[X]$ denotes the imaginary part of X. The ML estimate of phase error ($\widehat{\Delta\theta}$) is the solution to

$$\sum_{k=l}^{l+K-1} \frac{\sum_{u=0}^{M/2-1} \sinh\left[\frac{2C_2}{N_o}\Re[e^{-j\widehat{\Delta\theta}}e^{-ju2\pi/M}z_k]\right]\left[\frac{2C_2}{N_o}\Im[e^{-j\widehat{\Delta\theta}}e^{-ju2\pi/M}z_k]\right]}{\sum_{u=0}^{M/2-1}\cosh\left[\frac{2C_2}{N_o}\Re[e^{-j\widehat{\Delta\theta}}e^{-ju2\pi/M}z_k]\right]} = 0. \tag{2.14}$$

Owing to the nonlinear nature of (2.14), no obvious and simple solution for $\widehat{\Delta\theta}$ is possible. To arrive at one, approximations to sinh() and cosh() are required. For high signal-to-noise ratio, Gardner showed that the solution to (2.14) produces an estimator with a feedback loop [10]. Even more interesting, the resulting structures

for BPSK and QPSK are identical to the decision-directed tracker estimators. Ironically, solving for a NDA estimator by direct computation leads to a decision-directed tracking loop. Gardner then speculated that this implied the decision-directed estimator was the optimum estimator at high SNR. Since he proved the results only for $M = 2$ and $M = 4$, no generalization is possible. However, the result is expected to be applicable for all M. Therefore at this SNR extreme, no estimator can outperform the decision-directed tracking loop.

At low signal-to-noise ratio, we can safely say that $2C_2/N_o$ is low (recall C_2 absorbs energy term). Therefore, we can replace $\sinh(x)$ and $\cosh(x)$ by their low x approximations given below:

$$\sinh(x) \approx x + \frac{x^3}{3!} + \frac{x^5}{5!} + \frac{x^7}{7!} + \ldots \tag{2.15}$$

$$\cosh(x) \approx 1. \tag{2.16}$$

Using (2.15) and (2.16) in (2.14) produces

$$\sum_{k=l}^{l+K-1} \sum_{u=0}^{M/2-1} \left[\frac{\left(\frac{2C_2}{N_o} \Re[e^{-j\widehat{\Delta\theta}} e^{-ju2\pi/M} z_k] \right)}{1!} + \frac{\left(\frac{2C_2}{N_o} \Re[e^{-j\widehat{\Delta\theta}} e^{-ju2\pi/M} z_k] \right)^3}{3!} \right.$$

$$\left. + \frac{\left(\frac{2C_2}{N_o} \Re[e^{-j\widehat{\Delta\theta}} e^{-ju2\pi/M} z_k] \right)^5}{5!} + \ldots \right] \left[\frac{2C_2}{N_o} \Im[e^{-j\widehat{\Delta\theta}} e^{-ju2\pi/M} z_k] \right] = 0. \tag{2.17}$$

The above equation can be solved for all M. The solution is stated below ([10] see Appendix B).

$$\widehat{\Delta\theta} = \frac{1}{M} \arctan \left[\frac{\sum_{k=l}^{l+K-1} \Im[z_k{}^M]}{\sum_{k=l}^{l+K-1} \Re[z_k{}^M]} \right]. \tag{2.18}$$

This estimator is referred to as the digital X-M multiplier circuit.

Equation (2.18) represents an estimator which meets our two objectives - it does not require a large preamble, nor does it have feedback. Unfortunately, since approximations (2.15) and (2.16) were used, the estimator is optimum only at low SNR. At higher SNR, this estimator cannot outperform a decision-directed tracking

loop, and therefore the X-M multiplier should result in some loss of performance, when compared to the tracking loop. This loss is almost negligible for $M = 2$ or $M = 4$, but becomes more pronounced for $M > 4$. This degradation has been termed *nonlinear loss*, and is studied in [15, 17]. Consequently, this open-loop digital technique can not be used for all M. To deal with this possibility, Viterbi and Viterbi proposed a new estimator, with equation (2.18) as their starting point [12]. This new estimator fits under the class of nonlinear estimator shown in Figure 2.3. Essentially, one can argue that the purpose of the M'th power in equation (2.18) is modulation removal. Therefore, the M'th power can be replaced by another nonlinearity which multiplies the phase of z_k by M (to remove the effects of the $\{g_k\}$), and then performs a separate nonlinear operation on the magnitude of z_k. For this reason, this estimator has been renamed for this thesis as the nonlinear phase estimator with modulation removal (NPE/$\bar{\text{M}}$). The value of the estimate is

$$\widehat{\Delta\theta} = \frac{1}{M} \arctan \left[\frac{\sum_{k=l}^{l+K-1} \Im[F(|z_k|)e^{jM \arg(z_k)}]}{\sum_{k=l}^{l+K-1} \Re[F(|z_k|)e^{jM \arg(z_k)}]} \right] \tag{2.19}$$

where $F()$ represents some nonlinear operation on $|z_k|$. The advantage of this technique over the X-M digital multiplier emerges because the $F(|z_k|)$ can be chosen to optimize the variance . In fact, it has been shown that the optimum $F()$ produces results which approach the CRLB even at high SNR [18]. Note that when we select $F(|z_k|) = |z_k|^M$, the NPE/$\bar{\text{M}}$ reduces to a X-M digital multiplier.

The concept of nonlinear estimation can be expanded further. The main results so far have assumed that the frequency error is zero. If this were not the case, the Δf can be expected to severely degrade $\widehat{\Delta\theta}$, even for the NPE/$\bar{\text{M}}$. However by carefully choosing a nonlinearity, the effects of Δf can be eliminated. Therefore, a nonlinear estimator with modulation and frequency error removal is possible (will be denoted NPE/$\bar{\text{M}}\bar{\text{F}}$). This new proposed estimator, as well as the NPE/$\bar{\text{M}}$, are analyzed in Chapter 3.

2.1.2 ML Frequency Error Estimation

As was the case for ML phase error estimation, numerous data-aided and decision-directed strategies exist for frequency error estimation [19, 20]. For the same reasons outlined before, these estimators can not be used for burst-mode communications. As a result, the emphasis in this section will be on open-loop topologies.

For the purpose of finding the ML estimate for Δf, we will assume that $\Delta\theta = 0$. Hence, the likelihood function (2.11) becomes

$$\begin{aligned}\Lambda_1(\widetilde{\boldsymbol{A}}') &= \ln C_4 + \sum_{k=l}^{l+K-1} \ln\left(\sum_{u=0}^{M/2-1} \cosh\left[\frac{2C_2}{N_o}\Re[e^{-j2\pi\widetilde{\Delta f}T_S k} e^{-ju2\pi/M} z_k]\right]\right) \quad (2.20)\\ &= \Lambda_1(\widetilde{\Delta f}).\end{aligned}$$

We can now proceed to find the ML estimate of $\Delta f T_S$ (T_S is included in the estimate, and may be considered a normalizing constant). Firstly, we differentiate (2.20) with respect to $\widetilde{\Delta f}T_S$, replace $\widetilde{\Delta f}T_S$ by $\widehat{\Delta f}T_S$, and set the result equal to zero. The outcome of these steps is

$$\sum_{k=l}^{l+K-1} \frac{\sum_{u=o}^{M/2-1} \sinh\left[\frac{2C_2}{N_o}\Re[e^{-j2\pi\widehat{\Delta f}T_S k} e^{-ju2\pi/M} z_k]\right]\left[\frac{2C_2}{N_o} 2\pi k \Im[e^{-j2\pi\widehat{\Delta f}T_S k} e^{-ju2\pi/M} z_k]\right]}{\sum_{u=o}^{M/2-1} \cosh\left[\frac{2C_2}{N_o}\Re[e^{-j2\pi\widehat{\Delta f}T_S k} e^{-ju2\pi/M} z_k]\right]} = 0. \quad (2.21)$$

In order to solve this equation for $\widehat{\Delta f}T_S$, approximations to the hyperbolic functions are again needed. Therefore, using the low SNR approximations to $\sinh(x)$ and $\cosh(x)$ given in equations (2.15) and (2.16), and following the same inductive reasoning that led to (2.18), we can reduce (2.21) to

$$\sum_{k=l}^{l+K-1} k\Im[e^{-j2\pi\widehat{\Delta f}T_S kM} {z_k}^M] = 0,$$

which implies that

$$\sum_{k=l}^{l+K-1} k \sin[\arg({z_k}^M) - 2\pi\widehat{\Delta f}T_S kM] = 0. \quad (2.22)$$

To solve explicitly for $\widehat{\Delta f}T_S$, one further assumption is made. Namely, we will assume that the estimate is very close to the unknown parameter ($\widehat{\Delta f} \approx \Delta f$). If

the resulting estimate is efficient, then this assumption is justified. As a result, the sine function can be approximated by a first order expansion. That is, $\sin(x) \approx x$ and so

$$\sum_{k=l}^{l+K-1} [k \arg(z_k{}^M) - 2\pi \widehat{\Delta f} T_S k^2 M] = 0.$$

The $\widehat{\Delta f} T_S$ term can now be isolated, such that

$$\widehat{\Delta f} T_S = \frac{\sum_{k=l}^{l+K-1} k \arg(z_k{}^M)}{2\pi M \sum_{k=l}^{l+K-1} k^2}. \tag{2.23}$$

As will be shown later, the resulting open-loop frequency error estimator is identical to the least-squares frequency estimator. Its analysis is presented in Chapter 4, where it will be shown that the estimate is efficient, justifying our assumption. However, the conditions for efficiency are easily violated. Note that it had not been shown in the literature that the least-squares estimate of $\Delta f T_S$ is in fact a low SNR approximation to the ML estimate.

One final note on frequency estimation is appropriate. In order to solve for $\widehat{\Delta f} T_S$, it was assumed that there was no phase error ($\Delta\theta = 0$). Consequently, this allowed us to use a first order approximation to $\sin(x)$. However, it is possible to use the concept of nonlinear estimation to obtain a pseudo-ML estimate for $\Delta f T_S$, even when $\Delta\theta$ is not zero. This nonlinear frequency estimator (NFE) is modelled after the Intermediate Frequency (IF) version proposed by Simon and Divsalar [21]. Two consecutive samples are used to convert the frequency error into a phase error. Thereafter, a nonlinear phase type estimator, similar to the NPE/MF, is used to solve for $\widehat{\Delta f} T_S$. Since the technique results in an open-loop topology, it will also be studied in Chapter 4.

2.2 Cramer-Rao Lower Bound

The Cramer-Rao lower bound on the variance of the estimated parameters is known to be equal to the diagonal elements of the inverse of Fisher's information matrix

$\boldsymbol{J}$[14]. Since the matrix is defined for discrete-time observations, we cannot apply it directly to our analog received waveform. Instead, we apply it to the I & D samples.

The first step is to find the probability density function (pdf) of these samples. These results are extremely important and are used quite often in the thesis. The results are derived assuming that the transmitted symbols ($\{g_k\}$) are given (in a probabilistic sense). If so, $r(t)$ is a sample function of a Gaussian process, and the x_k and y_k are samples of Gaussian random variables. This last property is due to the fact that x_k and y_k are outputs of a linear transformation operating on a Gaussian input. Solving for the in-phase component (x_k),

$$\begin{aligned}
x_k &= \int_{(k-1/2)T_S}^{(k+1/2)T_S} r(t)\sqrt{2/T_S}\sin(2\pi f_o t + \theta_o)dt \\
&= \int_{(k-1/2)T_S}^{(k+1/2)T_S} \sum_{j=l}^{l+K-1} \sqrt{2E_S}\sin(2\pi(f_o+\Delta f)t + g_j 2\pi/M + \theta_o + \Delta\theta)p(t-jT_S) \bullet \\
&\quad \sqrt{2/T_S}\sin(2\pi f_o t + \theta_o)dt + \int_{(k-1/2)T_S}^{(k+1/2)T_S} n(t)\sqrt{2/T_S}\sin(2\pi f_o t + \theta_o)dt \\
&= \int_{(k-1/2)T_S}^{(k+1/2)T_S} (\sqrt{E_S}/T_S)\cos(2\pi\Delta f t + g_k 2\pi/M + \Delta\theta)dt + n_k^i \\
&= \sqrt{E_S}\cos(2\pi\Delta f k T_S + g_k 2\pi/M + \Delta\theta)\frac{\sin\pi\Delta f T_S}{\pi\Delta f T_S} + n_k^i \\
&\approx \sqrt{E_S}\cos(2\pi\Delta f k T_S + g_k 2\pi/M + \Delta\theta) + n_k^i \qquad (2.24) \\
&\stackrel{def}{=} \alpha_k + n_k^i \qquad\qquad l \le k \le l+K-1.
\end{aligned}$$

The above approximation holds for $\sin(\pi\Delta f T_S)/\pi\Delta f T_S \approx 1$. From Figure 2.4, we see that this restricts the $\Delta f T_S$ to be less than 0.1, which is well within the limits for most communication oscillators. Therefore, it will be assumed that this condition is always satisfied.

A similar result holds for the quadrature component (y_k). Namely,

$$\begin{aligned}
y_k &= \sqrt{E_S}\sin(2\pi\Delta f k T_S + g_k 2\pi/M + \Delta\theta) + n_k^q \qquad (2.25) \\
&\stackrel{def}{=} \beta_k + n_k^q \qquad\qquad l \le k \le l+K-1.
\end{aligned}$$

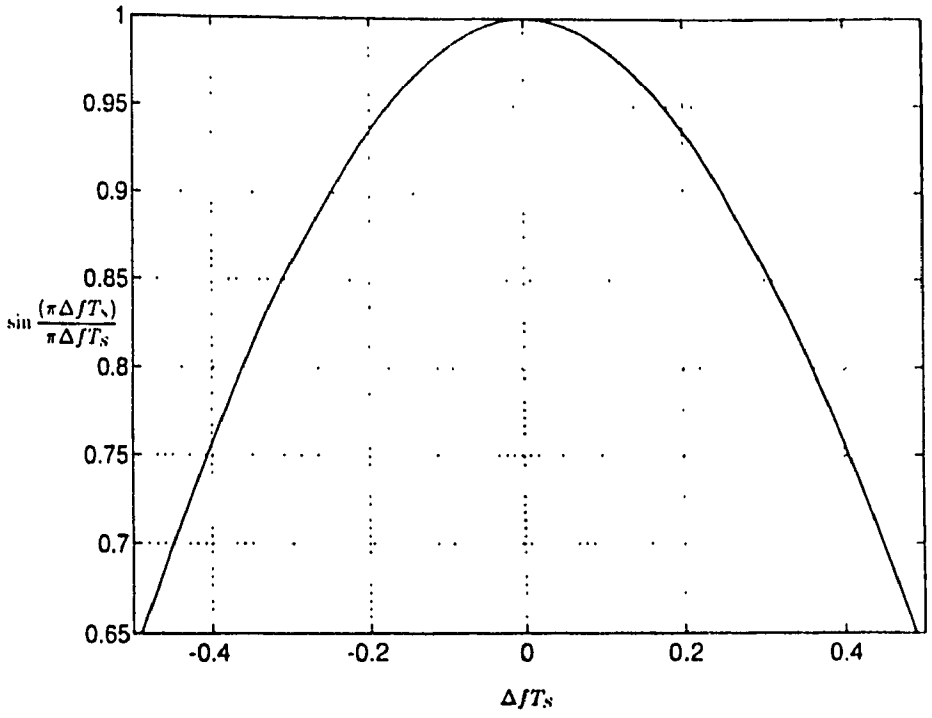

Figure 2.4: Plot of $\sin(\pi\Delta fT_S)/(\pi\Delta fT_S)$

The values of n_k^i and n_k^q are given below:

$$n_k^i = \int_{(k-1/2)T_S}^{(k+1/2)T_S} n(t)\sqrt{2/E_S}\sin(2\pi f_o t + \theta_o)dt$$
$$n_k^q = \int_{(k-1/2)T_S}^{(k+1/2)T_S} n(t)\sqrt{2/E_S}\cos(2\pi f_o t + \theta_o)dt.$$

To find the joint pdf of X_k and Y_k, namely $f_{X_k,Y_k}(x_k, y_k)$, the moments of the noise samples must be determined. We first note that the random variables N_k^i and N_k^q are Gaussian. Their mean and variance are determined by using properties of $N(t)$. That is, $\mathrm{E}[N(t)] = 0$ and $\mathrm{E}[N(t)N(\lambda)] = (N_o/2)\delta^\dagger(t-\lambda)$. Therefore,

$$\mathrm{E}[N_k^i] = \mathrm{E}[N_k^q] = 0 \tag{2.26}$$
$$\mathrm{E}[N_k^i N_j^i] = \mathrm{E}[N_k^q N_j^q] = \begin{cases} 0 & k \neq j \\ N_o/2 & k = j \end{cases} \tag{2.27}$$
$$\mathrm{E}[N_k^i N_k^q] = 0 \tag{2.28}$$

$^\dagger\delta(x)$ is the Dirac delta function

The above results imply that N_k^i and N_k^q are independent random variables with zero mean and variance $\sigma^2 = N_o/2$.

Given the transmitted symbols ($\{g_k\}$), α_k and β_k are constant. As a result, X_k and Y_k are Gaussian, with moments

$$\begin{aligned} \mathrm{E}[X_k|\{g_k\}] &= \alpha_k & (2.29)\\ \mathrm{VAR}[X_k|\{g_k\}] &= N_o/2 & (2.30)\\ \mathrm{E}[Y_k|\{g_k\}] &= \beta_k & (2.31)\\ \mathrm{VAR}[Y_k|\{g_k\}] &= N_o/2 & (2.32)\\ \mathrm{E}[X_kY_k|\{g_k\}] &= \alpha_k\beta_k & (2.33)\\ \mathrm{COV}[X_kY_k|\{g_k\}] &= 0. & (2.34) \end{aligned}$$

Since X_k and Y_k are Gaussian and uncorrelated, they are also independent. This ensures that their joint pdf can be written as

$$\begin{aligned} f_{X_k,Y_k}(x_k,y_k|\{g_k\}) &= f_{X_k}(x_k|\{g_k\})f_{Y_k}(y_k|\{g_k\}) \\ &= \frac{1}{\pi N_o}\exp\left[-\frac{{x_k}^2+{y_k}^2}{N_o}+\frac{\alpha_k x_k+\beta_k y_k}{N_o/2}-\frac{{\alpha_k}^2+{\beta_k}^2}{N_o}\right] \\ &= \frac{1}{\pi N_o}\exp\left[-\frac{{x_k}^2+{y_k}^2}{N_o}+\frac{\alpha_k x_k+\beta_k y_k}{N_o/2}-\frac{E_S}{N_o}\right] \\ & \qquad -\infty < x_k, y_k < \infty \qquad (2.35) \end{aligned}$$

where the substitution $E_S = {\alpha_k}^2+{\beta_k}^2$ was made. Since the samples are independent for different k, the joint pdf of all random X_k's and Y_k's, denoted by vectors $\boldsymbol{X}$ and $\boldsymbol{Y}$ respectively, is given by

$$\begin{aligned} f_{\boldsymbol{X},\boldsymbol{Y}}(\boldsymbol{x},\boldsymbol{y}|\{g_k\}) &= \prod_{k=l}^{l+K-1} f_{X_k,Y_k}(x_k,y_k|\{g_k\}) \\ &= \frac{1}{(\pi N_o)^K}\exp\left[\sum_{k=l}^{l+K-1}\left(-\frac{({x_k}^2+{y_k}^2)+E_S}{N_o}+\frac{\alpha_k x_k+\beta_k y_k}{N_o/2}\right)\right] \\ & \qquad -\infty < \forall x_k, y_k < \infty. \qquad (2.36) \end{aligned}$$

Taking the natural logarithm,

$$\ln f_{\boldsymbol{X},\boldsymbol{Y}}(\boldsymbol{x},\boldsymbol{y}|\{g_k\}) = D+\frac{2}{N_o}\sum_{k=l}^{l+K-1}(\alpha_k x_k+\beta_k y_k) \qquad -\infty < \forall x_k, y_k < \infty \quad (2.37)$$

where D includes all terms which are independent of $\Delta\theta$ or Δf. The three remaining unknowns in equation (2.37) are Δf, $\Delta\theta$, and $\{g_k\}$. In determining the Cramer-Rao lower bound, it will be assumed that modulation is absent. Since most of the literature uses this unmodulated bound, the above assumption is generally accepted. In fact, any modulation is expected to introduce degradation, and therefore this estimate cannot have a variance lower than the unmodulated bound. In accordance, all the estimators in this paper will be compared to this lower bound.

The elements of $\boldsymbol{J}$ (as defined on page 20 of [14]) are given by

$$\begin{aligned} J_{11} &= \text{element (1,1) of matrix } \boldsymbol{J} \\ &= \mathrm{E}\left[\frac{\partial \ln f_{\boldsymbol{X},\boldsymbol{Y}}(\boldsymbol{X},\boldsymbol{Y}|\{g_k\})}{\partial\Delta\theta}\frac{\partial \ln f_{\boldsymbol{X},\boldsymbol{Y}}(\boldsymbol{X},\boldsymbol{Y}|\{g_k\})}{\partial\Delta\theta}\right] \qquad (2.38) \\ J_{22} &= \text{element (2,2) of matrix } \boldsymbol{J} \\ &= \mathrm{E}\left[\frac{\partial \ln f_{\boldsymbol{X},\boldsymbol{Y}}(\boldsymbol{X},\boldsymbol{Y}|\{g_k\})}{\partial\Delta f}\frac{\partial \ln f_{\boldsymbol{X},\boldsymbol{Y}}(\boldsymbol{X},\boldsymbol{Y}|\{g_k\})}{\partial\Delta f}\right] \qquad (2.39) \\ J_{12} = J_{21} &= \mathrm{E}\left[\frac{\partial \ln f_{\boldsymbol{X},\boldsymbol{Y}}(\boldsymbol{X},\boldsymbol{Y}|\{g_k\})}{\partial\Delta f}\frac{\partial \ln f_{\boldsymbol{X},\boldsymbol{Y}}(\boldsymbol{X},\boldsymbol{Y}|\{g_k\})}{\partial\Delta\theta}\right] \qquad (2.40) \end{aligned}$$

Noting that all g_k are zero, equations (2.38) to (2.40) can be solved, generating the folowing matrix

$$\boldsymbol{J} = \frac{2}{N_o}\begin{bmatrix} E_S K & 2\pi T_S E_S \sum_{k=l}^{l+K-1} k \\ 2\pi T_S E_S \sum_{k=l}^{l+K-1} k & 4\pi^2 {T_S}^2 E_S \sum_{k=l}^{l+K-1} k^2 \end{bmatrix}. \qquad (2.41)$$

The inverse of (2.41) is

$$\boldsymbol{J}^{-1} = \frac{6N_o}{4\pi^2 {T_S}^2 {E_S}^2 K^2(K^2-1)}\begin{bmatrix} 4\pi^2 {T_S}^2 E_S \sum_{k=l}^{l+K-1} k^2 & -2\pi T_S E_S \sum_{k=l}^{l+K-1} k \\ -2\pi T_S E_S \sum_{k=l}^{l+K-1} k & E_S K \end{bmatrix}. \qquad (2.42)$$

As shown in the text by Van Trees, the lower bound on the variance of the estimates is given by

$$\mathrm{COV}[[\widehat{\Delta\Theta}, \widehat{\Delta F}][\widehat{\Delta\Theta}, \widehat{\Delta F}]^{T\S}] \geq \boldsymbol{J}^{-1}.$$

§ $()^T$ denotes transpose

Therefore,

$$\mathrm{VAR}[\widehat{\Delta\Theta}] \geq \frac{6}{(E_S/N_o)K^2(K^2-1)} \sum_{k=l}^{l+K-1} k^2 \tag{2.43}$$

$$\geq \frac{3}{(E_b/N_o)K^2(K^2-1)} \sum_{k=l}^{l+K-1} k^2 \quad \text{for QPSK} \tag{2.44}$$

$$\mathrm{VAR}[\widehat{\Delta fT_S}] \geq \frac{6}{4\pi^2 K(K^2-1)(E_S/N_o)} \tag{2.45}$$

$$\geq \frac{3}{4\pi^2 K(K^2-1)(E_b/N_o)} \quad \text{for QPSK.} \tag{2.46}$$

Note that the bound on the variance of $\widehat{\Delta fT_S}$ is independent of the initial starting point of the samples. On the other hand, the bound for the variance of $\widehat{\Delta\Theta}$ is dependent on this initial starting point. In fact, there is an optimum value of l which produces the lowest bound, as was noted by Rife and Boorstyn [22]. Mimimizing equation (2.43) with respect l yields the optimum l as

$$l = -\frac{K-1}{2}. \tag{2.47}$$

With this value of l, the lower bound on the variance of the phase error estimate reduces to

$$\mathrm{VAR}[\widehat{\Delta\Theta}] = \frac{1}{2K(E_S/N_o)}. \tag{2.48}$$

The fact that the lowest bound is obtained for $l = -(K-1)/2$ is a very important result. It implies that a phase estimator employing discrete time observations will have a minimum variance if the frequency error of the observations ($2\pi k\Delta fT_S$) is symmetric about a zero frequency error. Obviously our samples do not fall into this symmetric structure. However, if we were to redefine the phase error per window as $\Delta\theta'$, where

$$\Delta\theta' = \Delta\theta + 2\pi\Delta fT_S(l + \frac{K-1}{2}) = \Delta\theta + 2\pi\Delta fT_S(l+N) \tag{2.49}$$

then the samples could be denoted as

$$x_k = \sqrt{E_S}\cos(2\pi\Delta fT_S(k-l-N) + \Delta\theta' + g_k 2\pi/M) + n_k^i \tag{2.50}$$

$$y_k = \sqrt{E_S}\sin(2\pi\Delta fT_S(k-l-N) + \Delta\theta' + g_k 2\pi/M) + n_k^q. \tag{2.51}$$

Observation Window									
Symbol	l	$l+1$	$\cdots$	$l+\frac{K-3}{2}$	$l+\frac{K-1}{2}$	$l+\frac{K+1}{2}$	$\cdots$	$l+K-2$	$l+K-1$
Before Redefinition Phase error	$\Delta\theta$	$\Delta\theta$	$\cdots$	$\Delta\theta$	$\Delta\theta$	$\Delta\theta$	$\cdots$	$\Delta\theta$	$\Delta\theta$
Freq. error ($*2\pi\Delta fT_S$)	l	$l+1$	$\cdots$	$l+\frac{K-3}{2}$	$l+\frac{K-1}{2}$	$l+\frac{K+1}{2}$	$\cdots$	$l+K-2$	$l+K-1$
After Redefinition Phase error	$\Delta\theta'$	$\Delta\theta'$	$\cdots$	$\Delta\theta'$	$\Delta\theta'$	$\Delta\theta'$	$\cdots$	$\Delta\theta'$	$\Delta\theta'$
Freq. error ($*2\pi\Delta fT_S$)	$-N$	$-N+1$	$\cdots$	-1	0	1	$\cdots$	$N-1$	N

Figure 2.5: Redefinition of Phase Error per Window

In the above, $N = (K-1)/2$. Note that the frequency error of these modified samples does meet the symmetry requirements (See Figure 2.5). However in such a case, the synchronizer no longer estimates $\Delta\theta$, but rather $\Delta\theta'$. This is permitted since $2\pi\Delta fT_S(l+N)$ is constant for every window. The reader should also note that this redefinition would have no effect on the bound for $\widehat{\Delta FT_S}$, since equation (2.45) is independent of l. It is now possible to conclude that every window can be made symmetric, simply by redefining the phase error per window as $\Delta\theta'$.

The CRLB for both phase and frequency error are shown in Figures 2.6 and 2.7. The results are plotted for QPSK, and for various levels of E_b/N_o. The phase error is assumed to have been redefined, and so the observation window is symmetric ($l = -(K-1)/2$). Since this is the lowest variance attainable, all estimates should have variance close to this bound. Furthermore, these estimates should be unbiased. That is, the mean of the estimate should be equal to the parameter which is being

estimated.

$$\mathrm{E}[\widehat{\Delta\Theta'}] = \Delta\theta' \tag{2.52}$$

$$\mathrm{E}[\widehat{\Delta F}] = \Delta f. \tag{2.53}$$

For an estimator to be useful, it must possess both these properties. In such a case, the estimate is said to be efficient.

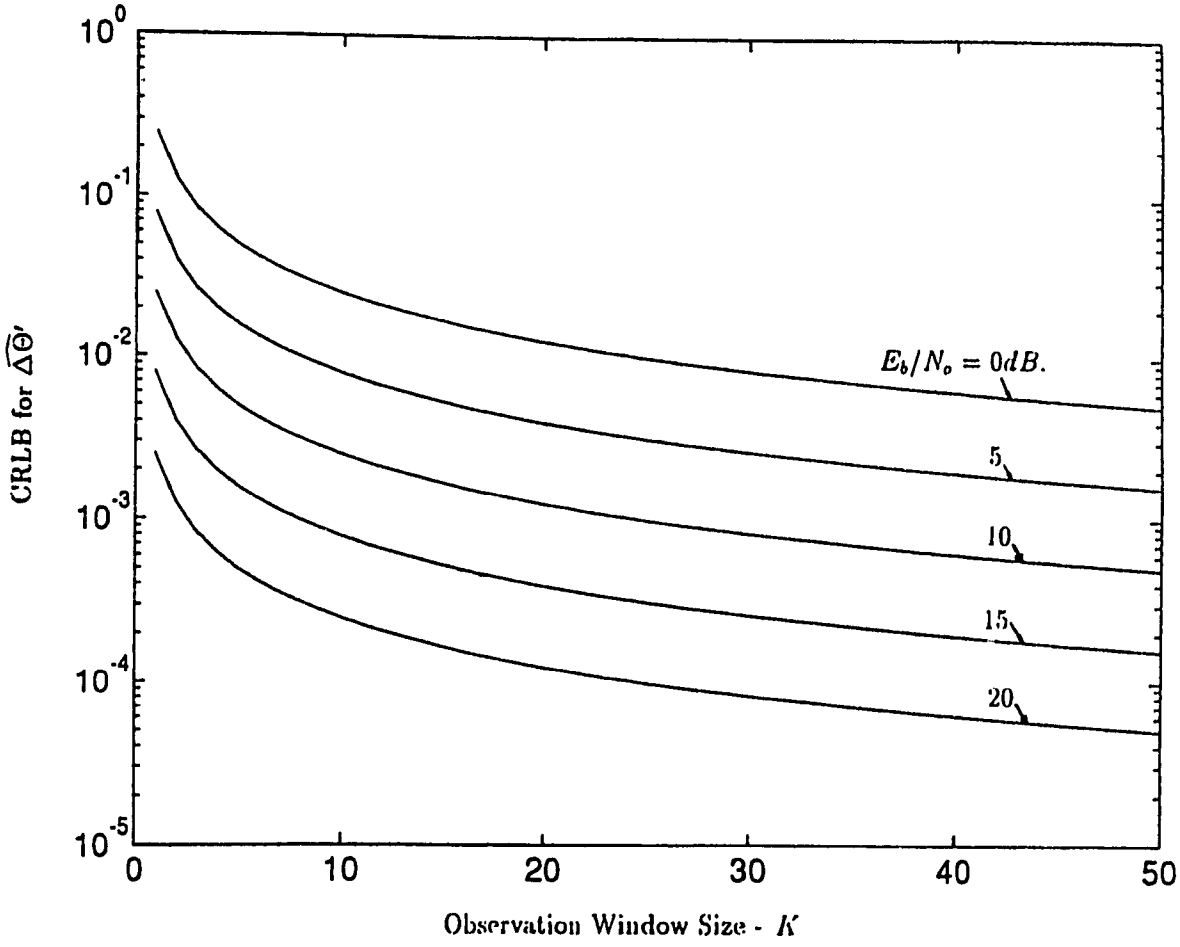

Figure 2.6: CRLB for Phase Error Estimation

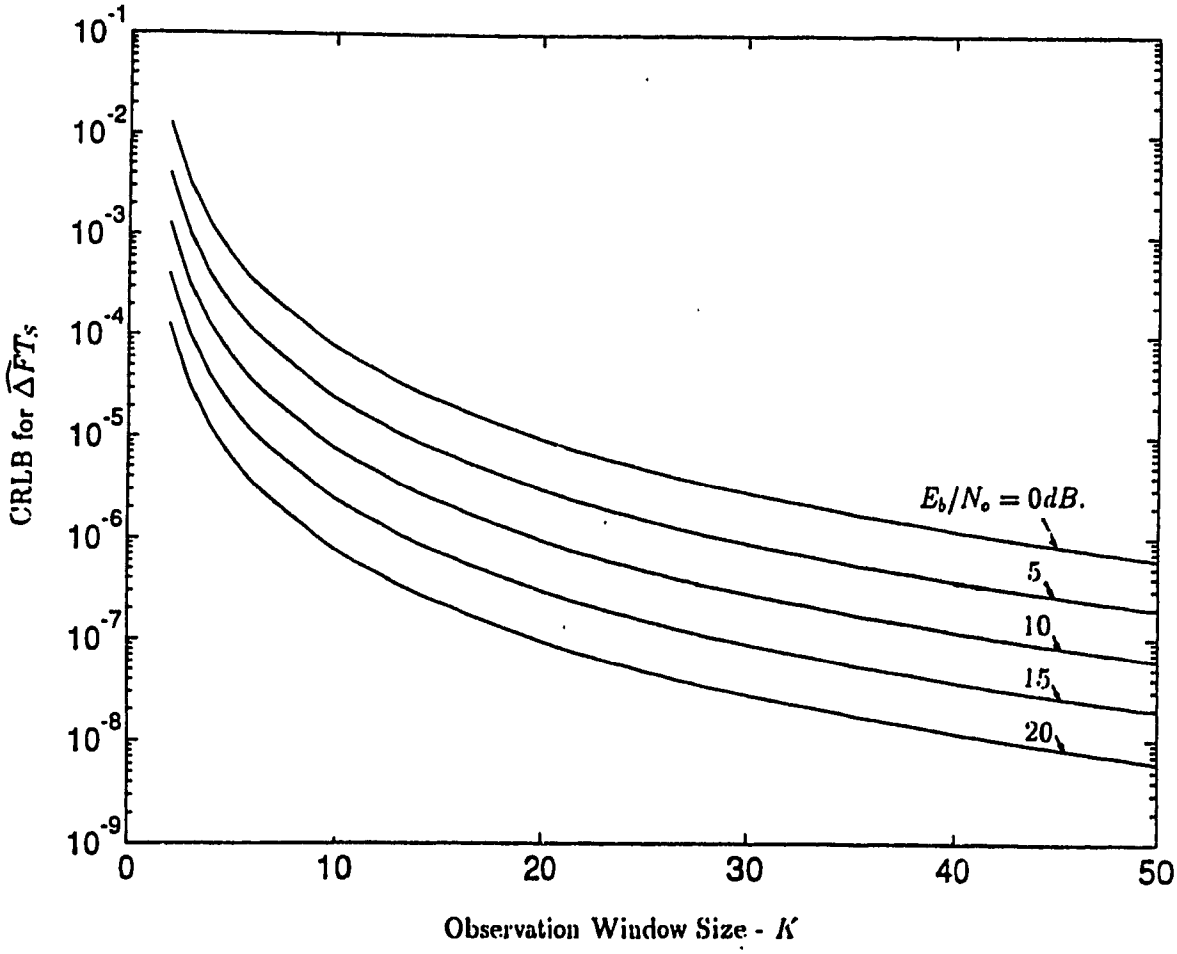

Figure 2.7: CRLB for Normalized Frequency Error Estimation

Chapter 3

Techniques for Phase Estimation

Two of the more important results of the last chapter are listed below:

- Integrate-and-dump samples are sufficient for phase error and frequency error estimation.
- Symmetric observation windows yield minimum variance for phase error estimates.

In accordance with these two results, the phase estimate (as well as the frequency estimate) should be determined from the samples

$$\begin{aligned} x_k &= \sqrt{E_S}\cos(2\pi\Delta f T_S(k-l-N)+\Delta\theta'+g_k 2\pi/M)+n_k^i \\ y_k &= \sqrt{E_S}\sin(2\pi\Delta f T_S(k-l-N)+\Delta\theta'+g_k 2\pi/M)+n_k^q \\ & \qquad\qquad l\le k\le l+K-1. \end{aligned} \tag{3.1}$$

These samples generate a complex quantity z_k, such that

$$\begin{aligned} z_k &= x_k + jy_k \\ &= \sqrt{E_S}e^{j(2\pi\Delta f T_S(k-l-N)+\Delta\theta'+g_k 2\pi/M)}+n_k^i+jn_k^q \\ &\stackrel{def}{=} \rho_k e^{j(2\pi\Delta f T_S(k-l-N)+\Delta\theta'+g_k 2\pi/M+\zeta_k)} \\ &= \rho_k e^{j\psi_k} \qquad l\le k\le l+K-1. \end{aligned} \tag{3.2}$$

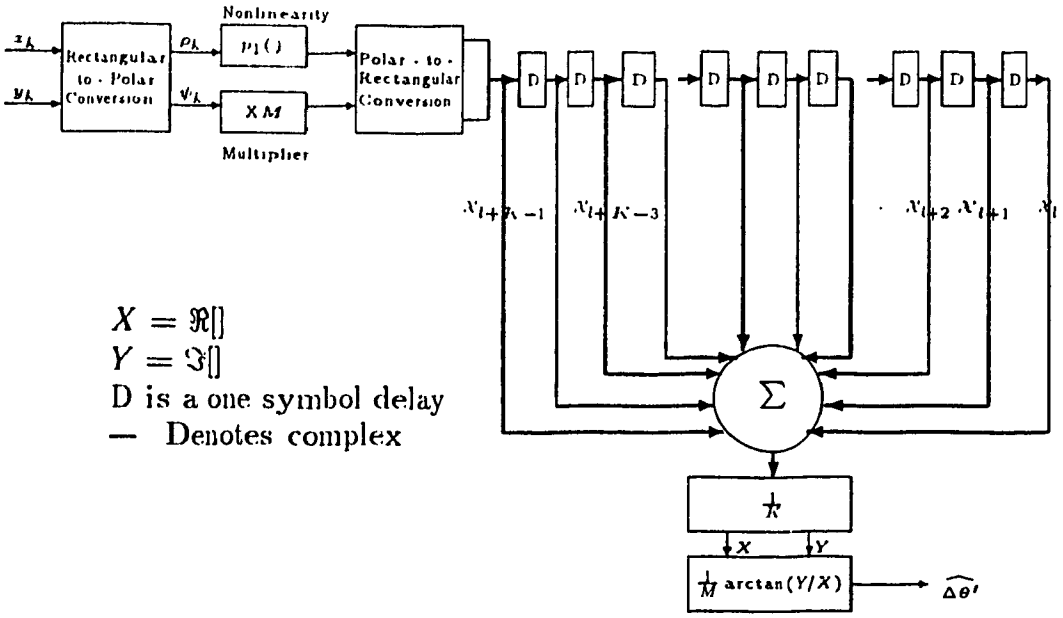

Figure 3.1: Nonlinear Phase Estimator with Modulation Removal (NPE/$\bar{\text{M}}$)

We introduce the polar form, since it simplifies the analysis presented in this chapter. Note that the random variables ρ_k and ϵ_k completely characterize the noise N_k^i and N_k^q.

3.1 Presentation of Techniques

The two estimation techniques studied in this chapter, both fall under the category of nonlinear phase estimators. These were the only synchronizers mentioned in Chapter 2 which were open-loop, and thus were appropriate for burst-mode TDMA systems. The major difference between the two techniques is the manner in which the samples x_k and y_k are manipulated. For the NPE/$\bar{\text{M}}$ (Figure 3.1), the samples are converted to polar form ($\rho_k e^{j\psi_k}$), after which the phase is multiplied by M (to remove the dependence on the modulation) and the magnitude is passed through some nonlinearity $p_1(\rho_k)$. The result is then reconverted back to rectangular form,

yielding

$$\begin{aligned}
\mathcal{V}_k &= p_1(\rho_k)e^{j(M\psi_k)} \\
&= p_1(\rho_k)e^{j(2\pi\Delta f T_S(k-l-N)M+M\Delta\theta'+M\epsilon_k+g_k 2\pi)} \\
&= p_1(\rho_k)e^{j(2\pi\Delta f T_S(k-l-N)M+M\Delta\theta'+M\epsilon_k)} \\
&= p_1(\rho_k)\cos(2\pi\Delta f T_S(k-l-N)M + M\Delta\theta' + M\epsilon_k) \\
&\quad + jp_1(\rho_k)\sin(2\pi\Delta f T_S(k-l-N)M + M\Delta\theta' + M\epsilon_k). \qquad (3.3)
\end{aligned}$$

An estimate of $M\Delta\theta'$, denoted $\widehat{M\Delta\theta'}$, is then found by averaging the K complex samples $\mathcal{V}_k$, and determining the corresponding argument of this mean.

If noise were absent, $\mathcal{V}_k$ would be given by

$$\begin{aligned}
\mathcal{V}_k &= p_1(\sqrt{E_S})e^{j(2\pi\Delta f T_S(k-l-N)+g_k 2\pi/M+\Delta\theta')M} \\
&= p_1(\sqrt{E_S})e^{j(2\pi\Delta f T_S(k-l-N)M+M\Delta\theta')}.
\end{aligned}$$

Therefore,

$$M\widehat{\Delta\theta'} = \arg\left[\frac{1}{K}\sum_{k=l}^{l+K-1}\mathcal{V}_k\right]$$

$$\widehat{\Delta\theta'} = \frac{1}{M}\arctan\left[\frac{\frac{1}{K}\sum_{k=l}^{l+K-1}p_1(\sqrt{E_S})\sin\left(2\pi\Delta f T_S(k-l-N)M + M\Delta\theta'\right)}{\frac{1}{K}\sum_{k=l}^{l+K-1}p_1(\sqrt{E_S})\cos\left(2\pi\Delta f T_S(k-l-N)M + M\Delta\theta'\right)}\right].$$

After using the trigonometric identity

$$a + \arctan\left[\frac{y}{x}\right] = \arctan\left[\frac{x\sin(a)+y\cos(a)}{x\cos(a)-y\sin(a)}\right],$$

the above equation reduces to

$$\begin{aligned}
\widehat{\Delta\theta'} &= \Delta\theta' + \frac{1}{M}\arctan\left[\frac{\frac{1}{K}\sum_{k=l}^{l+K-1}p_1(\sqrt{E_S})\sin\left(2\pi\Delta f T_S(k-l-N)M\right)}{\frac{1}{K}\sum_{k=l}^{l+K-1}p_1(\sqrt{E_S})\cos\left(2\pi\Delta f T_S(k-l-N)M\right)}\right] \\
&= \Delta\theta'.
\end{aligned}$$

The last equality is due to the fact that the numerator of the arctan function evaluates to zero. Surprisingly, even though the samples on which the estimate is based are a function of Δf, the final estimate is not. This property is attributed directly to

the symmetry of the frequency error for samples at opposite ends of the observation window ($\mathcal{X}_{l+r}$ and $\mathcal{X}_{l+K-r-1}$). That is,

$$p_1(\sqrt{E_S})\sin(2\pi\Delta f T_S(r-N)M) = -p_1(\sqrt{E_S})\sin(2\pi\Delta f T_S(N-r)M)\ .$$

However as soon as noise is considered, the above relation no longer holds since each sample is corrupted by independent random noise. That is,

$$\begin{aligned} & p_1(\rho_{l+r})\sin(2\pi\Delta f T_S(r-N)M + M\epsilon_{l+r}) \\ & \neq \ -p_1(\rho_{l+K-r-1})\sin(2\pi\Delta f T_S(N-r)M + M\epsilon_{l+K-r-1}), \end{aligned}$$

and as a result, the final estimate would be a function of both noise and frequency error.

$$\widehat{\Delta\theta'} = \frac{1}{M}\arctan\left[\frac{\frac{1}{K}\sum_{k=l}^{l+K-1} p_1(\rho_k)\sin(2\pi\Delta f T_S(k-l-N)M + M\Delta\theta' + M\epsilon_k)}{\frac{1}{K}\sum_{k=l}^{l+K-1} p_1(\rho_k)\cos(2\pi\Delta f T_S(k-l-N)M + M\Delta\theta' + M\epsilon_k)}\right] \quad (3.4)$$

$$= \Delta\theta' + \frac{1}{M}\arctan\left[\frac{\frac{1}{K}\sum_{k=l}^{l+K-1} p_1(\rho_k)\sin(2\pi\Delta f T_S(k-l-N)M + M\epsilon_k)}{\frac{1}{K}\sum_{k=l}^{l+K-1} p_1(\rho_k)\cos(2\pi\Delta f T_S(k-l-N)M + M\epsilon_k)}\right] \quad (3.5)$$

$$= \Delta\theta' + \text{degradation}(\Delta f T_S,\ \rho_k,\ \epsilon_k \text{ for } l \le k \le l+K-1)\ . \quad (3.6)$$

In the next section, it will be shown that even a small $\Delta f T_S$ severely degrades the performance of the estimator. Hence, a method of generating samples $\mathcal{X}'_k$ independent of Δf would be beneficial. The NPE/$\bar{\text{M}}\bar{\text{F}}$, shown in Figure 3.2, produces such samples. Essentially, the estimator performs a second operation on the z_k's, prior to averaging. The output of this operation should be independent of Δf, but should still be a strong function of the parameter to be estimated – $\Delta\theta'$. The reasoning behind the particular choice of operation, lies in the fact that the frequency error for sample $\mathcal{X}_{l+r}$, is the negative of that for $\mathcal{X}_{l+K-r-1}$ – i.e. $2\pi\Delta f T_S(r-N)M = -2\pi\Delta f T_S(N-r)M$. Adding the arguments of these two samples by complex multiplication, produces an output which is only a function of noise and $\Delta\theta'$. Namely,

$$\mathcal{X}'_r \ = \ \mathcal{X}_{l+r}\mathcal{X}_{l+K-r-1}$$

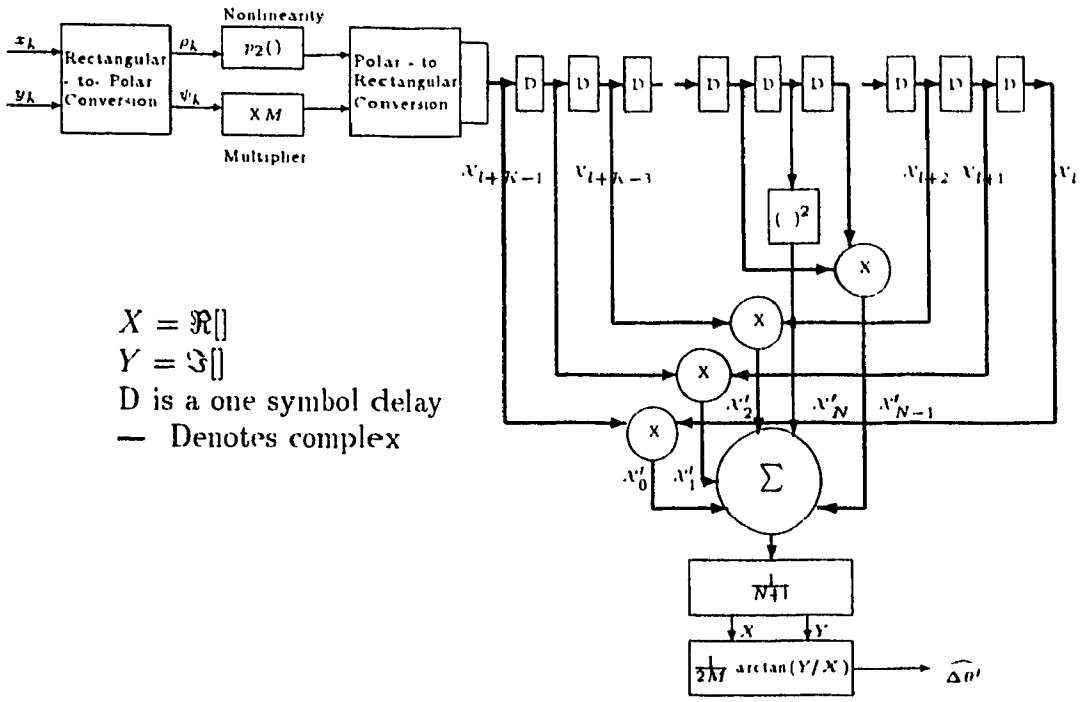

Figure 3.2: Nonlinear Phase Estimator with Modulation and Frequency Error Removal (NPE/$\bar{\text{M}}\bar{\text{F}}$)

$$
\begin{aligned}
&= p_2(\rho_{l+r})e^{j(2\pi\Delta f T_S(r-N)M+M\Delta\theta'+M\epsilon_{l+r})} \bullet \\
&\quad p_2(\rho_{l+K-r-1})e^{j(2\pi\Delta f T_S(N-r)M+M\Delta\theta'+M\epsilon_{l+K-r-1})} \\
&= p_2(\rho_{l+r})p_2(\rho_{l+K-r-1})e^{j(2M\Delta\theta'+M\epsilon_{l+r}+M\epsilon_{l+K-r-1})} \quad \text{for } 0 \le r \le N \ . \quad (3.7)
\end{aligned}
$$

Special consideration must be paid to the middle symbol of the observation window, corresponding to $r = N$. This sample, $\mathcal{X}_{l+N}$, is characterized as having a counterpart which corresponds to itself (i.e. $\mathcal{X}_{l+N} = \mathcal{X}_{l+K-N-1}$), and by being already independent of Δf. Therefore for $r = N$, equation (3.7) becomes $\mathcal{X}'_N = p_2^2(\rho_{l+N})e^{j(2M\Delta\theta'+2M\epsilon_{l+N})}$, which is simply $\mathcal{X}_{l+N}$ squared.

The estimate is then found from these $\mathcal{X}'_r$ for $0 \le r \le N$, using the same averaging technique as used by the NPE/$\bar{\text{M}}$.

$$\widehat{\Delta\theta'} = \frac{1}{2M}\arctan\left[\frac{\frac{1}{N+1}\sum_{r=0}^{N} p_2(\rho_{l+r})p_2(\rho_{l+K-r-1})\sin(2M\Delta\theta' + M\epsilon_{l+r} + M\epsilon_{l+K-r-1})}{\frac{1}{N+1}\sum_{r=0}^{N} p_2(\rho_{l+r})p_2(\rho_{l+K-r-1})\cos(2M\Delta\theta' + M\epsilon_{l+r} + M\epsilon_{l+K-r-1})}\right] \quad (3.8)$$

$$= \Delta\theta' + \frac{1}{2M}\arctan\left[\frac{\frac{1}{N+1}\sum_{r=0}^{N} p_2(\rho_{l+r})p_2(\rho_{l+K-r-1})\sin(M\epsilon_{l+r} + M\epsilon_{l+K-r-1})}{\frac{1}{N+1}\sum_{r=0}^{N} p_2(\rho_{l+r})p_2(\rho_{l+K-r-1})\cos(M\epsilon_{l+r} + M\epsilon_{l+K-r-1})}\right] \quad (3.9)$$

$$= \Delta\theta' + \text{degradation}(\rho_k, \epsilon_k \text{ for } l \le k \le l+K-1)\,. \quad (3.10)$$

Notice that there is no $\Delta f T_S$ dependent degradation and that $\widehat{\Delta\theta'} = \Delta\theta'$ for the noiseless case.

At first glance, comparison of equations (3.4) and (3.8) may suggest that the NPE/$\bar{\text{M}}\bar{\text{F}}$ is placed at an immediate disadvantage with respect to the NPE/$\bar{\text{M}}$, since the process of multiplying $\mathcal{X}_{l+r}$ and $\mathcal{X}_{l+K-r-1}$ effectively doubles the noise ($M\epsilon_{l+r} + M\epsilon_{l+K-r-1}$ as compared to $M\epsilon_k$). However, the fact that these $\mathcal{X}'_r$ have twice the signal level of the wanted parameter ($2M\Delta\theta'$ versus $M\Delta\theta'$) compensates for the increased noise.

At this point we can determine the processing times (T_P) of both estimators in terms of the number of real addition operations, real multiplication operations, and *ROM look-up* operations. If the time for each of these operations is known (T_A, T_M and T_{LU}, respectively), then the absolute time required to determine the estimates can be obtained. However, we will not attempt to substitute values for these times, since they are strongly dependent on the technology used for implementation.

All the operations of the two estimators can be reduced to some combination of the three *base* operations:

- 1. real addition: addition of two real quantities
- 2. real multiplication: multiplication of two real quantities
- 3. Table look-up: input is index to a ROM table and value of table is the required output.

For the NPE/$\bar{\text{M}}$, for instance, the generation of the $\mathcal{X}_k$ as well as the arctangent operation can both be implemented by table look-ups. Furthermore, the K term

complex addition corresponds to $2(K-1)$ real additions ($K-1$ additions for $\Re[.Y_k]$ and $K-1$ additions for $\Im[.Y_k]$) where we recall that a summation of two terms requires only a single addition. Lastly, the multiplication of the complex sum by $1/K$ requires 2 real multiplications. Therefore, the processing time for the NPE/M is given by

$$T_P = 2(K-1)T_A + 2T_M + 2T_{LU} \qquad \text{:NPE/M.}$$

A similar reasoning holds for the NPE/MF. The only extra feature of this estimator is that it requires $(K+1)/2$ complex multiplications. Each complex multiplication can be implemented by 4 real multiplications and 2 real additions $((a+jb)(c+jd) = ((ac-bd)+j(ad+bc))$. Using this last result, the processing time for the NPE/MF is given by

$$T_P = 2KT_A + (2K+4)T_M + 2T_{LU} \qquad \text{: NPE/MF.}$$

3.2 Comparison of Techniques

In this section, we find the pdf of the random estimates ($\widehat{\Delta\Theta}'$). We note from equations (3.5) and (3.9) that both estimators are of the form

$$\widehat{\Delta\Theta}' = \Delta\theta' + \delta \tag{3.11}$$

where δ is a random degradation component dependent on the random variables ρ_k and ϵ_k, for all k. It turns out that the pdf of δ is all that is required for a comparison of the two techniques. To find this function, we first require the joint pdf of ρ_k and ϵ_k. The steps involved are outlined below. First, we recall the joint pdf of X_k and Y_k given in equation (2.35).

$$f_{X_k,Y_k}(x_k, y_k|\text{modulation}) =$$
$$\frac{1}{\pi N_o}\exp\left[-\frac{({x_k}^2+{y_k}^2)}{N_o} + \frac{\alpha_k x_k + \beta_k y_k}{N_o/2} - \frac{E_S}{N_o}\right] \quad -\infty < x_k, y_k < \infty\ . \tag{3.12}$$

where

$$\begin{aligned} \alpha_k &= \sqrt{E_S}\cos(2\pi\Delta f T_S(k-l-N)+g_k 2\pi/M+\Delta\theta') \\ \beta_k &= \sqrt{E_S}\sin(2\pi\Delta f T_S(k-l-N)+g_k 2\pi/M+\Delta\theta') \end{aligned}$$

and where the redefined $\Delta\theta'$ is used. We proceed with the following transformation of variables

$$\begin{cases} \rho_k = \sqrt{{X_k}^2+{Y_k}^2} \\ \epsilon_k = (\arctan(Y_k/X_k) - 2\pi\Delta f T_S(k-l-N) - \Delta\theta' - g_k 2\pi/M)\mathrm{mod}(2\pi) \end{cases} . \tag{3.13}$$

The final result of the transformation is

$$f_{\rho_k,\epsilon_k}(\rho_k,\epsilon_k|\{g_k\}) = \frac{\rho_k}{\pi N_o}\exp\left[-\frac{{\rho_k}^2}{N_o}+\frac{\sqrt{E_S}\rho_k\cos\epsilon_k}{N_o/2}-\frac{E_S}{N_o}\right] \quad \begin{matrix} 0\le\rho_k<\infty \\ -\pi\le\epsilon_k<\pi \end{matrix} . \tag{3.14}$$

Notice that (3.14) is not explicitly dependent on the modulation. Furthermore, the same pdf is obtained for all $l \le k \le l+K-1$. Therefore, we may rewrite the pdf without the modulation condition, and without the k'th sample subscript. That is,

$$f_{\rho,\epsilon}(\rho,\epsilon) = \frac{\rho}{\pi N_o}\exp\left[\frac{-\rho^2}{N_o}+\frac{\sqrt{\gamma}\rho\cos\epsilon}{\sqrt{N_o/2}}-\frac{\gamma}{2}\right] \quad \begin{matrix} 0\le\rho<\infty \\ -\pi\le\epsilon<\pi \end{matrix} \tag{3.15}$$

where the substitution $\gamma = 2E_S/N_o$ was made. This γ is a measure of the channel signal-to-noise ratio.

The pdf of δ can now be found from application of the central limit theorem (CLT). The method described below is an expansion to the procedure put forth by Hagmann and Hubermann [24], which was applied to the unmodulated ($M = 1$) Viterbi and Viterbi phase estimator (equivalent to the NPE/$\bar{M}$). For this estimator, we recall that δ is defined as,

$$\delta = \frac{1}{M}\arctan\left[\frac{\frac{1}{K}\sum_{k=l}^{l+K-1}p_1(\rho_k)\sin(2\pi\Delta f T_S(k-l-N)M+M\epsilon_k)}{\frac{1}{K}\sum_{k=l}^{l+K-1}p_1(\rho_k)\cos(2\pi\Delta f T_S(k-l-N)M+M\epsilon_k)}\right] .$$

Since ρ_k, ϵ_k are independent from ρ_l, ϵ_l ($k \ne l$), both numerator and denominator of the arctangent function are sums of independent random variables. By the

CLT, these sums, denoted as ξ and η, can be assumed to be Gaussian distributed. Therefore,

$$\begin{aligned}
\delta &= \frac{1}{M}\arctan\left[\frac{\xi}{\eta}\right] \qquad \text{and} \qquad (3.16)\\
\xi &= \frac{1}{K}\sum_{k=l}^{l+K-1} p_1(\rho_k)\sin\left(2\pi\Delta f T_S(k-l-N)M + M\epsilon_k\right)\\
\eta &= \frac{1}{K}\sum_{k=l}^{l+K-1} p_1(\rho_k)\cos\left(2\pi\Delta f T_S(k-l-N)M + M\epsilon_k\right).
\end{aligned}$$

The moments of ξ and η are derived in Appendix C, and shown below:

$$\begin{aligned}
\mu_\xi &= 0 \qquad (3.17)\\
\sigma_\xi^2 &= \frac{\mathrm{E}[{p_1}^2(\rho)]}{2K} - \frac{\mathrm{E}[{p_1}^2(\rho)\cos(2M\epsilon)]}{2K} S_K(2M\Delta f T_S) - \\
&\qquad \frac{\mathrm{E}^2[p_1(\rho)\cos(M\epsilon)]}{2K}[1 - S_K(2M\Delta f T_S)] \qquad (3.18)\\
\mu_\eta &= \mathrm{E}[p_1(\rho)\cos(M\epsilon)]S_K(M\Delta f T_S) \qquad (3.19)\\
\sigma_\eta^2 &= \frac{\mathrm{E}[{p_1}^2(\rho)]}{2K} + \frac{\mathrm{E}[{p_1}^2(\rho)\cos(2M\epsilon)]}{2K} S_K(2M\Delta f T_S) - \\
&\qquad \frac{\mathrm{E}^2[p_1(\rho)\cos(M\epsilon)]}{2K}[1 + S_K(2M\Delta f T_S)] \qquad (3.20)\\
\mathrm{COV}[\eta,\xi] &= 0 \qquad \text{and where}\\
S_K(2M\Delta f T_S) &= \frac{\sin(2K\pi\Delta f T_S M)}{K\sin(2\pi\Delta f T_S M)}. \qquad (3.21)
\end{aligned}$$

If we define random variables Z_1 and Z_2 as,

$$\begin{aligned}
Z_1 &= \frac{1}{M}\arctan\left[\frac{\xi}{\eta}\right] \qquad -\pi/M \le Z_1 < \pi/M \qquad (3.22)\\
Z_2^2 &= \xi^2 + \eta^2 \qquad 0 \le Z_2 < \infty, \qquad (3.23)
\end{aligned}$$

then it is possible to find $f_{Z_1,Z_2}(z_1,z_2)$ from $f_{\eta,\xi}(\eta,\xi)$ by transformation of variables. We can then determine $f_\delta(\delta)$ by noting that $Z_1 = \delta$, and solving for the marginal probability distribution of Z_1. These steps are carried out in Appendix D, where the desired pdf is obtained.

$$f_\delta(\delta) = \frac{Me^{-\mu_\eta{}^2/2\sigma_\eta^2}}{2\pi}\frac{\sigma_\eta\sigma_\xi}{\sigma_\eta^2\sin^2(M\delta)+\sigma_\xi^2\cos^2(M\delta)}\left\{1+\frac{\mu_\eta}{\sqrt{2}\sigma_\eta}\sqrt{\pi}\sqrt{\frac{\sigma_\xi^2\cos^2(M\delta)}{\sigma_\eta^2\sin^2(M\delta)+\sigma_\xi^2\cos^2(M\delta)}}\right.$$
$$\left.\exp\left[\frac{\mu_\eta{}^2}{2\sigma_\eta^2}\frac{\sigma_\xi^2\cos^2(M\delta)}{\sigma_\eta^2\sin^2(M\delta)+\sigma_\xi^2\cos^2(M\delta)}\right]\left[1+\mathrm{erf}\left(\frac{\mu_\eta}{\sqrt{2}\sigma_\eta}\sqrt{\frac{\sigma_\xi^2\cos^2(M\delta)}{\sigma_\eta^2\sin^2(M\delta)+\sigma_\xi^2\cos^2(M\delta)}}\right)\right]\right\}$$
$$-\pi/M \le \delta < \pi/M \qquad (3.24)$$

where μ_η, σ_η^2, and σ_ξ^2 are as defined in equations (3.18) - (3.21).

A similar analysis is possible for the NPE/$\bar{\mathrm{M}}\bar{\mathrm{F}}$. The degradation δ and the random variables ξ and η are defined below.

$$\delta = \frac{1}{2M}\arctan\left[\frac{\xi}{\eta}\right]$$
$$\xi = \frac{1}{N+1}\sum_{r=0}^{N} p_2(\rho_{l+r})p_2(\rho_{l+K-r-1})\sin\left(M\epsilon_{l+r}+M\epsilon_{l+K-r-1}\right)$$
$$\eta = \frac{1}{N+1}\sum_{r=0}^{N} p_2(\rho_{l+r})p_2(\rho_{l+K-r-1})\cos\left(M\epsilon_{l+r}+M\epsilon_{l+K-r-1}\right).$$

The moment derivations are again shown in Appendix C.

$$\mu_\xi = 0 \qquad (3.25)$$
$$\sigma_\xi^2 = \frac{N\mathrm{E}^2[p_2{}^2(\rho)]-N\mathrm{E}^2[p_2{}^2(\rho)\cos(2M\epsilon)]+\mathrm{E}[p_2{}^4(\rho)]}{2(N+1)^2} - \frac{\mathrm{E}[p_2{}^4(\rho)\cos(4M\epsilon)]}{2(N+1)^2} \qquad (3.26)$$
$$\mu_\eta = \frac{N\mathrm{E}^2[p_2(\rho)\cos(M\epsilon)]+\mathrm{E}[p_2{}^2(\rho)\cos(2M\epsilon)]}{(N+1)} \qquad (3.27)$$
$$\sigma_\eta^2 = \frac{N\mathrm{E}^2[p_2{}^2(\rho)]+N\mathrm{E}^2[p_2{}^2(\rho)\cos(2M\epsilon)]-2N\mathrm{E}^4[p_2(\rho)\cos(M\epsilon)]}{2(N+1)^2} + \frac{\mathrm{E}[p_2{}^4(\rho)]+\mathrm{E}[p_2{}^4(\rho)\cos(4M\epsilon)]-2\mathrm{E}^2[p_2{}^2(\rho)\cos(2M\epsilon)]}{2(N+1)^2} \qquad (3.28)$$
$$\mathrm{COV}[\eta,\xi] = 0.$$

Using the same method as was used for the NPE/$\bar{\mathrm{M}}$, the pdf of δ is obtained as

$$f_\delta(\delta) = \frac{2Me^{-\mu_\eta^2/2\sigma_\eta^2}}{2\pi} \frac{\sigma_\eta\sigma_\xi}{\sigma_\eta^2\sin^2(2M\delta)+\sigma_\xi^2\cos^2(2M\delta)} \left\{1 + \frac{\mu_\eta}{\sqrt{2}\sigma_\eta}\sqrt{\pi}\sqrt{\frac{\sigma_\xi^2\cos^2(2M\delta)}{\sigma_\eta^2\sin^2(2M\delta)+\sigma_\xi^2\cos^2(2M\delta)}}\right.$$
$$\left.\exp\left[\frac{\mu_\eta^2}{2\sigma_\eta^2}\frac{\sigma_\xi^2\cos^2(2M\delta)}{\sigma_\eta^2\sin^2(2M\delta)+\sigma_\xi^2\cos^2(2M\delta)}\right]\left[1+\mathrm{erf}\left(\frac{\mu_\eta}{\sqrt{2}\sigma_\eta}\sqrt{\frac{\sigma_\xi^2\cos^2(2M\delta)}{\sigma_\eta^2\sin^2(2M\delta)+\sigma_\xi^2\cos^2(2M\delta)}}\right)\right]\right\}$$
$$-\pi/2M \le \delta < \pi/2M \qquad (3.29)$$

where μ_η, σ_η^2, and σ_ξ^2 are defined by (3.26) - (3.28). Note that the only difference in $f_\delta(\delta)$ between the two estimators ((3.24) and (3.29)) is in the definitions of μ_η, σ_η^2, and σ_ξ^2, and in the factor of 2 attached to the M for the NPE/MF. At this point, we can draw the following conclusion — ξ and η are sums of K random variables for the NPE/$\bar{\mathrm{M}}$, but only $N+1$ random variables for the new proposed estimator. Since application of the CLT is justified if the sums are taken over many random variables, the Gaussian approximation is better suited for the NPE/$\bar{\mathrm{M}}$, particularly if observation window size (K) is small.

3.2.1 Moment Analysis

The mean of the estimates can be obtained from (3.11), as

$$\mathrm{E}[\widehat{\Delta\Theta}'] = \Delta\theta' + \mathrm{E}[\delta]. \qquad (3.30)$$

Notice from the definitions of $f_\delta(\delta)$ in (3.24) and (3.29), that $f_\delta(\delta) = f_\delta(-\delta)$. Since δ is symmetrically distributed about $\delta = 0$, it's mean evaluates to zero. Consequently, both estimators produce unbiased results. This further implies that the variance of $\widehat{\Delta\Theta}'$ is equal to the variance of δ. That is,

$$\mathrm{VAR}[\widehat{\Delta\Theta}'] = \mathrm{E}[(\widehat{\Delta\Theta}' - \Delta\theta)^2] = \mathrm{E}[\delta^2]. \qquad (3.31)$$

The problem has now been reduced to finding this latter variance for a given M, observation window size (K), and channel signal-to-noise ratio ($\gamma = 2E_S/N_o$). When these parameters are specified, the moments μ_η, σ_η^2, and σ_ξ^2 become constant. To determine their values, expectations of the form $\mathrm{E}[h^R(\rho)]$ and $\mathrm{E}[h^U(\rho)\cos(UM\epsilon)]$

must be evaluated, where $h(\rho)$ is $p_1(\rho)$ for the NPE/$\bar{\text{M}}$ and $p_2(\rho)$ for the NPE/$\bar{\text{M}}\bar{\text{F}}$. Analytic expressions for these expectations were derived in [12] for nonlinearities of the form $h(\rho) = \rho^l$, where $l \leq M$ and even. The results are presented here without proof.

$$\mathrm{E}[h^R(\rho)] = (N_o/2)^{Rl/2} \sum_{n=0}^{Rl/2} \binom{Rl/2}{n}^2 2^n n! \gamma^{Rl/2-n} \qquad \text{for all } l \qquad (3.32)$$

$$\mathrm{E}[h^U(\rho)\cos(UM\epsilon)] = \begin{cases} (N_o/2)^{0.5Ul}\gamma^{0.5Ul} \sum_{n=0}^{0.5U(l+M)} \frac{(0.5U(M-l)+n-1)!(0.5U(M+l))!}{(0.5U(M-l)-1)!(0.5U(M+l)-n)!n!}(-2/\gamma)^n \\ -(N_o)^{0.5Ul}e^{-\gamma/2}(2/\gamma)^{0.5Ul+1} \sum_{n=0}^{0.5U(M-l)-1} \frac{(0.5U(M+l)+n)!}{(0.5U(M-l)-n-1)!n!}(2/\gamma)^n \\ \qquad\qquad l \leq M-2 \qquad (3.33) \\ (N_o/2)^{0.5Ul}\gamma^{0.5Ul} \qquad\qquad l = M\,. \qquad (3.34) \end{cases}$$

The variance of δ can then be found by integrating $\delta^2 f_\delta(\delta)$ over $|\delta| \leq \pi/uM$, where $u = 1$ for the NPE/$\bar{\text{M}}$, and $u = 2$ for the NPE/$\bar{\text{M}}\bar{\text{F}}$. Since p_1 and p_2 can be any function of ρ, it is very difficult to compare the two estimators on a fair basis when the nonlinearities are chosen randomly. Therefore, only the nonlinearity $p_1(\rho) = p_2(\rho) = \rho^0 = 1$ will be considered. For this case, the estimates are based solely on the phase of the received samples $(x_k + jy_k)$, and consequently neither is placed at a disadvantage.

Owing to the nonlinear nature of $f_\delta(\delta)$, the evaluation of $\int_{-\pi/uM}^{\pi/uM} x^2 f_\delta(x)dx$ cannot be carried out analytically. However, variance curves can be obtained by numerical integration. Figures 3.3 and 3.4 show the results for variance plotted versus the observation window size, for various channel E_b/N_o and for $\Delta f = 0$. The Cramer-Rao lower bound is also plotted on these graphs. Since all graphs are plotted for QPSK, $\gamma = 2E_s/N_o = 4E_b/N_o$. The graphs show that both estimators are efficient for $E_b/N_o > 10dB$..

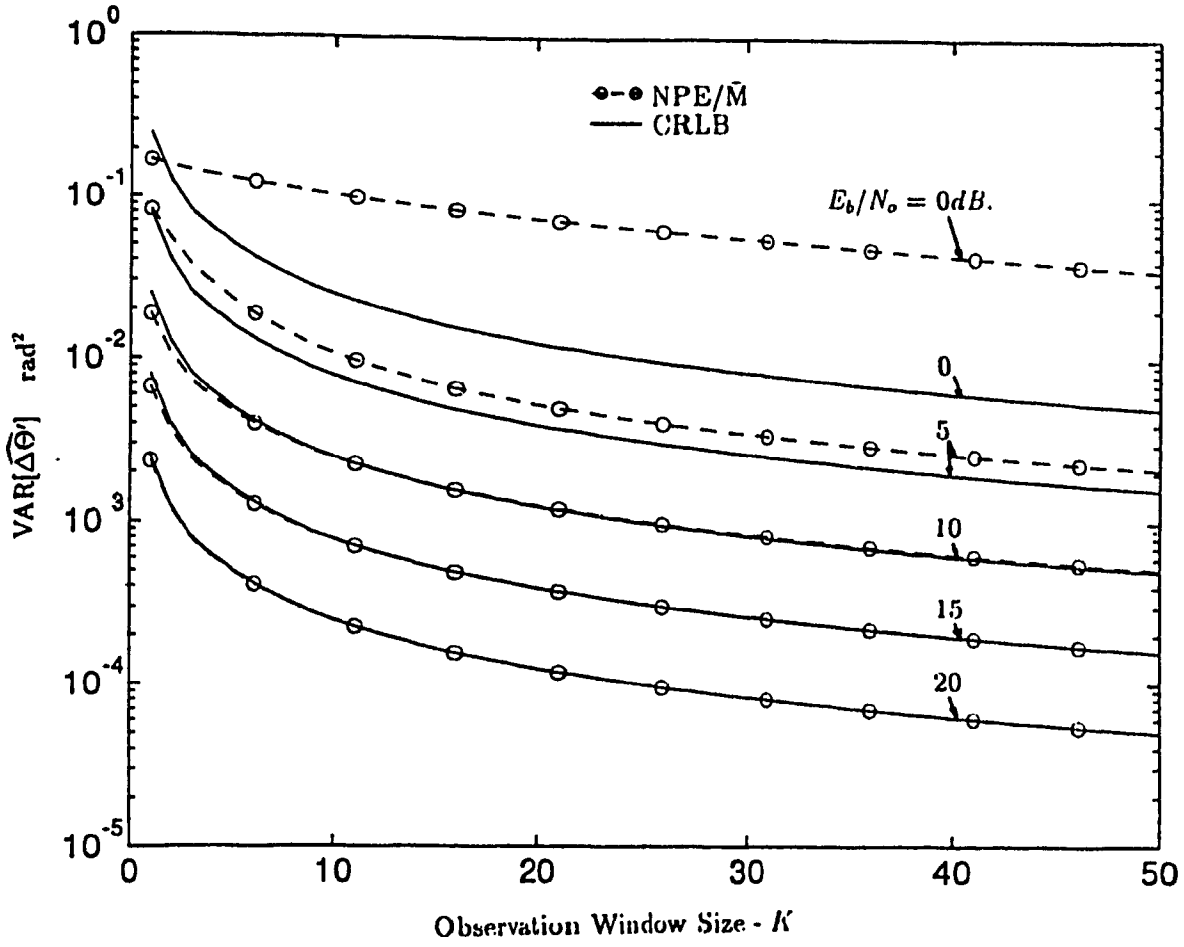

Figure 3.3: Variance of NPE/$\bar{M}$ for case ($\Delta f = 0$)

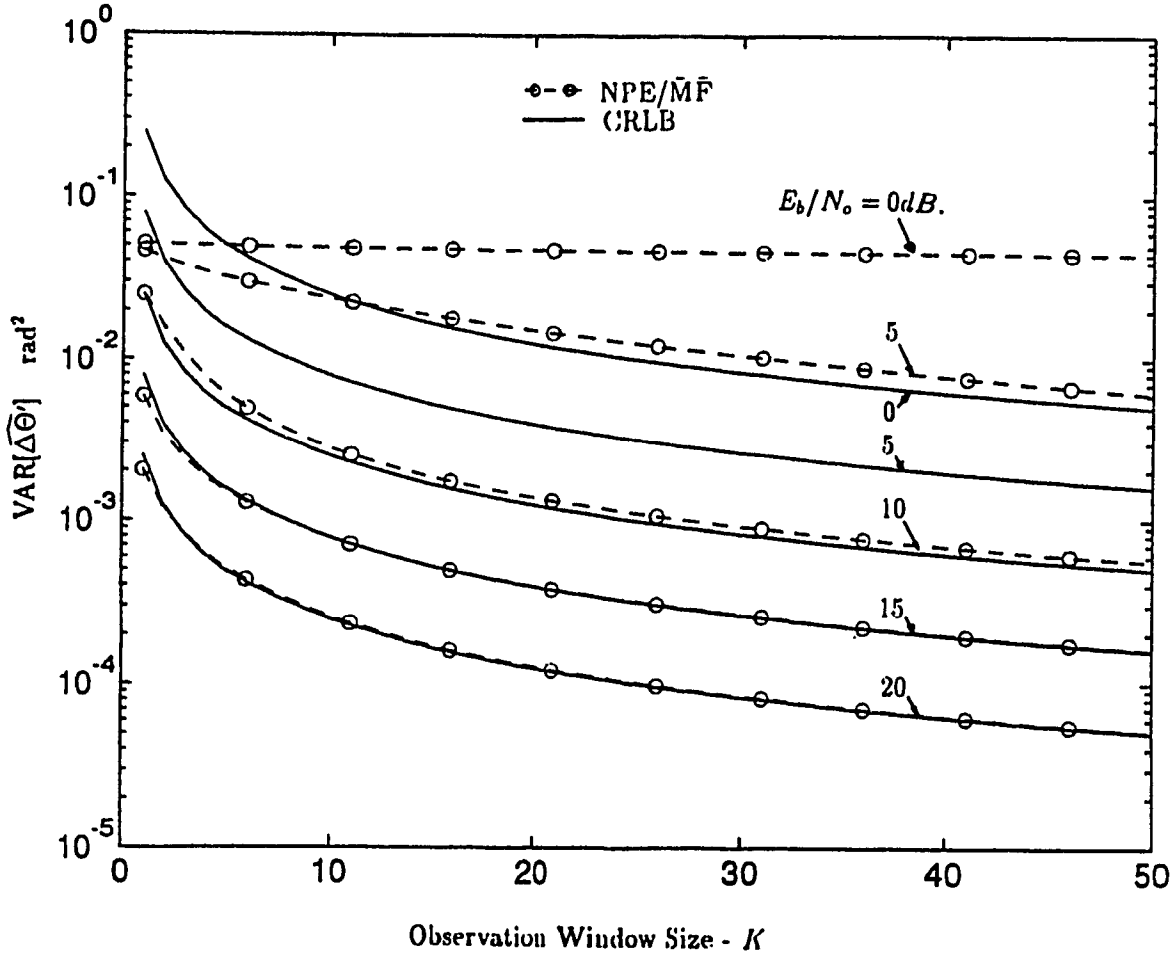

Figure 3.4: Variance of NPE/$\bar{\text{M}}\bar{\text{F}}$ for case ($\Delta f = 0$)

A side-by-side comparison of the variance of the two estimators for $\Delta f = 0$, is shown in Figure 3.5. Apparently for $\Delta f = 0$, the NPE/MF is as good as its NPE/$\bar{\text{M}}$ counterpart for $E_b/N_o > 8dB$. and for $E_b/N_o < 0dB$.. This advantage at low SNR is not considered, since neither estimator is efficient at this SNR. An additional comment must be made concerning the variance of the NPE/$\bar{\text{M}}$. We notice from Figure 3.5 that the curve has a knee at low E_b/N_o. This phenomenon has been observed through simulation, and has been documented in numerous articles [12, 25]. However the theoretical analysis presented in the paper by Viterbi and Viterbi fails to show such a characteristic. This may be attributed to the linearizing assumptions made in that paper. We therefore conclude that the method of variance analysis proposed in this thesis is more generally applicable and seems to provide results which are closer to simulation.

The true advantage of this new estimator is best displayed when considering the variance for environments where a small frequency error exists ($\Delta f T_S < 0.1$). These results are presented in Figure 3.6, for two levels of SNR. In both cases, the variance is plotted against the normalized frequency error ($\Delta f T_S$) for an observation window size of $K = 25$. Notice that at both levels of E_b/N_o, the variance of the NPE/$\bar{\text{M}}$ increases steeply with $\Delta f T_S$. In contrast, for a fixed K and E_b/N_o, the variance of the new estimator remains constant, regardless the frequency error. In other words, a crossover point exists, denoted C_o, for which the new estimator outperforms the traditional NPE/$\bar{\text{M}}$, when $\Delta f T_S > C_o$. One also concludes that C_o decreases as the signal-to-noise ratio increases, implying that this advantage is even more pronounced at this higher SNR.

3.2.2 Phase Ambiguity Resolution

The problem of phase ambiguity is due to the multiplication of the received phase by M, and then division in equations (3.4) and (3.8) by uM (recall that $u = 1$ for the NPE/$\bar{\text{M}}$ and $u = 2$ for the new estimator). To see why this problem occurs, consider

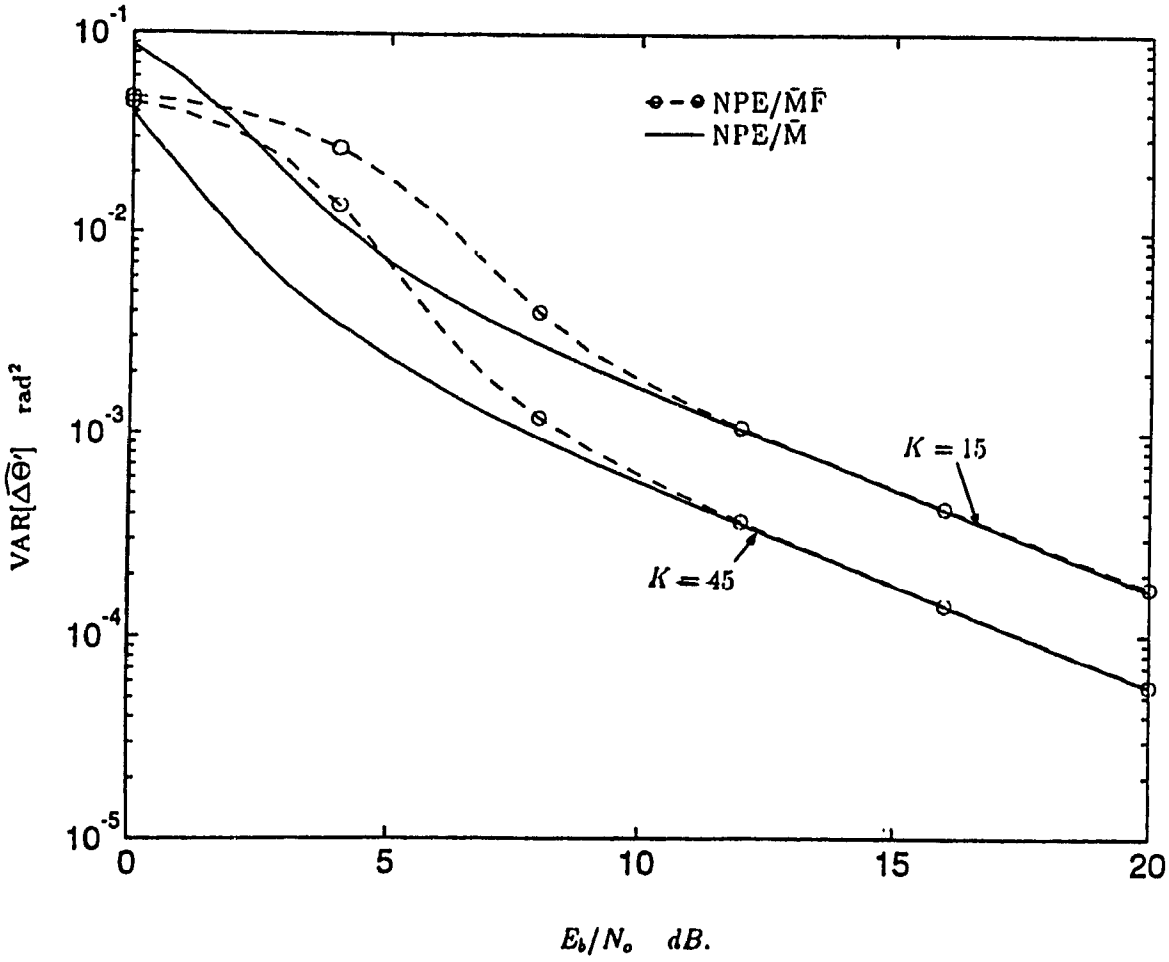

Figure 3.5: Comparison of Two Techniques for $\Delta f = 0$

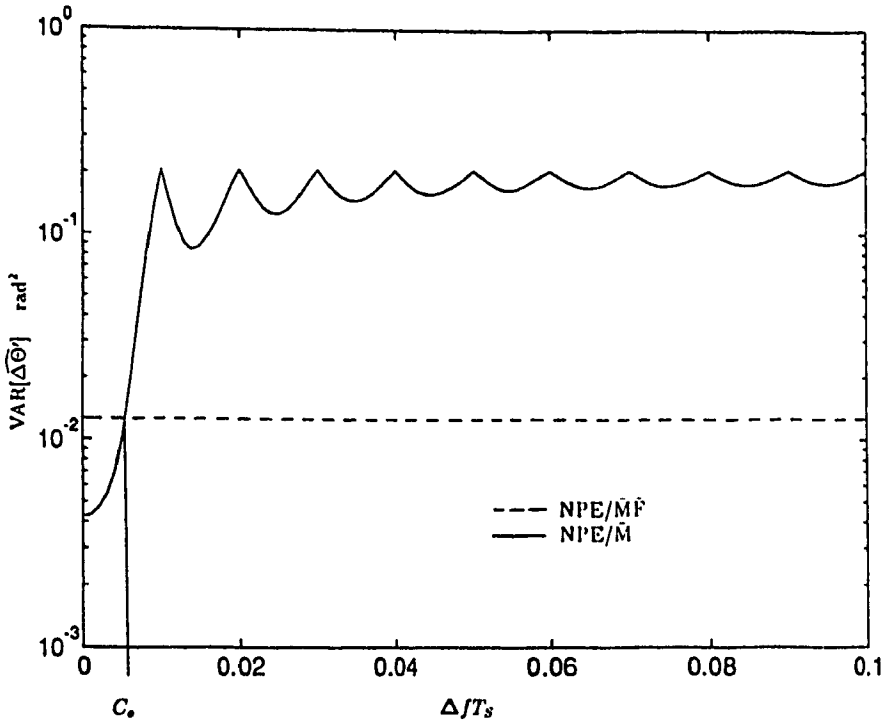

a) $E_b/N_o = 5dB$.

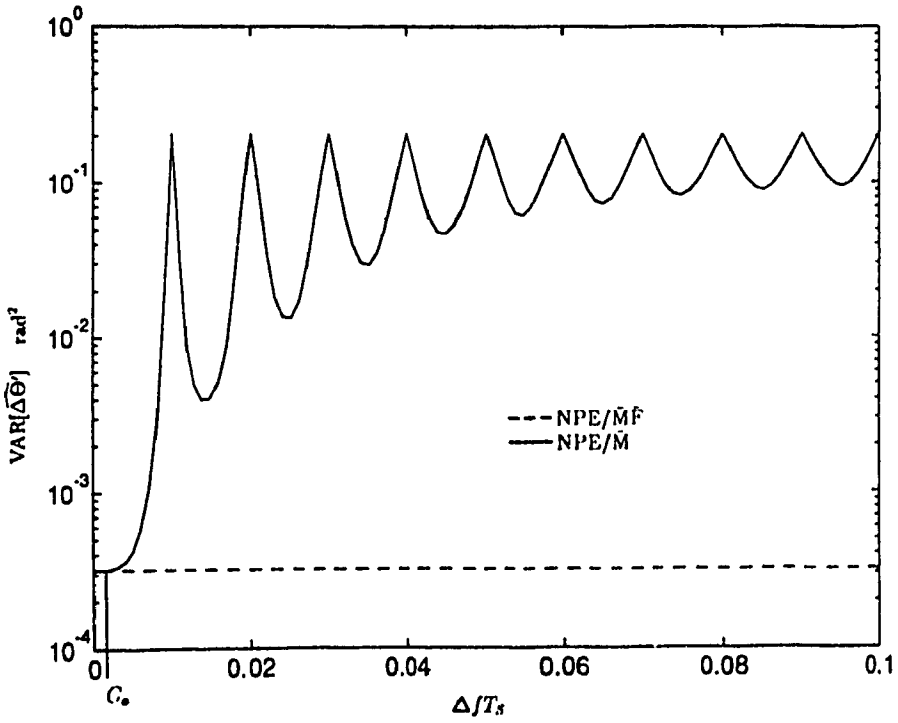

b) $E_b/N_o = 15dB$.

Figure 3.6: Variance of Phase Estimators as a Function of Frequency Error ($K = 25$)

a simple example where all angles are modulo 2π ($-\pi \leq$ angle $< \pi$), and where ϕ is linear in time (See Figure 3.7). Multiplication of ϕ by 4, and subsequent division by 4, results in the ϕ' shown. Since 4ϕ is modulo 2π, ϕ' exists only in $[-\pi/4, \pi/4)$. Therefore, ϕ' is no longer equal to $\phi \mathrm{mod}(2\pi)$ but rather to $\phi \mathrm{mod}(\pi/2)$. Notice that this implies that $\phi = (\phi' + 2\pi m/4)\mathrm{mod}(2\pi)$, where $m = 0, 1, 2, \text{or } 3$. The above is an example of 4-fold phase ambiguity. A similar situation applies to both phase error estimators. Essentially, the unknown phase ($\Delta\theta'$) is multiplied by M, and then divided by uM. Hence, the phase that is being estimated is in reality $\Delta\theta' \mathrm{mod}(2\pi/uM)$, and not $\Delta\theta' \mathrm{mod}(2\pi)$. This is intuitively satisfying, since close examination of Figures 3.1 and 3.2 shows that the obtained estimates cannot assume values outside $-\pi/uM \leq \widehat{\Delta\theta'} < \pi/uM$ (output of the arctangent operation must lie in $[-\pi, \pi)$). Therefore the estimate obtained can be written as

$$\begin{aligned} \widehat{\Delta\theta'} &= (\Delta\theta' \mathrm{mod}(2\pi/uM) + \delta \mathrm{mod}(2\pi/uM)) \,\mathrm{mod}(2\pi/uM) \\ &= (\Delta\theta' + \delta)\mathrm{mod}(2\pi/uM). \end{aligned} \tag{3.35}$$

The modulo 2π estimate (denoted $\widehat{\Delta\theta'}_a$) is then a phase rotated version of $\widehat{\Delta\theta'}$, where

$$\widehat{\Delta\theta'}_a = \left(\widehat{\Delta\theta'} + \frac{2\pi m}{uM}\right) \mathrm{mod}(2\pi) \tag{3.36}$$

and where

$$m = 0, 1, 2, 3, \ldots, \text{or } M-1 \;\&\; u = 1 \quad \text{for the NPE/}\bar{\mathrm{M}}$$
$$m = 0, 1, 2, 3, \ldots, \text{or } 2M-1 \;\&\; u = 2 \quad \text{for the NPE/}\bar{\mathrm{M}}\bar{\mathrm{F}}.$$

Notice that the new estimator exhibits $2M$-fold ambiguity, while the NPE/$\bar{\mathrm{M}}$ exhibits only M-fold phase ambiguity.

If the ambiguity is resolved correctly, then the variance results obtained in the last section apply also to the estimate $\widehat{\Delta\theta'}_a$ (*i.e.* $\mathrm{VAR}[\widehat{\Delta\Theta'}_a] = \mathrm{VAR}[\widehat{\Delta\Theta'}] = \mathrm{VAR}[\delta]$). Once the estimate $\widehat{\Delta\theta'}$ is obtained, $\widehat{\Delta\theta'}_a$ is found from (3.36) by determining the value of m. This procedure is referred to as ambiguity resolution.

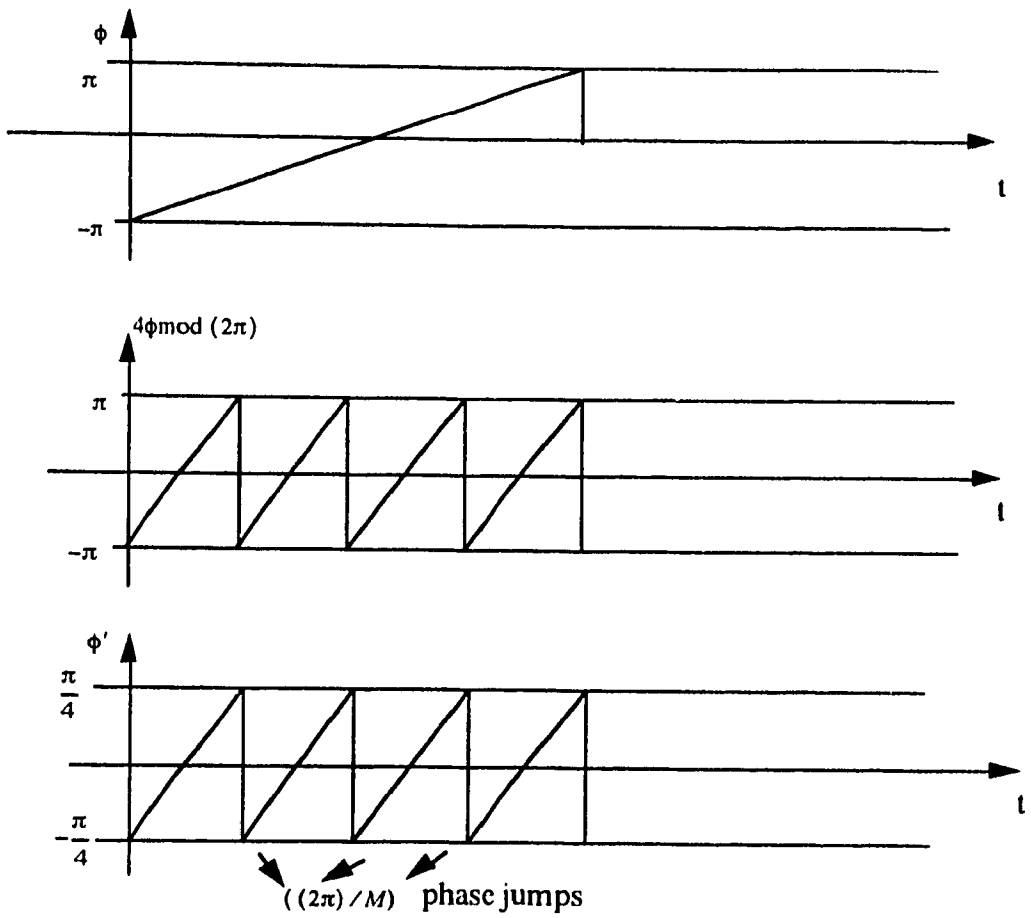

Figure 3.7: Cause of Phase Ambiguity

Before analyzing the different resolution techniques, it will prove helpful to see the effect of an ambiguous phase on a received symbol. To investigate this situation, consider the k'th symbol output of the phase rotator of Figure 2.2, which is referred to as the decision vector (DV). Since we are assuming no phase ambiguity resolution, decisions are based on this DV. The phase rotator is a device which rotates the input vector $(x_k + jy_k)$ by an amount determined by the estimators $(\widehat{\Delta\theta'} + 2\pi\widehat{\Delta f}T_S(k-l-N))$. It will be assumed that there is no noise, and as a result both estimators are exact, except for a possible phase ambiguity error which is present after phase estimation. As will be shown in Chapter 4, the frequency estimators do not suffer from ambiguity problems. Therefore,

$$x'_k + jy'_k = \sqrt{E_S}e^{j(g_k 2\pi/M + \Delta\theta' + 2\pi\Delta f T_S(k-l-N))}e^{-j(\widehat{\Delta\theta'} + 2\pi\widehat{\Delta f}T_S(k-l-N))}.$$

We know from equations (3.35) and (3.36) that for this noiseless case,

$$\begin{aligned}
\widehat{\Delta\theta'} &= \Delta\theta' \mathrm{mod}(2\pi/uM) \\
\widehat{\Delta\theta'}_a &= \Delta\theta' \mathrm{mod}(2\pi) \\
&= (\widehat{\Delta\theta'} + 2\pi m/uM)\mathrm{mod}(2\pi)
\end{aligned}$$

and so

$$\begin{aligned}
x'_k + jy'_k &= \sqrt{E_S}e^{j(g_k 2\pi/M + (\widehat{\Delta\theta'} + 2\pi m/uM)\mathrm{mod}(2\pi) - \widehat{\Delta\theta'})} \\
&= \sqrt{E_S}e^{j(g_k 2\pi/M + 2\pi m/uM)}. \qquad (3.37)
\end{aligned}$$

The last equality holds since the mod(2π) condition can be removed from the exponential. If the transmitted symbol was $g_k = i$, where $i = 0, 1, 2,$ or 3, then the DV should have phase $2\pi i/M$. However the phase ambiguity *pushes* the decision vector by $2\pi m/uM$, leading to an error if m is nonzero.

One difference between the two estimators is apparent at this point. First, let us define the *received* signal constellation as the possible locations of the DV's in the (x'_k, y'_k) signal space, when noise is absent. For the NPE/$\bar{\mathrm{M}}$, the possible shifts of

the decision vectors are multiples of $2\pi/M$, and so the received signal constellation retains its original shape, regardless the value of m (See Figure 3.8a). On the other hand, for the NPE/$\bar{\text{M}}\bar{\text{F}}$ the shifts are multiples of π/M. The signal constellation can therefore assume one of two shapes (Figure 3.8b). The expected constellation is obtained for $m = 0, 2, 4,$ or 6, while a new shape is exhibited for $m = 1, 3, 5,$ or 7.

When noise is considered (ϵ_k), the overall effect is to rotate the the DV's randomly about their nominal location, shown in Figure 3.8. The pdf of this random noise is easily determined by finding the marginal density of ϵ_k, from the joint pdf of ϵ_k and ρ_k, given in equation (3.14). The result of this operation is

$$\begin{aligned} f_{\epsilon_k}(\epsilon_k) &= \int_0^\infty f_{\rho_k,\epsilon_k}(\rho_k, \epsilon_k) d\rho_k \\ &= \frac{e^{-E_S/N_o}}{2\pi}\left\{1 + \sqrt{\frac{E_S}{N_o}}\sqrt{\pi}\cos\epsilon_k \exp\left[\frac{E_S}{N_o}\cos^2\epsilon_k\right]\right. \\ &\qquad \left.\left[1 + \text{erf}\left(\sqrt{\frac{E_S}{N_o}}\cos\epsilon_k\right)\right]\right\} - \pi \le \epsilon_k < \pi. \end{aligned} \tag{3.38}$$

A plot of this pdf is shown in Figure 3.9, for various E_b/N_o.

The two methods of resolving phase ambiguity, namely by differential detection and by unique word preambles, are analyzed below.

Differential Detection: In this first technique, the ambiguity resolution is resolved indirectly. First, the modulation is restricted to be differentially coherent PSK (DCPSK), where information is transmitted via phase changes rather than absolute modulo 2π phases . Since the phase ambiguity error is constant for every symbol within the observation window, it has no effect on the phase difference between two consecutive DV's. For differentially coherent QPSK, for example, each input symbol corresponds to a specific phase change. Therefore, all input symbols can be encoded in a phase change if an initial preamble symbol is sent. Such an encoding scheme is specified in Table 3.1.

At the receiver, a corresponding decoding scheme is required. For the encoding scheme of Table 3.1, the decoding scheme required is shown in Table 3.2. Decisions

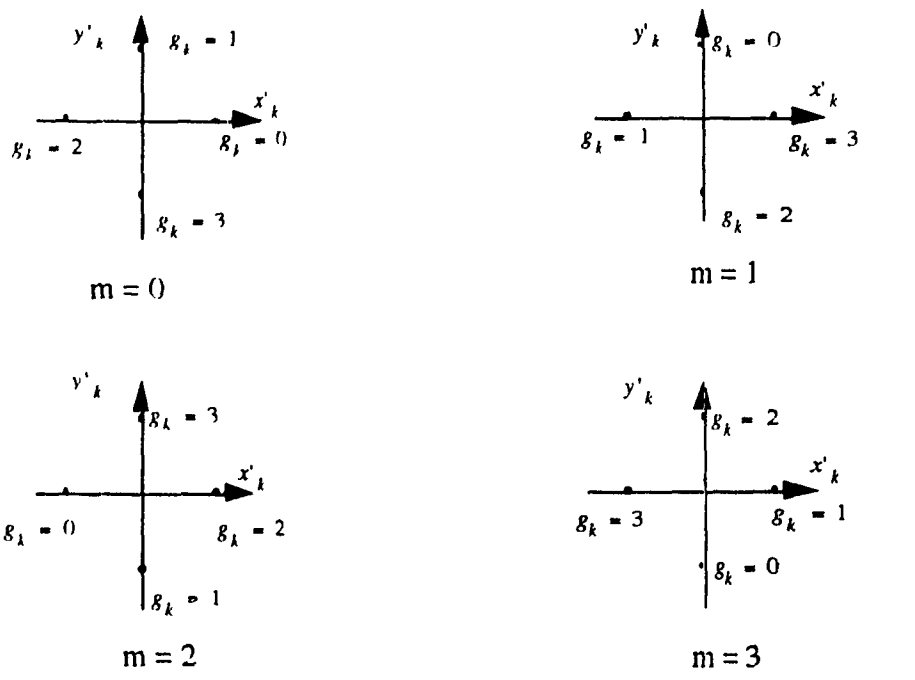

a) NPE/$\bar{M}$

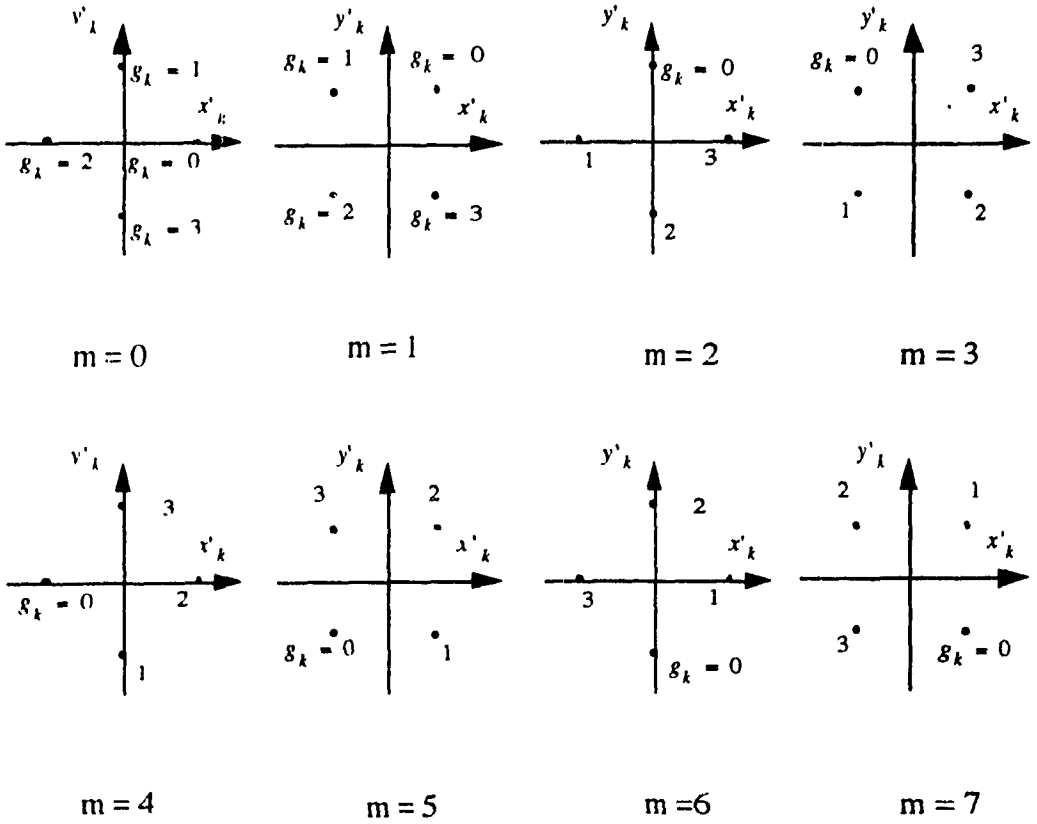

b) NPE/$\bar{M}\bar{F}$

Figure 3.8: Possible Received Signal Constellations for QPSK

Table 3.1: Typical Encoding Scheme for QPSK System

Previous Encoded Symbol	Input Symbol	New Encoded Symbol
0	0	3
0	1	1
0	2	0
0	3	2
1	0	0
1	1	2
1	2	1
1	3	3
2	0	1
2	1	3
2	2	2
2	3	0
3	0	2
3	1	0
3	2	3
3	3	1

Table 3.2: Typical Decoding Scheme for QPSK System

Previous Received Symbol	Current Received Symbol	Decoded Symbol
0	0	2
0	1	1
0	2	3
0	3	0
1	0	0
1	1	2
1	2	1
1	3	3
2	0	3
2	1	0
2	2	2
2	3	1
3	0	1
3	1	3
3	2	0
3	3	2

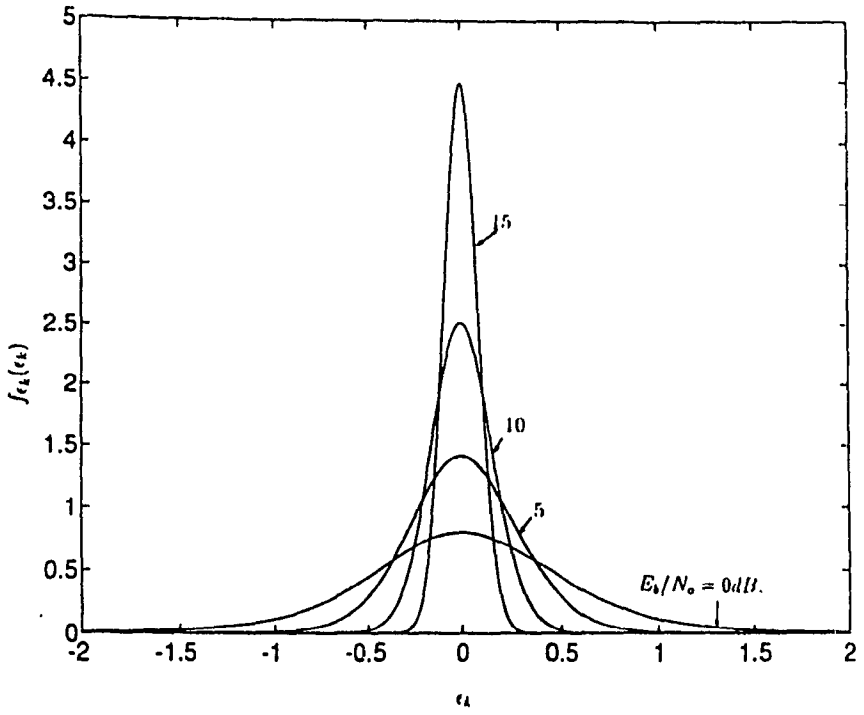

Figure 3.9: Plot of pdf of ϵ_k (for QPSK)

are made by means of a phase discriminator, and are based on the location of the DV in the receiver signal space. A QPSK phase discriminator is shown in Figure 3.10. The ML decision rule is as follows: decide transmitted symbol is g_i, if DV falls in Region i. Notice that for QPSK (as well as for any other MPSK signalling format) only the phase of the DV is important for decisions. For the moment, consider a receiver using a NPE/$\bar{\text{M}}$ producing an estimate with ambiguity $m = 2$. Furthermore, assume that the signal-to-noise ratio is quite high ($\epsilon_k \approx 0$). As a result of ambiguity, two consecutive transmitted symbols (g_i and g_{i+1}) are demodulated as $(g_i+2)\text{mod}(4)$ and $(g_{i+1}+2)\text{mod}(4)$. Although the absolute values of the symbols are incorrect, the relative difference between the two remains intact. That is, the output of decoder is independent of m (*e.g.* decoder output is 3 if consecutive input symbols are (0,2) or (1,3) or (2,0) or (3,1)).

Special consideration must be given to the NPE/$\bar{\text{M}}$. Depending on the value

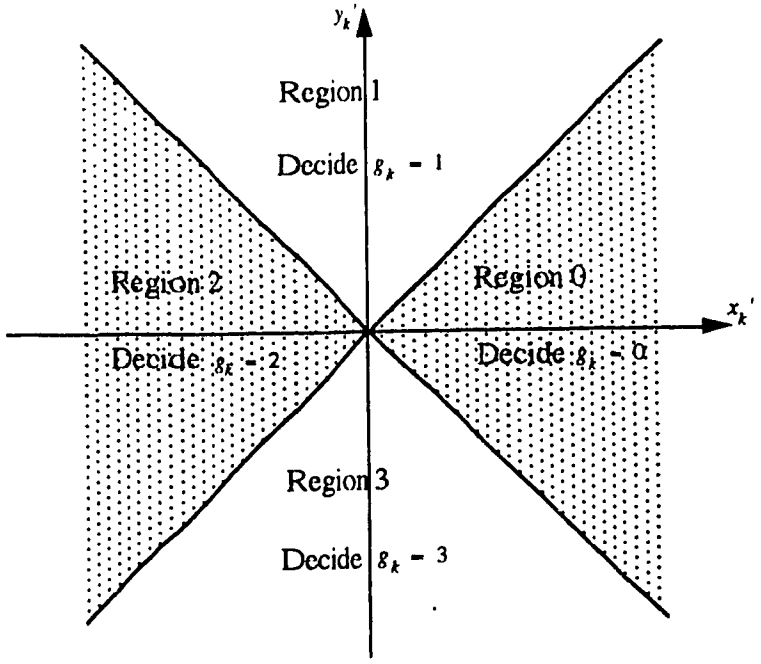

Figure 3.10: Phase Discriminator for QPSK

of m, different phase discriminators may be required. When m is even, the phase discriminator with characteristic shown in Figure 3.10 is appropriate. However when m is odd, Figure 3.8 suggests that a π/M shifted version is needed. Since the state of m (m even or odd) is not known, the receiver does not know which phase discriminator to apply when it first receives the data. To resolve this problem, the state of m must be determined. For instance, if the state is known to be even, then the phase dis riminator of Figure 3.10 can be used. Similarly, if the state is known to be odd, then the DV's can be phase rotated by an additional π/M, essentially adding a known phase ambiguity. After rotation, the resulting receiver signal constellation must be one of the m even ones. Therefore, if the state can be correctly determined, only a single phase discriminator is required.

The problem for the NPE/$\bar{\text{M}}\bar{\text{F}}$ then reduces to determining the state of m. Since this procedure uses random quantities, there is always a probability of making an error. This event will be denoted as E, and its probability as P_E.

$$\begin{aligned} P_E &= \Pr[\text{Deciding the wrong state of } m] \\ &= \Pr[\text{Decide } m \text{ is even} | m \text{ is odd}] \end{aligned}$$

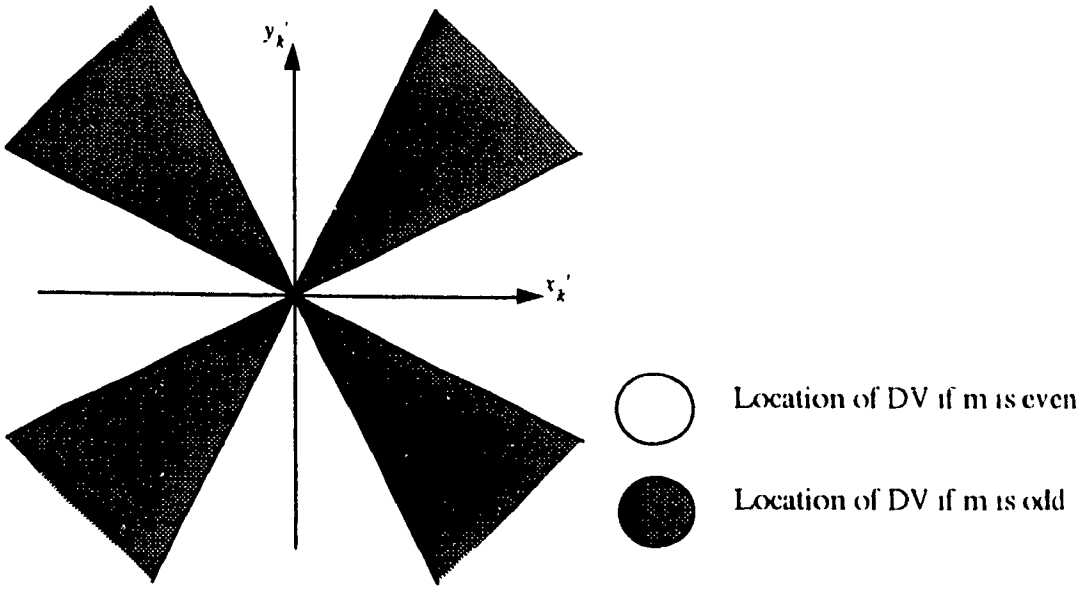

Figure 3.11: Determining State of m (for QPSK)

$$= \Pr[\text{Decide } m \text{ is odd } | m \text{ is even}].$$

To determine the state we examine the location of the $(2N+1)$ received DV's. The phase of these vectors is randomly located anywhere on the received signal space. Owing to noise, we see that each DV is rotated from its nominal point by an angle ϵ_k, whose pdf is given by (3.38). This pdf suggests that the phase of the received DV is likely to be close to the nominal point. As a result, if a received DV falls in one of the the shaded regions of Figure 3.11, then it is likely that m is odd. Obviously if ϵ_k is large, then it is possible that noise has pushed the DV into this region, and an error is made. To improve the chances of determining state, we examine the location of all $(2N+1)$ received DV's, and then apply a majority decision rule. If more than $N+1$ DV's fall into the shaded region, we say that m is odd. Otherwise, we say that m is even. An error is made on a symbol if ϵ_k is such that it pushes the DV into a region with opposite m state. This event is denoted as A, where

$$A : \{\pi/2M \leq |\epsilon_k| < 3\pi/2M \text{ or } 5\pi/2M \leq |\epsilon_k| < 7\pi/2M \text{ or } \ldots$$
$$(2M-3)\pi/2M \leq |\epsilon_k| < (2M-1)\pi/2M\}.$$

Given the pdf of ϵ_k, Pr[A] can be easily evaluated by numerical integration. That is,

$$\begin{aligned} p = \Pr[\mathrm{A}] &= \Pr[\pi/2M \le |\epsilon_k| < 3\pi/2M] + \Pr[5\pi/2M \le |\epsilon_k| < 7\pi/2M] + \cdots \\ &\quad + \Pr[(2M-3)\pi/2M \le |\epsilon_k| < (2M-1)\pi/2M]. \end{aligned} \tag{3.39}$$

If more than $N+1$ out of the K DV's result in event A, then a wrong decision about state is made. This probability is given by

$$\begin{aligned} P_E = \Pr[E] &= \sum_{k=N+1}^{2N+1} \Pr[\text{event A occurs for } k \text{ DV's}] \\ &= \sum_{k=N+1}^{2N+1} \binom{2N+1}{k} p^k (1-p)^{2N+1-k}. \end{aligned} \tag{3.40}$$

The results for P_E as a function of K are shown in Figure 3.12.

Since P_E is rather small for $E_b/N_o > 5dB.$, we can safely assume that determining the state will not affect the results of the decoding. Consequently, the only difference between the two estimators is in the added processing required to determine the state. One final note on differential detection for ambiguity resolution is required. Namely, every symbol demodulation error gives rise to two transition errors upon differential decoding. This results in an approximate doubling of the bit error rate (BER) as compared to conventional PSK systems. Thus, if one wishes to use DCPSK and obtain the same BER performance of a conventional PSK system, the transmitted signal energy must be increased by about 3 dB..

Unique Word Preamble: The second method of ambiguity resolution entails appending a small preamble to the observation window, which could then be used to uniquely determine the value of m. Consider transmitting the symbol $g_k = 0$ in a noiseless system. Depending on the value of m, the DV will land on one of its uM possible locations (See Figure 3.8a and 3.8b). For instance, if the NPE/$\bar{\mathrm{M}}$ is employed and the DV has an angle of π, then it is known that $m = 2$. Rotating the

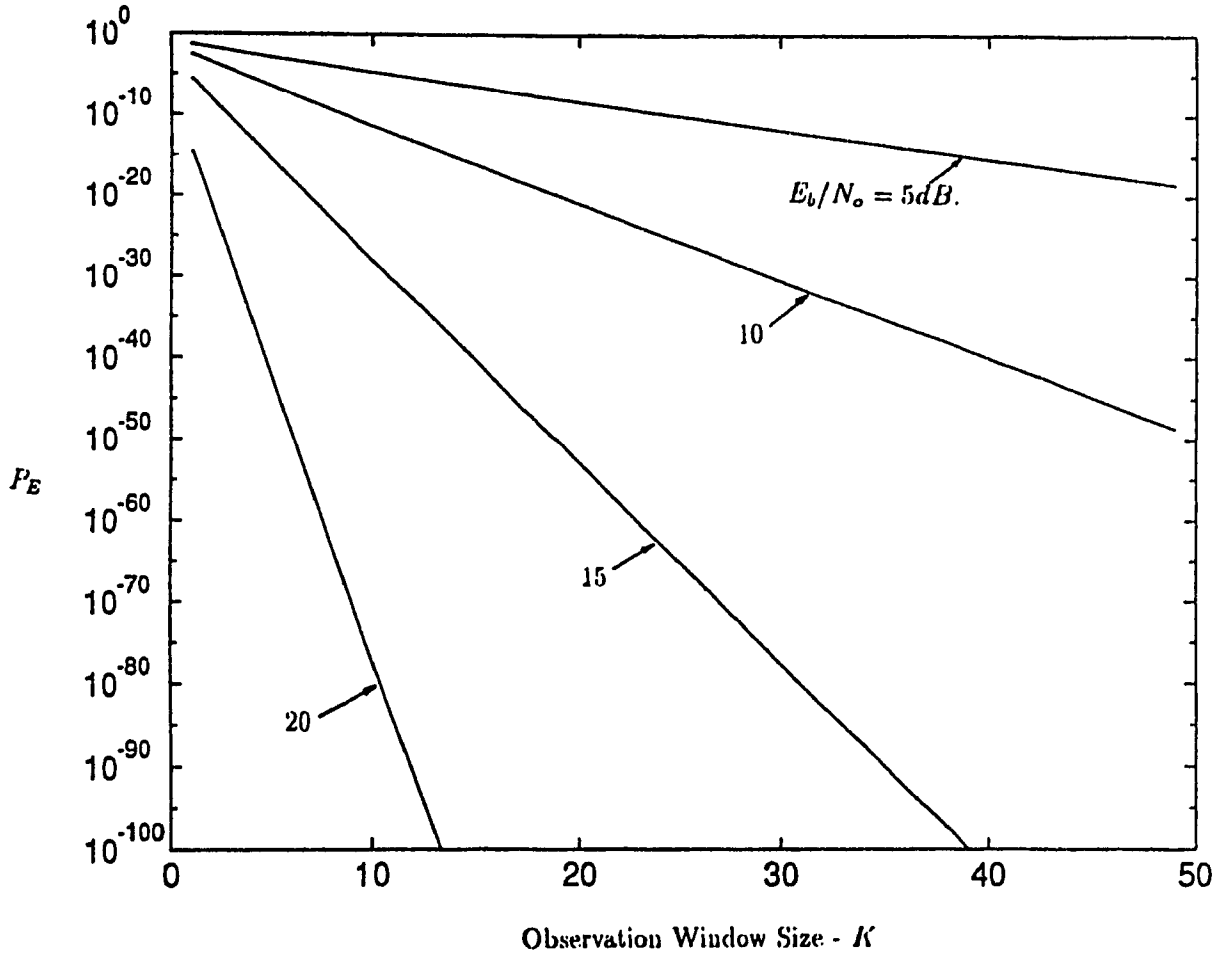

Figure 3.12: Probability of Incorrectly Determining State of m (for QPSK)

vectors of the observation window by an additional $-2\pi m/uM$ would correct the ambiguity problem, and allow for coherent detection.

Clearly, if phase noise is zero ($\epsilon_k = 0$), then a one symbol preamble is sufficient to unequivocally determine the value of m for each observation window. Unfortunately, the noise has the effect of rotating the DV's about their nominal locations. Consider the same example mentioned in the previous paragraph. The received DV should fall somewhere in region 2. However, the noise may be such that it pushes the DV into regions 0,1,or 3. In either case, the phase noise causes a region error. In addition, if the preamble includes only this symbol, then the wrong choice for m is made, leading to an ambiguity resolution error. Since every symbol is corrupted by independent noise, we could foresee transmitting an L symbol preamble per observation window, and choosing m on the basis of a majority decision, much as was done to determine the state of m. For instance, consider sending an all zero preamble. If the largest number of DV's fall into region k, we can decide that $m = k$. The increase in performance will be reflected in a decrease in the probability of ambiguity resolution error (P_{ARE}) for larger values of L.

In order to find expressions for P_{ARE}, we make the following assumption - random phase noise (ϵ_k) is such that only adjacent region errors are permitted (*i.e.* $-3\pi/M \leq |\epsilon_k| < 3\pi/M$). This assumption is made quite often in the literature, and seems quite acceptable for QPSK when $E_b/N_o > 5dB$.. Figure 3.9 implies that at this SNR, ϵ_k is only significant for $|\epsilon_k| < \pi/3$.

The L symbol preamble is decoded by the ambiguity resolution device. Of these L symbols, n_c will have $-\pi/M \leq \epsilon_k < \pi/M$ and will not produce a region error, n_{e1} will have $\pi/M \leq \epsilon_k < 3\pi/M$ and will produce a region error, and n_{e2} will have $-3\pi/M \leq \epsilon_k < -\pi/M$ also producing a region error. Since it was assumed that only adjacent region errors are possible, $|\epsilon_k|$ is never in $[3\pi/M, \pi)$. The value of m will be determined correctly if $n_c > \max(n_{e1}, n_{e2})$. Note that correction is also possible for $n_c = \max(n_{e1}, n_{e2})$. However when we have this equality, the correct m

is only chosen half the time, and so this case is not considered in the evaluation of P_{ARE}. The final expression for the NPE/M is derived in Appendix E, and the result is shown below.

$$P_{ARE} = \sum_{\forall n_c \leq \max(n_{e1}, n_{e2})} \frac{L!}{n_c! n_{e1}! n_{e2}!} p_r^{n_{e1}+n_{e2}} (1-2p_r)^{n_c} \qquad \text{:NPE/M} \qquad (3.41)$$

where

$$\begin{aligned} p_r &= \text{probability of a specific adjacent region error} \\ &= \int_{\pi/M}^{3\pi/M} f_{\epsilon_k}(x) dx. \end{aligned} \qquad (3.42)$$

For the NPE/$\bar{\text{M}}\bar{\text{F}}$, the state of m is first required prior to applying the technique outlined above. Given the state is correctly determined (event $\bar{\text{E}}$), then Pr[Ambiguity resolution error|$\bar{\text{E}}$] is as found for the NPE/$\bar{\text{M}}$. If the state is incorrectly determined, then it will be assumed that an ambiguity resolution error definitely occurs - Pr[Ambiguity resolution error|E] = 1. Consequently, by the total probability theorem,

$$\begin{aligned} P_{ARE} &= \Pr[\text{Ambiguity resolution error}|\bar{\text{E}}]\Pr[\text{E}] \\ &\quad + \Pr[\text{Ambiguity resolution error}|\text{E}]\Pr[\text{E}] \\ &= \Pr[\text{Ambiguity resolution error}|\bar{\text{E}}][1-P_E] + P_E. \end{aligned} \qquad (3.43)$$

Therefore,

$$P_{ARE} = \left[\sum_{\forall n_c \leq \max(n_{e1}, n_{e2})} \frac{L!}{n_c! n_{e1}! n_{e2}!} p_r^{n_{e1}+n_{e2}} (1-2p_r)^{n_c} \right] (1-P_E) + P_E \text{ :NPE/MF.} \qquad (3.44)$$

The results for P_{ARE} for both estimators are shown in Figure 3.13 for two values of E_b/N_o, and for $K = 25$. Given a channel SNR, these graphs can be used to determine the required L to meet a probability of ambiguity resolution error specification. It becomes apparent from the graphs that the two estimation techniques provide essentially the same performance for small preamble lengths. The only drawback

of our new estimator is the added processing required to determine the state. Note that at both levels of SNR, the curves begin to diverge as L is increased (for $L > 8$ at $E_b/N_o = 5dB.$ and for $L > 6$ at $E_b/N_o = 15dB.$) For these ranges of L, P_E in equation (3.44) becomes the dominant term. In fact, the P_E places a floor on the minimum P_{ARE} which can be obtained for the NPE/$\bar{\text{M}}\bar{\text{F}}$.

Given an L and a K, the useful information throughput per observation window can be defined as follows

$$\begin{aligned} \text{Throughput} &= \frac{\text{useful number of information symbols per observation window}}{\text{total number of symbols per observation window}} \\ &= \frac{K-L}{K}. \end{aligned}$$

The throughput reflects the fraction of the window which is used to transmit information, and should be kept as high as possible. Therefore, even though P_{ARE} decreases as L increases, this gain must be weighted against the corresponing loss in throughput.

The probability of symbol error (P_S) for coherent QPSK transmission is given by [3],

$$\begin{aligned} P_S &= \text{erfc}\left(\sqrt{E_b/N_o}\right) \\ &= 1.2 \text{ x } 10^{-2} \qquad \text{for } E_b/N_o = 5db. \\ &= 1.8 \text{ x } 10^{-15} \qquad \text{for } E_b/N_o = 15db. \end{aligned}$$

Therefore for $L > 10$, P_{ARE} is so low that it would have no effect on the symbol error probability and as a result, such high values of L are not expected to be required.

3.2.3 Cycle Skipping

Cycle skipping is a phenomenon which has received a great deal of attention for analog PLL type synchronizers [26]. On the other hand, cycle skipping for the nonlinear phase estimator has only received minor consideration in the literature.

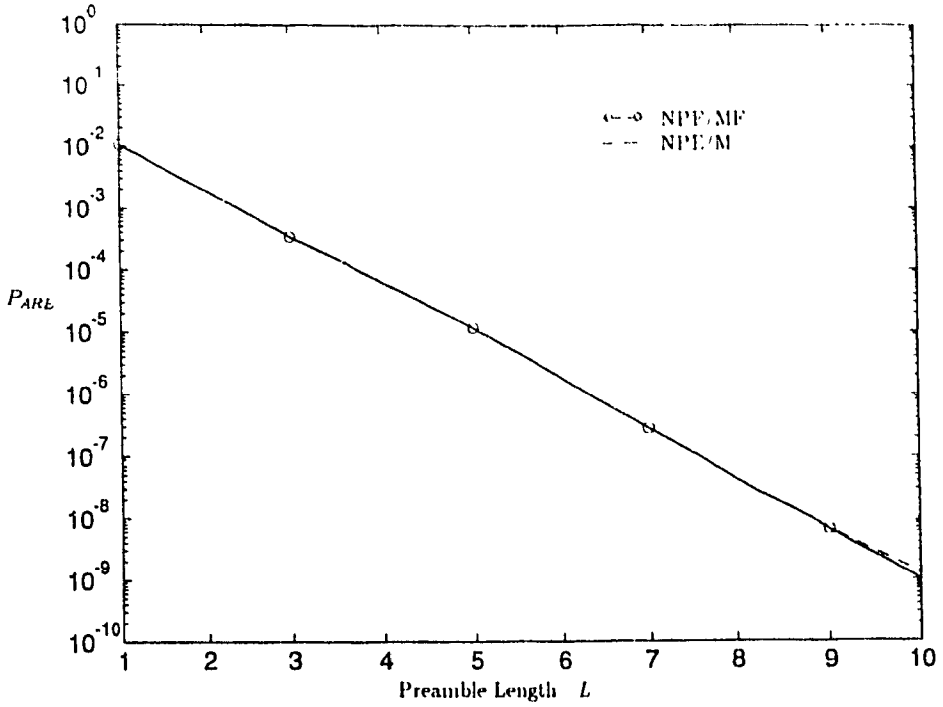

a) $E_b/N_o = 5dB$.

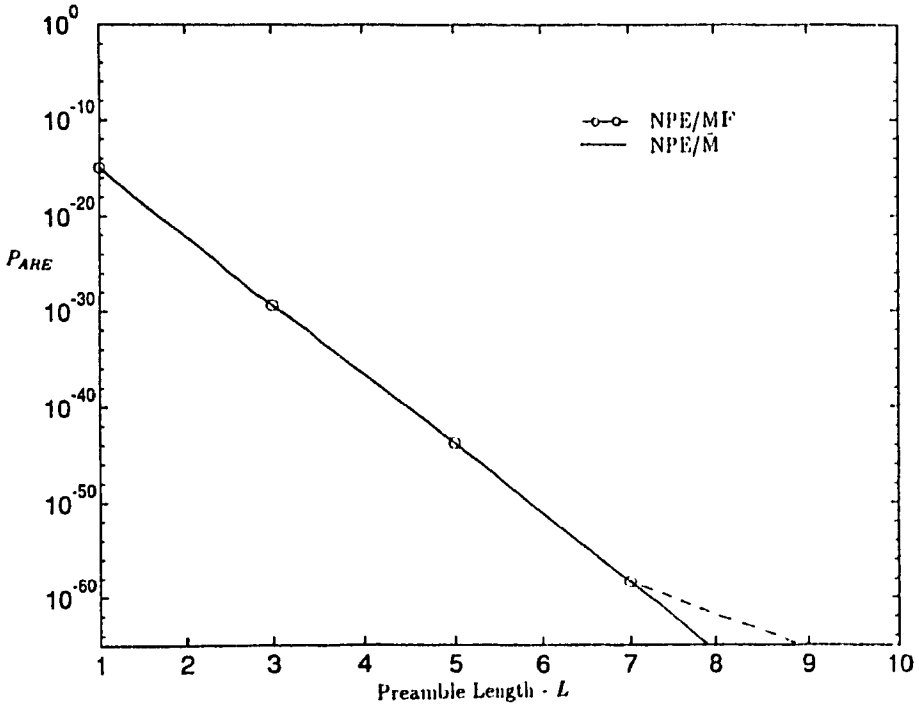

b) $E_b/N_o = 15dB$.

Figure 3.13: Probability of Ambiguity Resolution Error

The results which have been obtained were derived empirically, and thus they will not be considered here [27, 28]. Instead, the probability of cycle skipping (P_{CS}) will be found for both estimators, and then compared.

For nonlinear phase estimators, cycle skipping arises only when there are multiple estimates per burst. Essentially a cycle skip occurs when the value of m changes from one observation window to another. If some form of ambiguity resolution is used on a per window basis, then the value of m is known for every window, and no cycle skipping may occur. As a result, cycle skipping could be avoided if one of the two resolution techniques described in the last section were used for each window (See Figure 3.14)

From this figure, one may conclude that a large portion of a burst may be devoted to ambiguity resolution if a preamble is appended to every observation window. Therefore, we may inquire as to the probability of cycle skipping, given that a preamble is used only for the first window in the burst. This implies that the value of m determined for the first window is used to correct ambiguity resolution for all subsequent windows (See Figure 3.15). To determine P_{CS}, we first assume that the phases to be estimated are uncorrelated from one observation window to another. This assumption is justified, particularly when we discuss the redefined phase error $\widehat{\Delta\theta'}$. Owing to the $2\pi\Delta f T_S(l+N)$ term added to each $\Delta\theta$ for every observation window (equation (2.49)), each of the phases $\widehat{\Delta\theta'}$ can assume any value in the interval $[-\pi, \pi)$. For convenience, let us also assume that these phases are uniformly distributed. This assumption is made in much of the literature, and does seem acceptable.

Therefore, the pdf of $\Delta\Theta'$ is

$$f_{\Delta\Theta'}(\Delta\theta') = \frac{1}{2\pi} \qquad -\pi \leq \Delta\theta' < \pi. \tag{3.45}$$

Lastly, assume that m was determined to be zero for the first window. The estimate

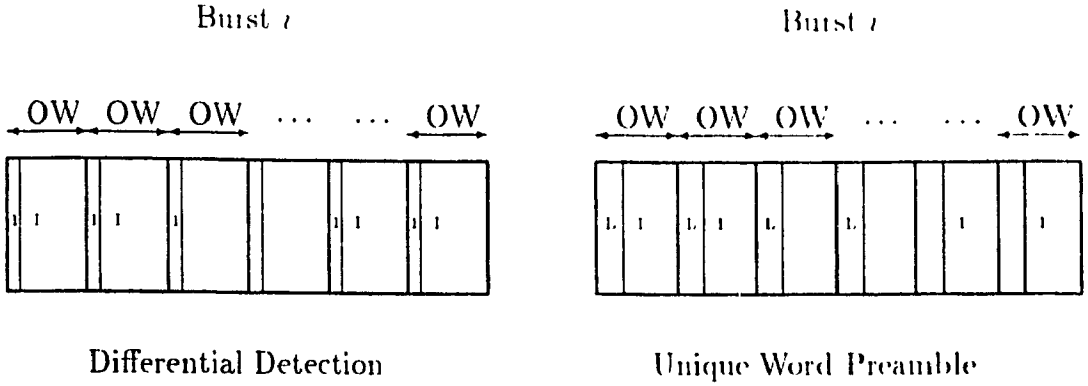

1 : one symbol preamble
L : L symbol preamble
I : Useful information part of observation window
OW: Observation Window

Figure 3.14: Ambiguity Resolution applied to each Window

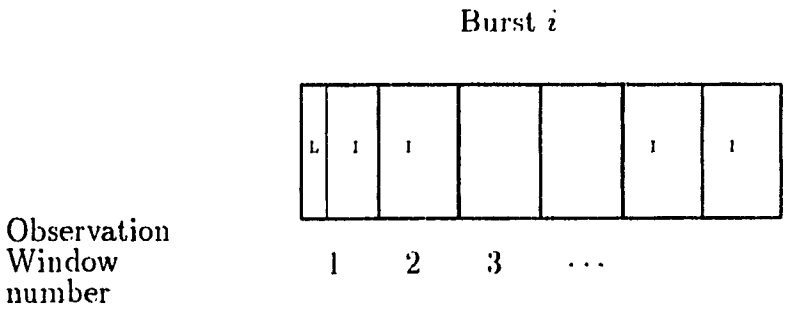

L : L symbol preamble
I : Useful information part of observation window

- m is found for observation window 1
- same m is used for windows 2,3,... in burst i

Figure 3.15: Ambiguity Resolution applied only to First Window

for this window is therefore,

$$\widehat{\Delta\theta'}(1) = \Delta\theta'(1) + \delta(1) \tag{3.46}$$

where $-\pi/uM \leq \widehat{\Delta\theta'}(1) < \pi/uM$, and where the index denotes the window number. Since $m = 0$, any subsequent estimate will also lie in $[-\pi/uM, \pi/uM)$. For the second window $\varphi \stackrel{def}{=} (\Delta\theta'(2) + \delta(2))$ can take any value. If $-\pi/uM \leq \varphi < \pi/uM$, then no cycle skip occurs since the value of m from window 1 is also valid for this window. If φ is outside this range, then a cycle skip will occur. To solve for the probability of this event, we need only find the pdf of the random variable φ. Since $\Delta\Theta'$ and δ are independent, the pdf of their sum can be found by convolving their respective pdf's [29].

$$f_\varphi(x) = f_{\Delta\Theta'}(x) * f_\delta(x) \tag{3.47}$$

where $f_{\Delta\Theta'}(x)$ is given by (3.45), and $f_\delta(x)$ is given by equation (3.24) for the NPE/$\bar{\text{M}}$ and by equation (3.29) for the NPE/$\bar{\text{M}}\bar{\text{F}}$. We need to evaluate the following integration

$$\int_{-\pi/uM}^{\pi/uM} f_\varphi(x)dx. \tag{3.48}$$

Therefore, we only require $f_\varphi(x)$ inside the interval $[-\pi/uM, \pi/uM)$. In this interval,

$$\begin{aligned} f_\varphi(x) &= \int_{x-\pi/uM}^{x+\pi/uM} \frac{1}{2\pi} f_\delta(x-\lambda)d\lambda \\ &= \frac{1}{2\pi}\int_{x-\pi/uM}^{x+\pi/uM} f_\delta(x-\lambda)d\lambda \\ &= \frac{1}{2\pi}. \end{aligned} \tag{3.49}$$

The probability of cycle skipping is equal to one minus the probability that φ is in $[-\pi/uM, \pi/uM)$. Therefore,

$$\begin{aligned}\Pr[\text{cycle skip}|m=0 \text{ for window 1}] &= 1-\Pr[-\pi/uM \le \varphi < \pi/uM] \\ &= 1-\int_{-\pi/uM}^{\pi/uM}\frac{1}{2\pi}dx \\ &= 1-\frac{1}{uM}.\end{aligned}$$

The same result applies for all assumed m for window 1, and so

$$\begin{aligned}P_{CS} &= \Pr[\text{cycle skip}|m=0 \text{ for window 1}] \\ &= 1-\frac{1}{uM}.\end{aligned} \tag{3.50}$$

If modulation is QPSK, the probability of cycle skipping is 0.75 for the NPE/M and 0.875 for our new estimator. Although the result is somewhat better for the NPE/$\bar{\text{M}}$, it remains too high to be acceptable. Consequently we have shown that both estimators require ambiguity resolution for all windows. Since this would ensure no cycle skips, neither estimator has an advantage.

3.3 Summary

When comparing the two estimators, the following points should be noted.

- In terms of cycle skipping, both estimators require ambiguity resolution for every window, and so the two estimators both have $P_{CS} = 0$.

- In terms of phase ambiguity resolution, the NPE/$\bar{\text{M}}\bar{\text{F}}$ performs about the same as the NPE/$\bar{\text{M}}$. However, it does require some additional processing to determine the state of m (regardless which resolution technique is selected). For resolution by unique word, the NPE/$\bar{\text{M}}$ shows an advantage for very large L, but such large preambles are not expected to be required to meet the specifications for P_{ARE}.

- In terms of variance, it has been shown that the new estimator performs almost as well as the NPE/$\bar{\text{M}}$ when $\Delta f = 0$. However, it outperforms this same estimator by a wide margin if a frequency error is present.

From the points listed above, we conclude that the NPE/$\bar{\text{M}}\bar{\text{F}}$ seems to be better suited for the burst-mode TDMA transmission scheme proposed.

Chapter 4

Techniques for Frequency Estimation

As mentioned in Chapter 2, the two open-loop methods for frequency error estimation to be studied in this thesis include the least-squares frequency estimator (LSFE) and the nonlinear frequency estimator (NFE). The analysis of the latter is very similar to the analysis of the phase estimators presented in the last chapter, and so the results will parallel those already shown. Since the same samples are to be used for both frequency and phase synchronizers, the frequency estimate is to be based on x_k and y_k ($l \leq k \leq l + K - 1$), given by (3.1).

4.1 Presentation of Techniques

The LSFE has already been shown to be an approximation to the ML estimate of Δf, under the condition that the estimate has small variance. The origins of this technique can be traced back to Kay, who found the LSFE for an unmodulated signal corrupted by AWGN [30]. The results were than extended by a host of others, including Bellini and Molinari, to cases with modulation [31].

With the samples as defined in (3.1), we see that because of redefinition, the

$2\pi\Delta f T_S M$ term is multiplied by $(k-l-N)$ rather than simply k (as was the case when deriving the ML estimate). Adjusting equation (2.23) to take this redefinition into account,

$$\begin{aligned}\widehat{\Delta f T_S} &= \frac{\sum_{k=l}^{l+K-1}(k-l-N)\arg(z_k{}^M)}{2\pi M\sum_{k=l}^{l+K-1}(k-l-N)^2} \\ &= \frac{\sum_{k=l}^{l+K-1}(k-l-N)(M\psi_k)\mathrm{mod}(2\pi)}{2\pi M\sum_{k=l}^{l+K-1}(k-l-N)^2}\end{aligned}$$

The modulo operation is required since the argument of $z_k{}^M$ is restricted.

To show that this estimator is in fact a LSFE, we examine $(M\psi_k)\mathrm{mod}(2\pi)$.

$$\begin{aligned}(M\psi_k)\mathrm{mod}(2\pi) &= (M(2\pi\Delta f T_S(k-l-N) - g_k 2\pi/M + \epsilon_k + \Delta\theta'))\mathrm{mod}(2\pi) \\ &= (2\pi\Delta f T_S(k-l-N)M + M\epsilon_k + M\Delta\theta')\mathrm{mod}(2\pi).\end{aligned}$$

These $(M\psi_k)\mathrm{mod}(2\pi)$ can be considered random points about a straight line with slope $2\pi\Delta f M$. Consequently, from [13], an estimate of the slope of this line is given by

$$2\pi\Delta f M = \frac{\sum_{k=l}^{l+K-1}(k-l-N)(M\psi_k)\mathrm{mod}(2\pi)}{T_S\sum_{k=l}^{l+K-1}(k-l-N)^2}$$

and so

$$\Delta f T_S = \frac{\sum_{k=l}^{l+K-1}(k-l-N)(M\psi_k)\mathrm{mod}(2\pi)}{2\pi M\sum_{k=l}^{l+K-1}(k-l-N)^2}.$$

Notice that this equation agrees exactly with that of the ML estimate of $\Delta f T_S$.

To proceed, we expand the summation in the denominator. Therefore

$$\begin{aligned}\widehat{\Delta f T_S} &= \frac{\sum_{k=l}^{l+K-1}(k-l-N)(M\psi_k)\mathrm{mod}(2\pi)}{2\pi M\frac{K(K^2-1)}{12}} \\ &= \frac{6\sum_{k=l}^{l+K-1}(k-l-N)(M\psi_k)\mathrm{mod}(2\pi)}{\pi MK(K^2-1)}. \qquad (4.1)\end{aligned}$$

From this equation, the block diagram of Figure 4.1 becomes obvious.

We can now expand ψ_k as $(2\pi\Delta f(k-l-N)T_S + \epsilon_k + \Delta\theta')$, and substitute this in equation (4.1).

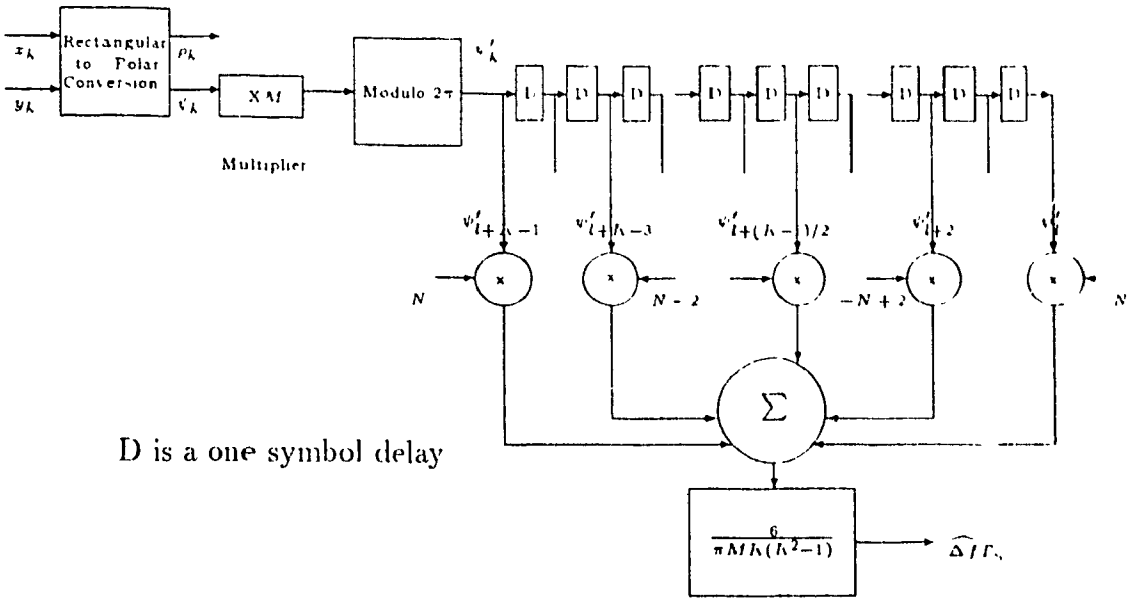

D is a one symbol delay

Figure 4.1: Least-Squares Frequency Estimator

$$\begin{aligned}\widehat{\Delta f}T_S &= \frac{6}{\pi MK(K^2-1)}\sum_{k=l}^{l+K-1}(k-l-N)(2\pi\Delta f(k-l-N)MT_S + M\epsilon_k \\ &\quad + M\Delta\theta')\mathrm{mod}(2\pi) \\ &= \frac{6}{\pi MK(K^2-1)}\sum_{k=l}^{l+K-1}((k-l-N)(2\pi\Delta f(k-l-N)MT_S + M\epsilon_k)\mathrm{mod}(2\pi) \\ &\quad + (k-l-N)(M\Delta\theta')\mathrm{mod}(2\pi)) \\ &= \frac{6}{\pi MK(K^2-1)}\sum_{k=l}^{l+K-1}(k-l-N)(2\pi\Delta f(k-l-N)MT_S + M\epsilon_k)\mathrm{mod}(2\pi) \quad (4.2)\end{aligned}$$

Even though the $(M\psi_k)\mathrm{mod}(2\pi)$ are dependent on the phase error, from equation (4.2) we see that the estimate of the normalized frequency error is not. Amazingly, symmetric windows remove the dependence on $\Delta\theta'$. Therefore, this implies that the ML estimate of frequency reduces to the LSF estimate not only in cases where $\Delta\theta = 0$, but in any and every case, provided the samples are symmetrically redefined.

At this point, we will assume that $(M\psi_k)\mathrm{mod}(2\pi)$ has no phase jumps. Therefore, $M\psi_k$ is restricted to $[-\pi, \pi)$, and so we can remove the $\mathrm{mod}(2\pi)$ operation. A discussion about the validity of this assumption appears at the end of this section.

Equation (4.2) reduces to

$$\begin{aligned}\widehat{\Delta fT_S} &= \frac{6M}{\pi M K(K^2-1)}\left[\sum_{k=l}^{l+K-1}(k-l-N)^2 2\pi\Delta fT_S + \sum_{k=l}^{l+K-1}(k-l-N)\epsilon_k\right] \\ &= \Delta fT_S + \frac{6}{\pi K(K^2-1)}\sum_{k=l}^{l+K-1}(k-l-N)\epsilon_k \qquad (4.3)\end{aligned}$$

This is the equation which will be used to determine the moments of $\widehat{\Delta FT_S}$.

In contrast, the NFE (Figure 4.2) operates on a totally different principle. Essentially, the frequency error is converted to a constant phase error by some nonlinear operation. First, the samples are passed through a rectangular-to-polar conversion block (again) . Then the phase is multiplied by M while the magnitude undergoes some nonlinear transformation ($p_3()$). The use of p_3 reflects the fact that this operation need not be the same as that used by either phase estimator. The result is then converted back into rectangular form yielding $\mathcal{Y}_k$, where

$$\begin{aligned}\mathcal{Y}_k &= p_3(\rho_k)e^{jM\psi_k} \\ &= p_3(\rho_k)\cos(M\psi_k) + jp_3(\rho_k)\sin(M\psi_k). \qquad (4.4)\end{aligned}$$

A second operation is then performed on $\mathcal{Y}_k$, in order to generate samples $\mathcal{Y}''_k$ which are dependent only on $2\pi\Delta fT_SM$ and noise. To determine this operation, consider two consecutive $\mathcal{Y}_k$'s. That is,

$$\begin{aligned}\mathcal{Y}_k &= p_3(\rho_k)e^{j(2\pi\Delta fT_S(k-l-N)M+M\Delta\theta'+M\epsilon_k)} \\ \mathcal{Y}_{k+1} &= p_3(\rho_{k+1})e^{j(2\pi\Delta fT_S(k-l-N)M+2\pi\Delta fT_SM+M\Delta\theta'+M\epsilon_{k+1})}.\end{aligned}$$

Notice that a suitable $\mathcal{Y}''_r$ could be obtained by multiplying $\mathcal{Y}_{l+2r+1}$ with the complex conjugate of $\mathcal{Y}_{l+2r}$. The result of this multiplication is,

$$\begin{aligned}\mathcal{Y}''_r &= \mathcal{Y}^*_{l+2r}\mathcal{Y}_{l+2r+1} \\ &= p_3(\rho_{l+2r})p_3(\rho_{l+2r+1})e^{j(2\pi\Delta fT_SM+M\epsilon_{l+2r+1}-M\epsilon_{l+2r})} \quad 0\le r<N. \qquad (4.5)\end{aligned}$$

Since $2\pi\Delta fT_SM$ can be treated as a constant for all r, we can use an averaging technique similar to the one used for the phase estimators. Namely

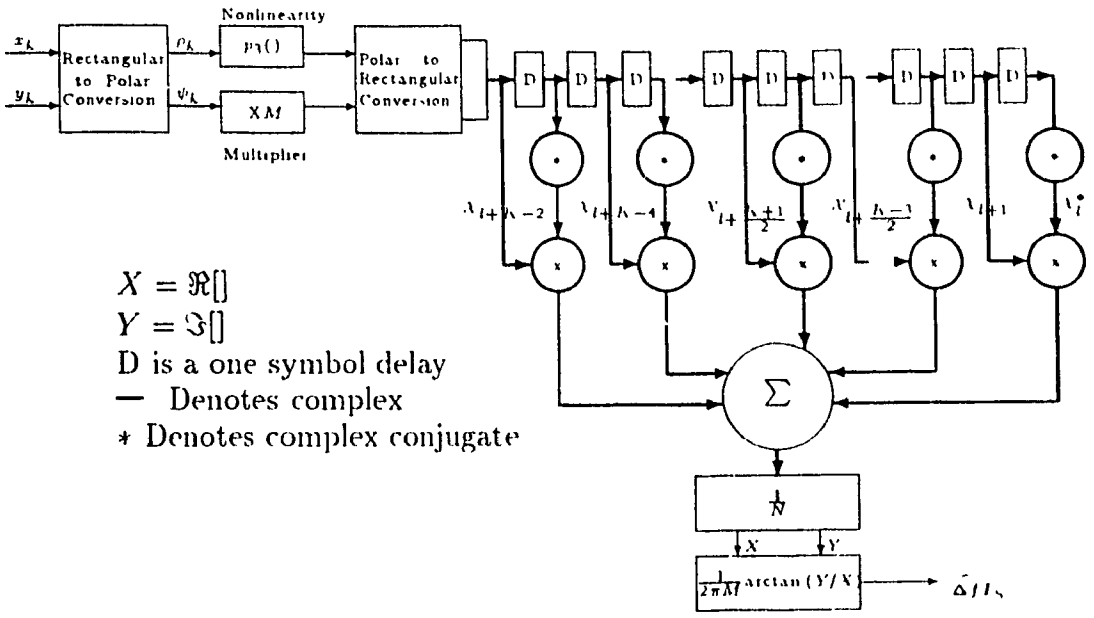

Figure 4.2: Nonlinear Frequency Estimator

$$
\begin{aligned}
2\pi\widehat{\Delta f}T_S M &= \arctan\left[\frac{\frac{1}{N}\sum_{r=0}^{N-1} p_3(\rho_{l+2r})p_3(\rho_{l+2r+1})\sin(2\pi\Delta f T_S M + M\theta_{l+2r+1} - M\theta_{l+2r})}{\frac{1}{N}\sum_{r=0}^{N-1} p_3(\rho_{l+2r})p_3(\rho_{l+2r+1})\cos(2\pi\Delta f T_S M + M\theta_{l+2r+1} - M\theta_{l+2r})}\right] \\
&= 2\pi\Delta f T_S M + \arctan\left[\frac{\frac{1}{N}\sum_{r=0}^{N-1} p_3(\rho_{l+2r})p_3(\rho_{l+2r+1})\sin(M\theta_{l+2r+1} - M\theta_{l+2r})}{\frac{1}{N}\sum_{r=0}^{N-1} p_3(\rho_{l+2r})p_3(\rho_{l+2r+1})\cos(M\theta_{l+2r+1} - M\theta_{l+2r})}\right] \\
\widehat{\Delta f}T_S &= \Delta f T_S + \frac{1}{2\pi M}\arctan\left[\frac{\frac{1}{N}\sum_{r=0}^{N-1} p_3(\rho_{l+2r})p_3(\rho_{l+2r+1})\sin(M\theta_{l+2r+1} - M\theta_{l+2r})}{\frac{1}{N}\sum_{r=0}^{N-1} p_3(\rho_{l+2r})p_3(\rho_{l+2r+1})\cos(M\theta_{l+2r+1} - M\theta_{l+2r})}\right] \qquad (4.6) \\
&= \Delta f T_S + \text{degradation}(\rho_k, \epsilon_k \text{ for } l \le k \le l+K-1) \qquad (4.7)
\end{aligned}
$$

Notice that equation (4.6) bears a strong similarity to equation (3.6) for the NPE/MF.

As with the phase estimators, expressions for the total processing time can also be obtained. Note that the NFE has a complex conjugate operation, which can be combined with the complex multiplication operation $((a+jb)(c+jd)^* =$

$(ac + bd) + j(bc - ad)$). Therefore, the total processing times are shown below

$$\begin{aligned} T_P &= (K-1)T_A + (K+1)T_M + T_{LU} \qquad \text{:LSFE} \\ T_P &= (2K-4)T_A + 2KT_M + 2T_{LU} \qquad \text{:NFE} \end{aligned}$$

4.2 Comparison of Techniques

4.2.1 Moment Analysis

For the LSFE, the moment analysis is straightforward. The mean of $\widehat{\Delta FT_S}$ is calculated below.

$$\begin{aligned} \mathrm{E}[\widehat{\Delta FT_S}] &= \mathrm{E}\left[\Delta f T_S + \frac{6}{\pi K(K^2-1)} \sum_{k=l}^{l+K-1} (k-l-N)\epsilon_k\right] \\ &= \Delta f T_S + \frac{6}{\pi K(K^2-1)} \sum_{k=l}^{l+K-1} (k-l-N)\mathrm{E}[\epsilon_k] \\ &= \Delta f T_S. \end{aligned} \tag{4.8}$$

The last step is possible since the expected value of random variable ϵ_k is zero. Equation (4.8) suggests that the LSFE is unbiased. Owing to results which will be presented later, we do not state this with certainty. The variance of the estimate is

$$\begin{aligned} \mathrm{VAR}[\widehat{\Delta FT_S}] &= \mathrm{E}[(\widehat{\Delta FT_S} - \Delta f T_S)^2] \\ &= \frac{36}{\pi^2 K^2(K^2-1)^2} \mathrm{E}\left[\sum_{k=l}^{l+K-1} (k-l-N)\epsilon_k \sum_{j=l}^{l+K-1} (j-l-N)\epsilon_j\right] \\ &= \frac{36}{\pi^2 K^2(K^2-1)^2} \sum_{k=l}^{l+K-1}\sum_{j=l}^{l+K-1} (k-l-N)(j-l-N)\mathrm{E}[\epsilon_k\epsilon_j] \\ &= \frac{36}{\pi^2 K^2(K^2-1)^2} \sum_{k=l}^{l+K-1} (k-l-N)^2\sigma_\epsilon^2 \\ &= \frac{3\sigma_\epsilon^2}{\pi^2 K(K^2-1)} \end{aligned} \tag{4.9}$$

where σ_ϵ^2 is the variance of each of the ϵ_k. This variance can be found from numerical integration of $f_{\epsilon_k}(\epsilon_k)$. Substitution into (4.9) would then give us the desired quantity.

A plot of this variance for various E_b/N_o is shown in Figure 4.3. The graph also shows a plot of the CRLB, and as expected, the LSFE has a variance very close to this bound. Note that this ensures that the variance is small, and so the approximation made in Chapter 2 ($\widehat{\Delta f} \approx \Delta f$) is justified.

To determine the variance of the NFE, we return to the analysis technique presented in Chapter 3. First, the degradation is defined as

$$\delta = \frac{1}{2\pi M} \arctan\left[\frac{\frac{1}{N}\sum_{r=0}^{N-1} p_3(\rho_{l+2r})p_3(\rho_{l+2r+1})\sin\left(M\epsilon_{l+2r+1} - M\epsilon_{l+2r}\right)}{\frac{1}{N}\sum_{r=0}^{N-1} p_3(\rho_{l+2r})p_3(\rho_{l+2r+1})\cos\left(M\epsilon_{l+2r+1} - M\epsilon_{l+2r}\right)}\right].$$

Again the CLT is invoked and both the numerator and denominator of the arctangent function are treated as Gaussian random variables, denoted respectively as ξ and η. Therefore,

$$\delta = \frac{1}{2\pi M} \arctan\left[\frac{\xi}{\eta}\right] \tag{4.10}$$

$$\xi = \frac{1}{N}\sum_{r=0}^{N-1} p_3(\rho_{l+2r})p_3(\rho_{l+2r+1})\sin\left(M\epsilon_{l+2r+1} - M\epsilon_{l+2r}\right) \tag{4.11}$$

$$\eta = \frac{1}{N}\sum_{r=0}^{N-1} p_3(\rho_{l+2r})p_3(\rho_{l+2r+1})\cos\left(M\epsilon_{l+2r+1} - M\epsilon_{l+2r}\right). \tag{4.12}$$

The moments of ξ and η are found in Appendix C. The results are

$$\mu_\xi = 0 \tag{4.13}$$

$$\sigma_\xi^2 = \frac{\mathrm{E}^2[{p_3}^2(\rho)]}{2N} - \frac{\mathrm{E}^2[{p_3}^2(\rho)\cos(2M\epsilon)]}{2N} \tag{4.14}$$

$$\mu_\eta = \mathrm{E}^2[p_3(\rho)\cos(M\epsilon)] \tag{4.15}$$

$$\sigma_\eta^2 = \frac{\mathrm{E}^2[{p_3}^2(\rho)]}{2N} + \frac{\mathrm{E}^2[{p_3}^2(\rho)\cos(2M\epsilon)]}{2N} - \frac{\mathrm{E}^4[p_3(\rho)\cos(M\epsilon)]}{N} \tag{4.16}$$

$$\mathrm{COV}[\xi,\eta] = 0. \tag{4.17}$$

The pdf of δ is found to be

$$f_\delta(\delta) = Me^{-\mu_\eta^2/2\sigma_\eta^2}\frac{\sigma_\eta\sigma_\xi}{\sigma_\eta^2\sin^2(2\pi M\delta)+\sigma_\xi^2\cos^2(2\pi M\delta)}\left\{1+\frac{\mu_\eta}{\sqrt{2}\sigma_\eta}\sqrt{\pi}\sqrt{\frac{\sigma_\xi^2\cos^2(2\pi M\delta)}{\sigma_\eta^2\sin^2(2\pi M\delta)+\sigma_\xi^2\cos^2(2\pi M\delta)}}\right.$$
$$\left.\exp\left[\frac{\mu_\eta^2}{2\sigma_\eta^2}\frac{\sigma_\xi^2\cos^2(2\pi M\delta)}{\sigma_\eta^2\sin^2(2\pi M\delta)+\sigma_\xi^2\cos^2(2\pi M\delta)}\right]\left[1+\mathrm{erf}\left(\frac{\mu_\eta}{\sqrt{2}\sigma_\eta}\sqrt{\frac{\sigma_\xi^2\cos^2(2\pi M\delta)}{\sigma_\eta^2\sin^2(2\pi M\delta)+\sigma_\xi^2\cos^2(2\pi M\delta)}}\right)\right]\right\}$$
$$-1/2M \le \delta < 1/2M \tag{4.18}$$

where μ_η, σ_η^2, and σ_ξ^2 are defined in equations (4.14) to (4.16).

The mean and variance of $\widehat{\Delta FT_S}$ can be obtained by noting that

$$\widehat{\Delta FT_S} = \Delta fT_S + \delta \ .$$

Therefore,

$$\begin{aligned} \mathrm{E}[\widehat{\Delta FT_S}] &= \Delta fT_S + \mathrm{E}[\delta] \\ &= \Delta fT_S \ . \end{aligned}$$

Consequently, the variance of $\widehat{\Delta FT_S}$ is equal to the variance of δ. This latter variance can be determined by numerically integrating $x^2 f_\delta(x)$ over the entire range of δ. Recall that the three terms μ_η, σ_η^2, and σ_ξ^2 are given by equations((3.32)-(3.34)). Numerical results are obtained only for the case $p_3(\rho) = \rho^0$. The variance is shown in Figure 4.4.

A side-by-side comparison of the two estimators is shown in Figure 4.5, for observation window lengths of 15 and 45.

In terms of variance, the better estimator seems obvious, since Figure 4.5 suggests an advantage for the LSFE (by almost three orders of magnitude). However, these results are somewhat misleading since much of this advantage is often lost. Recall that in deriving the LSF estimate, we assumed that the $M\psi_k (\stackrel{def}{=} \psi_k')$ did not exhibit phase jumps. However, this assumption is violated for most systems. Over the entire observation window, the phase ψ_k' changes by about $2\pi\Delta fT_S MK$. Even if ΔfT_S is small, the multiplication by KM will almost always ensure at least one phase jump. When phase jumps do occur, the ψ_k' must be corrected prior to using the technique of Figure 4.1 (See Figure 4.6). Unfortunately the noise in the ψ_k' can be so large ($M\epsilon_k$), that no correction procedure is full proof.

To examine the effects of an incorrect 2π phase jump, consider a single error for symbol $k = l + K - 1$ (last symbol in window). The estimator of Figure 4.1

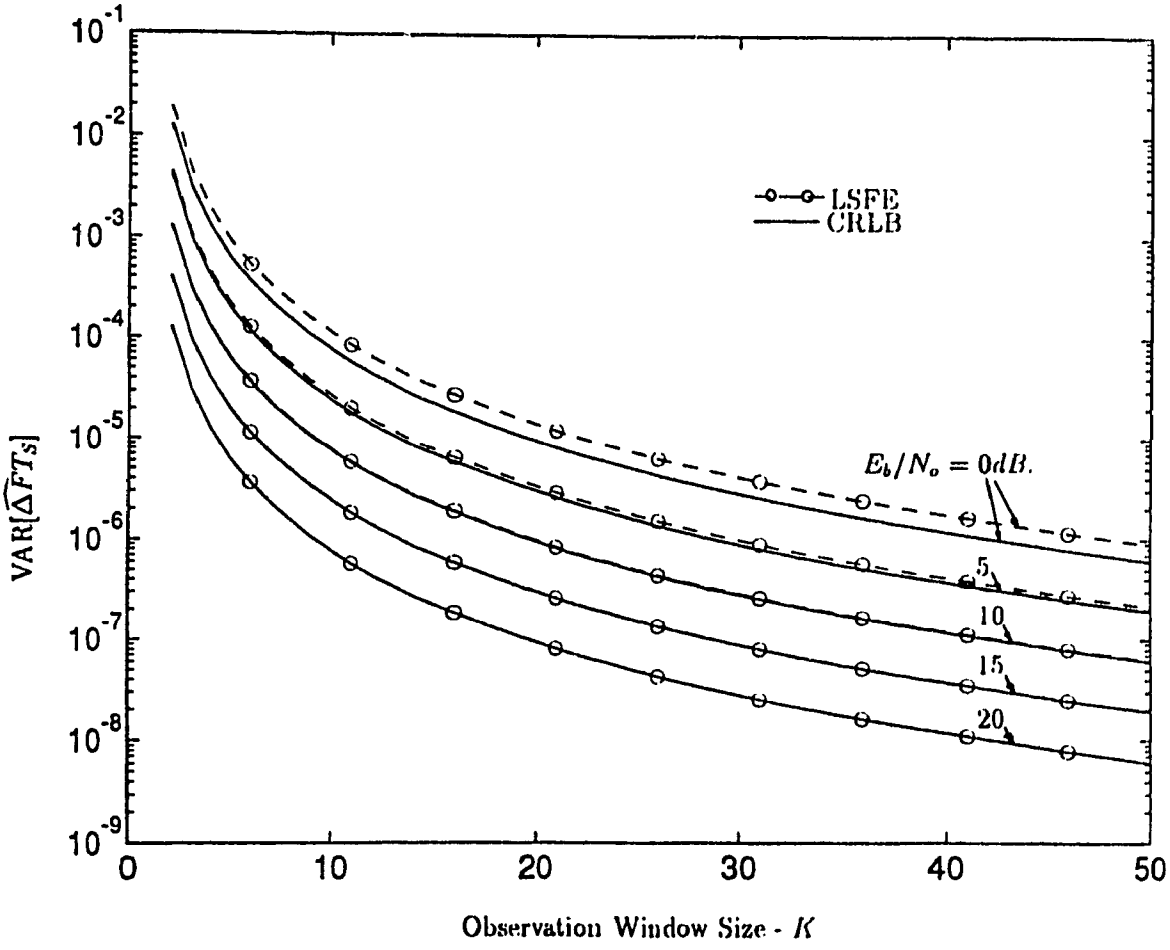

Figure 4.3: Variance of Least-Squares Frequency Estimator

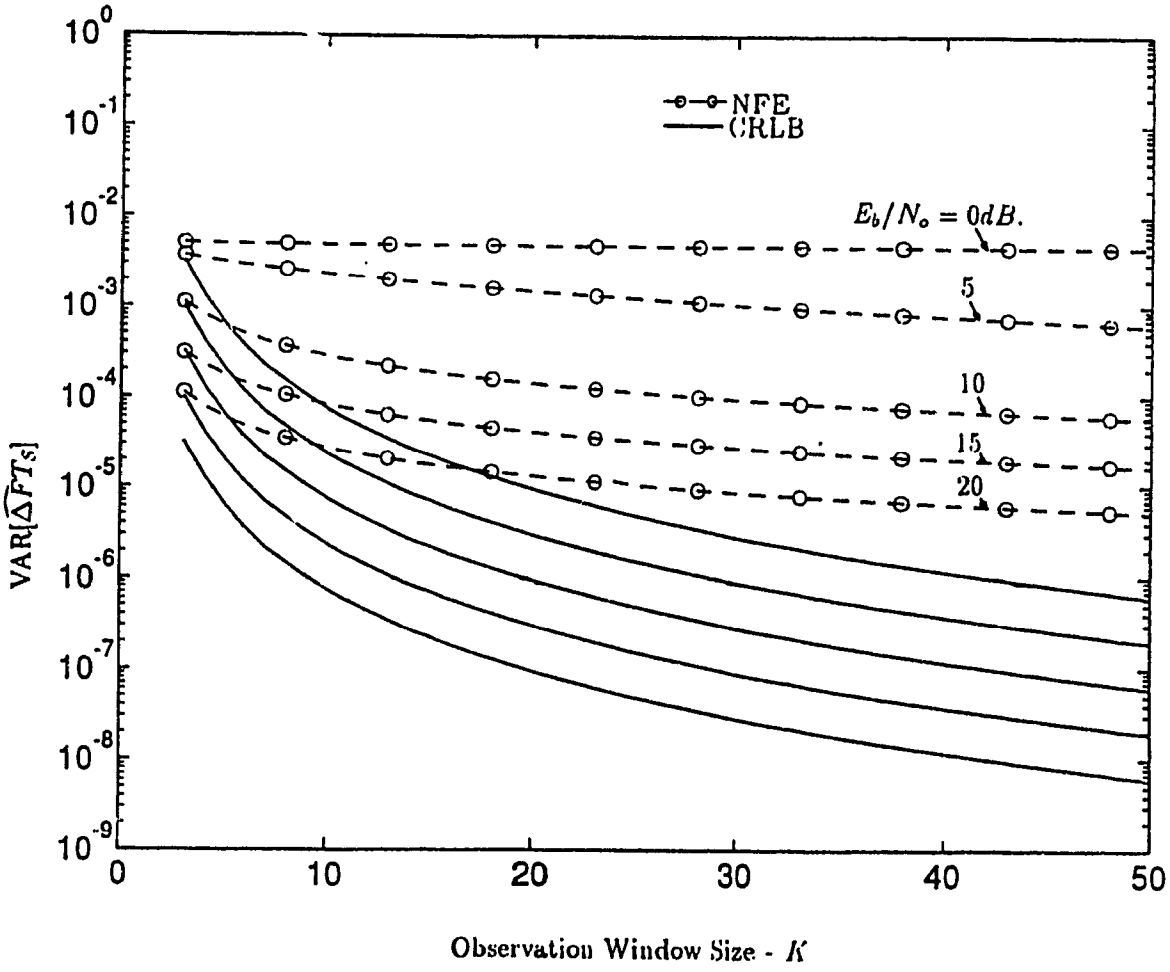

Figure 4.4: Variance of Nonlinear Frequency Estimator

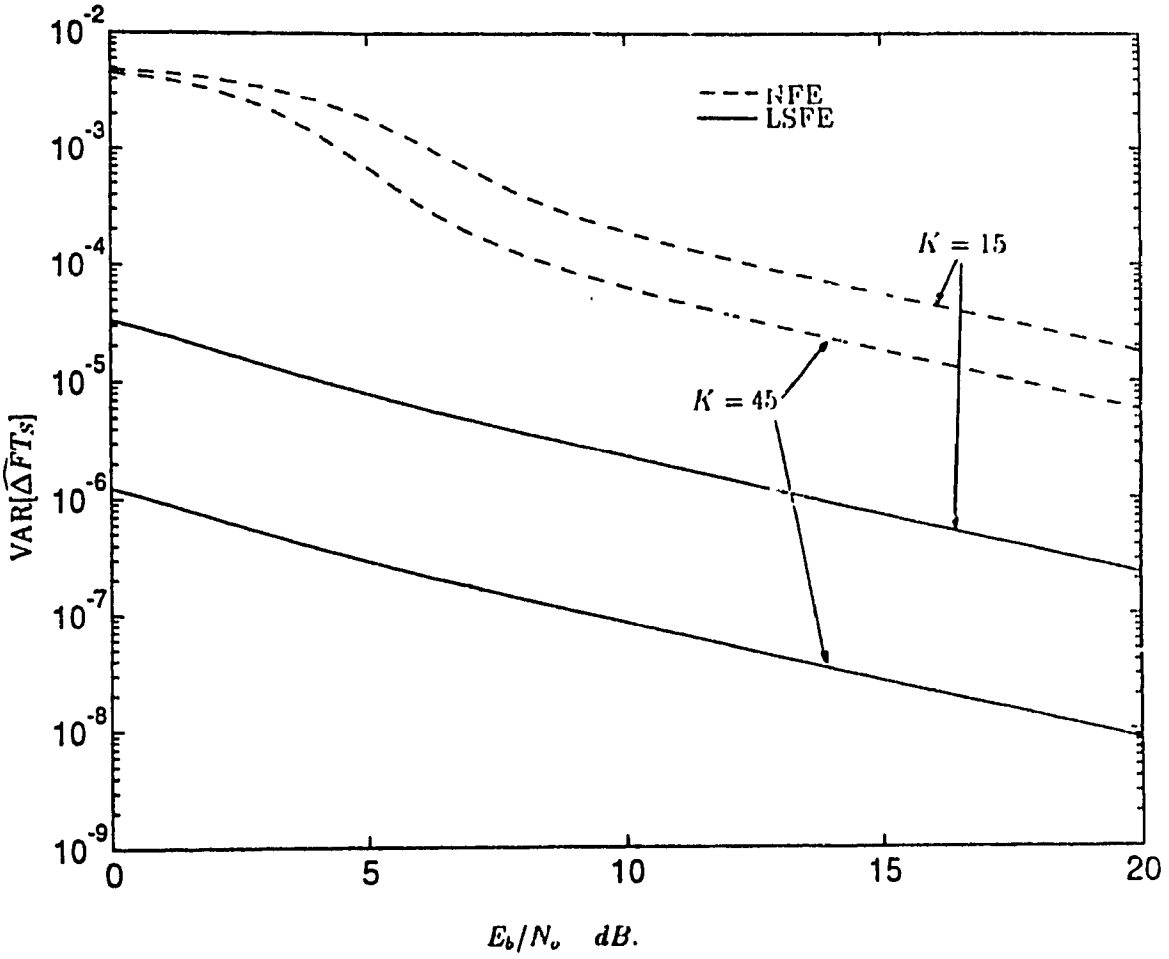

Figure 4.5: Comparison of Two Frequency Estimators

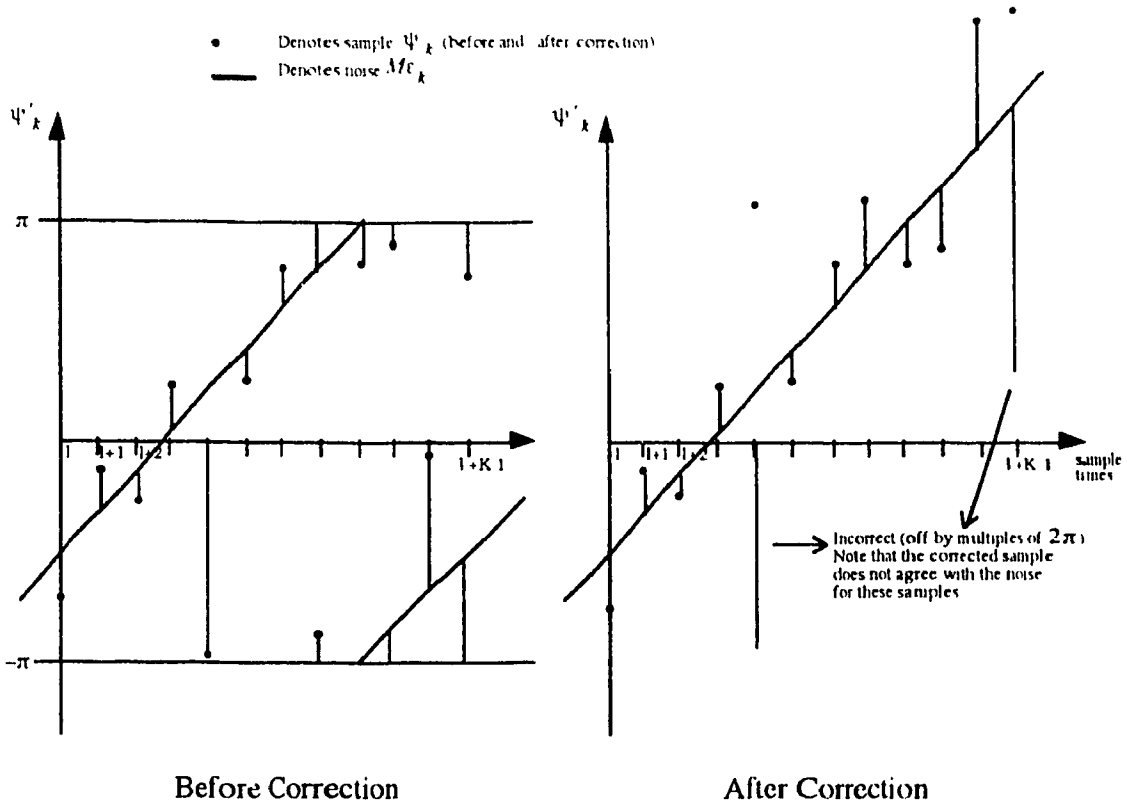

Figure 4.6: Typical set of ψ_k'

produces an estimate $\widehat{\Delta f T_S}$ based on ψ'_{l+K-1}, where

$$\widehat{\Delta f T_S} = \frac{6}{\pi M K(K^2-1)} \sum_{k=l}^{l+K-1} (k-l-N)\psi_k'.$$

On the other hand, the true LSFE requires the sample $\psi'_{l+K-1} \pm 2\pi$, and this true estimate is given by

$$\begin{aligned} \widehat{\Delta f T_{S,\text{true}}} &= \frac{6}{M\pi K(K^2-1)} \sum_{k=l}^{l+K-1} (k-l-N)\psi_k' \pm \frac{6}{M\pi K(K^2-1)} N 2\pi \\ &= \widehat{\Delta f T_S} \pm \frac{6}{MK(K+1)} \end{aligned}$$

We see that the estimate obtained by Figure 4.1 is not correct, since it is off by $6/(MK(K+1))$. For this simple example, the moments of $\widehat{\Delta F T_S}$ are evaluated below.

$$\mathrm{E}[\widehat{\Delta F T_S}] = \Delta f T_S \pm \frac{6}{MK(K+1)}$$

$$\begin{aligned} \mathrm{VAR}[\widehat{\Delta FT_S}] &= \mathrm{VAR}\left[\widehat{\Delta FT_{S,\mathrm{true}}} \mp \frac{6}{MK(K-1)}\right] \\ &= \mathrm{VAR}[\widehat{\Delta FT_{S,\mathrm{true}}}]. \end{aligned}$$

Therefore, a single incorrect phase jump produces a biased estimate. Since biased estimators are to be avoided , the attractiveness of this technique is greatly reduced.

4.2.2 Other Considerations

We recall from Chapter 3 that the phase estimators had an a ambiguity resolution problem. Since the NFE uses a technique very similar to the nonlinear phase estimators, there is a question concerning possible ambiguity of $\widehat{\Delta fT_S}$. The value of the estimate is repeated below

$$2\pi\widehat{\Delta fT_S}M = \arctan\left[\frac{\frac{1}{N}\sum_{r=0}^{N-1} p_3(\rho_{l+2r})p_3(\rho_{l+2r+1})\sin(2\pi\Delta fT_S M + M\epsilon_{l+2r+1} - M\epsilon_{l+2r})}{\frac{1}{N}\sum_{r=0}^{N-1} p_3(\rho_{l+2r})p_3(\rho_{l+2r+1})\cos(2\pi\Delta fT_S M + M\epsilon_{l+2r+1} - M\epsilon_{l+2r})}\right]$$

Since the arctangent function is modulo-2π, the estimate of ΔfT_S becomes modulo $(1/M)$, where $-1/2M \leq \widehat{\Delta fT_S} < 1/2M$. If the actual frequency error (ΔfT_S) can take a value outside this range, then ambiguity problems can occur. For QPSK this range evaluates to $-1/8 \leq \Delta fT_S < 1/8$. Considering that we restricted $|\Delta fT_S|$ to be less than 0.1, we see that there is no ambiguity problem.

4.3 Summary

From the analysis of this chapter, we conclude that the NFE seems better suited for frequency error estimation, than does the LSFE of Figure 4.1. Although the latter has a lower variance, its output is likely to be biased, rendering the estimate ineffective. Therefore, for our particular TDMA scheme, the NFE should be selected.

Chapter 5

Conclusions and Suggestions for Further Research

5.1 Conclusions

The major objective of this research was to propose fast and efficient phase error and frequency error estimation techniques. To do so, we studied the ML estimate and made three conclusions.

- ML estimation is achieved from the sampled received signal.
- Observation windows should be symmetric for minimum phase error variance.
- Nonlinear estimation can be considered a sub-class of ML estimation.

The techniques presented in this thesis are all open-loop digital topologies. For phase estimation, the existing Viterbi and Viterbi synchronizer (which we renamed as the NPE/$\bar{\text{M}}$) was analyzed and compared to a new estimator , the NPE/$\bar{\text{M}}\bar{\text{F}}$. The new estimator was shown to possess a marked advantage in terms of variance, when a frequency error is present. Even in cases where $\Delta f = 0$, the variance of the new estimator is comparable to that of the NPE/$\bar{\text{M}}$.

The two techniques were also contrasted for two additional criteria. The accepted methods of phase ambiguity resolution were presented and applied to each of the synchronizers. Except for some additional processing required by the NPE/$\bar{\text{M}}\bar{\text{F}}$ to determine the state of m, the two estimators exhibited similar performances. For ambiguity resolution by unique word preambles, expressions for P_{ARE} were obtained. Plots suggest an advantage for the NPE/$\bar{\text{M}}$ for large preamble sizes (L). However, as was mentioned, it may not be necessary to require such large L, and so this advantage rarely manifests itself. The estimators were also compared in terms of cycle skipping. The probability of cycle skipping was determined and shown to be high for both estimators (for QPSK: $P_{CS} = 0.75$ for the NPE/$\bar{\text{M}}$ and $P_{CS} = 0.875$ for the NPE/$\bar{\text{M}}\bar{\text{F}}$). Consequently, we established that ambiguity resolution is required for each window within a burst, effectively eliminating any chance of cycle skipping. On the basis of these findings, we concluded that the NPE/$\bar{\text{M}}\bar{\text{F}}$ is better suited for TDMA burst-mode communications.

For frequency estimation, it was shown that the LSFE is in fact the ML estimate of Δf if $(M\psi_k)\text{mod}(2\pi)$ exhibits no phase jumps. In such a case, the resulting estimator is efficient, even for relatively small observation window sizes. Unfortunately, the no phase jump condition is easily violated by most communication systems. Therefore, the estimate obtained by the LSFE of Figure 4.1 becomes biased, and as a result it is no longer efficient. Consequently, a nonlinear frequency estimator was proposed and shown to be unbiased. Although its variance is high, in comparison to that of the LSFE, it is expected that this may be the *lesser of two evils*. That is, the bias of the estimators is more significant than their variance.

In regards to the general receiver of Figure 2.2, we suggest using the NPE/$\bar{\text{M}}\bar{\text{F}}$ and the NFE in tandem. Since the performance of these estimators is as good or better than the currently existing estimation techniques, the performance of the overall receiver should be improved.

5.2 Suggestions for Further Research

The major results of this thesis clearly show the reasons for selecting the NPE/MF over the NPE/$\bar{\text{M}}$ and the NFE over the LSFE. However, this conclusion is based solely on a theoretical analysis. Therefore, before any definitive conclusions can be made more work must be undertaken. The aspects which remain to be studied include:

Simulation To get a complete comparison in terms of variance, ambiguity, *etc.* simulation results are to be studied. Initially, the channel model used in the thesis should be simulated to justify the theoretical results. Afterwards, the model may be expanded to include effects such as digital quantization of sampled signals, fading, *etc.*.

Bandlimited Channels The results presented in this report are applicable to channels with infinite bandwidth. Since bandlimitation can introduce ISI, the effects of this form of interference should be studied. This ISI will invalidate the assumption of Gaussian noise (N_k^i and N_k^q) in equations (2.24) and (2.25), which will then alter the joint pdf of ρ_k,ϵ_k given in (3.14). The ISI would further introduce dependence between the $\mathcal{X}_k$, making our method of variance analysis unapplicable. Therefore, a new method for determining the moments of the estimates would have to be obtained.

Gliding Window Accumulator All estimators considered in this work were of the block type. That is, every unique block of K symbols was used to determine $\widehat{\Delta\theta'}$ and $\widehat{\Delta f}$. It is possible to convert each of these into a *gliding* version, where each new input sample is used with the previous $K-1$ to obtain $\widehat{\Delta\theta'}$ and $\widehat{\Delta f}$. This technique offers excellent tracking capabilities, but has large processing time. For such estimators, the probability of cycle skipping would become a very important performance measure. However, since the phases in each window would be correlated, the cycle skipping analysis proposed in

this thesis would have to be extended (recall that we assumed uncorrelated phase errors per window). There is also a good chance that these gliding type estimators may require new performance measures.

Nonlinearities $p_1(\rho), p_2(\rho), p_3(\rho)$ For all three nonlinear estimators, these nonlinearities were chosen such that $p_1(\rho) = p_2(\rho) = p_3(\rho) = \rho^0 = 1$. Generally, it is possible to select these nonlinearities in order to minimize the variance, as was shown in [18]. It is very difficult to determine this optimum nonlinearity analytically since we have no explicit expression for the variance of the three estimators (all our variance results were obtained from numerical integration). Therefore, before proceeding with the optimization problem, expressions for the variance of the estimators as a function of signal-to-noise ratio and observation window size (K) must be obtained. One may have to resort to a two-dimensional curve fitting.

Bibliography

[1] F.M. Gardner, 'A BPSK/QPSK Timing-Error Detector for Sampled Receivers,' *IEEE Transactions on Communications*, Vol. COM-34, No. 5, pp. 423-429, May 1986.

[2] F.M. Gardner, *Phaselock Techniques*, New York: John Wiley and Sons, 1979.

[3] V.K. Bhargava, D. Haccoun, R. Matyas, and P. Nuspl, *Digital Communications by Satellite: Modulation, Multiple Access, and Coding*, New York: John Wiley and Sons, 1984.

[4] L.E. Franks, 'Carrier and Bit Synchronization in Data Communication-A Tutorial Review,' *IEEE Transactions on Communications*, Vol. COM-28, No. 8, pp. 1107-1120, August 1980.

[5] R.W.D. Booth, 'An Illustration of the MAP Estimation Method for Deriving Closed-Loop Phase Tracking Topologies: The MSK Signal Structure,' *IEEE Transactions on Communications*, Vol. COM-28, No. 8, pp. 1137-1142, August 1980.

[6] E. Del Re and R. Fantacci, 'Joint Carrier and Clock Recovery for QPSK and MSK Digital Communications,' *IEE Proc. I. Communications, Sound, and Vision*, Vol. 136, No. 3, pp. 208-212, June 1989.

[7] F.M. Gardner, 'Hangup in Phase-Lock Loops,' *IEEE Transactions on Communications*, Vol. COM-25, No. 10, pp. 1210-1214, October 1977.

[8] K.K Lee, T. Le-Ngoc, and V.K. Bhargava, 'A Feedforward Tracking Filter. Part 1: Principle and Tracking Behaviour,' *Journal of the Institution of Electronic and Radio Engineers*, Vol. 57, No. 6, pp. 262-271, Nov./Dec. 1987.

[9] K.K. Lee, T. Le-Ngoc, and V.K. Bhargava, 'A Feedforward Tracking Filter. Part 2: Noise Performance and Applications,' *Journal of the Institution of Electronic and Radio Engineers*, Vol. 57, No. 6, pp. 272-280, Nov./Dec. 1987.

[10] F.M. Gardner, 'Demodulator Reference Recovery Techniques Suited for Digital Implementation,' *Final Report to ESTEC Contract 6847/86/NL/DG*, August 1988.

[11] T. Jesupret, M. Moeneclaey, and G. Ascheid, 'Digital Demodulator Synchronization: Performance Analysis,' *Final Report to ESTEC Contract 8437/89/NL/RE*, June 1991.

[12] A.J. Viterbi and A.M. Viterbi, 'Nonlinear Estimation of PSK-Modulated Carrier Phase with Application to Burst Digital Transmission,' *IEEE Transactions in Information Theory*, Vol. IT-29. No. 4, pp. 543-551, July 1983.

[13] J.L. Melsa and D.L. Cohn, *Decision and Estimation Theory*, New York: McGraw-Hill Book Company, 1978.

[14] H.L. Van Trees, *Detection, Estimation, and Modulation Theory: Part 1*, New York: John Wiley and Sons, 1968.

[15] G. Ascheid, M. Oerder, J. Stahl, and H. Meyr, 'An all Digital Receiver Architecture for Bandwidth Efficient Transmission at High Data Rates,' *IEEE Transactions on Communications*, Vol. COM-37, No. 8, pp. 804-813, October 1989.

[16] P.Y. Kam, 'Maximum Likelihood Carrier Phase Recovery for Linear Suppressed-Carrier Digital Data Modulations,' *IEEE Transactions on Communications*, Vol. COM-34, No. 6, pp. 522-527, June 1986.

[17] S.A. Butman and J.R. Lesh, 'The Effects of Bandpass Limiters on n-Phase Tracking Systems,' *IEEE Transactions on Communications*, Vol. COM-25, No. 6, pp. 569-576, June 1977.

[18] B. Paden, 'A Matched Nonlinearity for Phase Estimation of a PSK-Modulated Carrier,' *IEEE Transactions in Information Theory*, Vol. IT-32. No. 3, pp. 419 422, May 1986.

[19] M.P. Fitz, 'Further Results in the Fast Estimation of a Single Frequency,' *Submitted to IEEE Transactions on Communications.*

[20] M. Luise and R. Reggiannini, 'Carrier Frequency Estimation in All-Digital Modems for Burst-Mode Transmissions,' *Submitted to IEEE Transactions on Communications.*

[21] M.K. Simon and D. Divsalar, 'Doppler-Corrected Differential Detection of MPSK,' *IEEE Transactions on Communications*, Vol. COM-37, No. 2, pp. 99 109, February 1989.

[22] D.C. Rife and R.R. Boorstyn, 'Single-Tone Parameter Estimation from Discrete-Time Observations,' *IEEE Transactions in Information Theory*, Vol. IT-20. No. 5, pp. 591-598, September 1974.

[23] R.A. Harris and M. Yarwood, 'Carrier Recovery and Inter-Burst Interference in a Symbol-Synchronous TDMA System,' *International Journal of Satellite Communications* Vol. 9, pp. 197-208, 1991.

[24] W. Hagmann and J. Hubermann, 'On the Phase Error Distribution of an Open Loop Phase Estimator,' *Proceedings ICC'88*, Philadelphia, pp. 1031-1037.

[25] P. Sanders and M. Moeneclaey, 'Performance of Digital Feedforward Carrier Synchronisers for M-PSK,' *Electronics Letters*, Vol. 25, No. 1, pp. 53-54, January 1989.

[26] G. Ascheid and H. Meyr, 'Cycle Skips in Phase-Locked Loops: A Tutorial Survey,' *IEEE Transactions on Communications*, Vol. COM-30, No. 10, pp. 2228-2241, October 1982.

[27] G. De Jonghe and M. Moeneclaey, 'The Effect of the Averaging Filter on the Cycle Slipping of NDA Feedforward Carrier Synchronizers for MPSK,' *Proceedings ICC'92*, Chicago, pp. 365-369.

[28] G. De Jonghe and M. Moeneclaey, 'Cycle Slipping behaviour of NDA Feedforward Carrier Synchronizers for time-varying Frequency-Nonselective fading Channels,' *Proceedings Globecom'92*, Orlando, pp. 350-354.

[29] A. Papoulis, *Probability, Random Variables, and Stochastic Processes*, New York: McGraw-Hill Book Company, 1991.

[30] S.M. Kay, 'A Fast and Accurate Single Frequency Estimator,' *IEEE Transactions on Acoustics, Speech, and Signal Processing*, Vol. 37, No. 12, pp. 1987-1990, December 1989.

[31] S. Bellini, C. Molinari, and G. Tartara, 'Digital Frequency Estimation in Burst Mode QPSK Transmission,' *IEEE Transactions on Communications*, Vol. COM-38, No. 7, pp. 959-961. July 1990.

[32] I.S. Gradshteyn and I.M. Ryzhik, *Table of Integrals, Series, and Products*, New York: Academic Press, Inc., 1965.

[33] R. Walpole and R. Myers, *Probability and Statistics for Engineers and Scientists*, New York: Macmillan Publishing Company, 1989.

Appendix A

Derivation of the Time Continuous Likelihood Function for White Gaussian Noise

The likelihood function is derived in [14] from classical estimation theory, and for a discrete set of observations. Given a set of received observations

$$r_i = S_i(\boldsymbol{A}) + n_i \quad i = 1, 2, 3, \ldots, K \tag{A.1}$$

the likelihood function $\mathrm{L}(\boldsymbol{r},\boldsymbol{A})$ is defined as $f_{\boldsymbol{R}|\boldsymbol{A}}(\boldsymbol{r}|\boldsymbol{A})$. In the above, $\boldsymbol{r} = [r_1, r_2, \ldots, r_K]$ denotes the vector of received observations, $\boldsymbol{A}$ represents the unknown parameters to be estimated, and the n_i denote sample values of independent Gaussian random noise with mean zero and variance $N_o/2$. Therefore,

$$\mathrm{L}(\boldsymbol{r}, \boldsymbol{A}) = f_{\boldsymbol{R}|\boldsymbol{A}}(\boldsymbol{r}|\boldsymbol{A}). \tag{A.2}$$

To proceed, we notice that

$$\begin{aligned} \mathrm{E}[R_i|\boldsymbol{A}] &= S_i(\boldsymbol{A}) \\ \mathrm{VAR}[R_i|\boldsymbol{A}] &= \mathrm{VAR}[N_i] = N_o/2. \end{aligned}$$

Owing to the form of the R_i's, we conclude that they are Gaussian and independent for different i. Therefore,

$$f_{R_i|\boldsymbol{A}}(r_i|\boldsymbol{A}) = \frac{1}{\sqrt{\pi N_o}} \exp\left[-\frac{|r_i - S_i(\boldsymbol{A})|^2}{N_o}\right],$$

and, as a result

$$f_{\boldsymbol{R}|\boldsymbol{A}}(\boldsymbol{r}|\boldsymbol{A}) = \prod_{i=1}^{K} \frac{1}{\sqrt{\pi N_o}} \exp\left[-\frac{|r_i - S_i(\boldsymbol{A})|^2}{N_o}\right] \tag{A.3}$$

$$= \frac{1}{(\pi N_o)^{K/2}} \exp\left[-\frac{1}{N_o}\sum_{i=1}^{K} |r_i - S_i(\boldsymbol{A})|^2\right]. \tag{A.4}$$

The ML estimate of $\boldsymbol{A}$ corresponds to the $\boldsymbol{A}$ which maximizes $\mathrm{L}(\boldsymbol{r},\boldsymbol{A})$. Notice that the factor $1/(\pi N_o)^{K/2}$ has no effect on this maximization, and can therefore be excluded from further consideration. The likelihood function can then be redefined as

$$\mathrm{L}(\boldsymbol{r}, \boldsymbol{A}) = \exp\left[-\frac{1}{N_o}\sum_{i=1}^{K} |r_i - S_i(\boldsymbol{A})|^2\right]. \tag{A.5}$$

The problem is now to apply equation (A.5) to time continuous signals

$$r(t) = s(t, \boldsymbol{A}) + n(t)$$

where $n(t)$ is a sample function of a white Gaussian noise process with mean zero and autocorrelation $\mathrm{E}[N(t)N(\lambda)] = (N_o/2)\delta(t-\lambda)$. To do this, we use the concept of random series expansion. That is, we refer to random process $R(t)$ by

$$R(t) = \underset{K\to\infty}{\text{l.i.m.}} \sum_{i=1}^{K} R_i \phi_i(t) \tag{A.6}$$

where t is in observation window, and where l.i.m. refers to the limit in the mean. In addition, the $\phi_i(t)$ refer to a complete orthonormal set of expansion functions. The R_i's can be used to completely describe the random process $R(t)$. Unfortunately, an infinite number is required for exact representation. For the moment, limit the expansion to only K terms, producing a vector $\boldsymbol{R}_K = [R_1, R_2, \ldots, R_K]$. Furthermore, denote the random process that uses this limited expansion as $R_K(t)$. When $R_K(t)$ is represented by $\boldsymbol{R}_K$, the problem is essentially a classical estimation problem.

Denote the K series expansion of $R_K(t)$, where

$$R_K(t) = \sum_{i=1}^{K} R_i \phi_i(t) \qquad t \epsilon T_{obs} \tag{A.7}$$

where the R_i are found by

$$R_i = \int_{T_{obs}} R(t)\phi_i(t)dt \qquad i = 1, 2, \ldots, K.$$

Similarly, K term expansions of $s(t, \boldsymbol{A})$ and $N(t)$ can be found.

$$\begin{aligned}
s_K(t, \boldsymbol{A}) &= \sum_{i=1}^{K} S_i(\boldsymbol{A})\phi_i(t) \qquad t \epsilon T_{obs}, \\
S_i(\boldsymbol{A}) &= \int_{T_{obs}} s(t, \boldsymbol{A})\phi_i(t)dt \qquad i = 1, 2, \ldots, K, \\
N_K(t) &= \sum_{i=1}^{K} N_i \phi_i(t) \qquad t \epsilon T_{obs}, \\
N_i &= \int_{T_{obs}} N(t)\phi_i(t)dt \qquad i = 1, 2, \ldots, K
\end{aligned}$$

The above can be used to relate R_i to $S_i(\boldsymbol{A})$ and N_i.

$$\begin{aligned}
R_i &= \int_{T_{obs}} R(t)\phi_i(t)dt \\
&= \int_{T_{obs}} (s(t, \boldsymbol{A}) + N(t))\phi_i(t)dt \\
&= S_i(\boldsymbol{A}) + N_i.
\end{aligned}$$

Ideally, the orthonormal expansion functions should be selected so that the N_i are uncorrelated. Since the random noise process is white Gaussian, this condition is satisfied for any set of $\phi_i(t)$. Therefore,

$$\mathrm{E}[N_i] = \mathrm{E}[N(t)] = 0 \tag{A.8}$$

$$\begin{aligned}
\mathrm{VAR}[N_i] &= \mathrm{E}\left[\int_{T_{obs}} N(t)\phi_i(t)dt \int_{T_{obs}} N(\lambda)\phi_i(\lambda)d\lambda\right] \\
&= \int_{T_{obs}} \int_{T_{obs}} \mathrm{E}[N(t)N(\lambda)]\phi_i(t)\phi_i(\lambda)dtd\lambda \\
&= N_o/2
\end{aligned} \tag{A.9}$$

This would then imply that $E[R_i|\boldsymbol{A}] = S_i(\boldsymbol{A})$ and $VAR[R_i|\boldsymbol{A}] = N_o/2$. The likelihood function for the R_K can then be written directly from (A.5).

$$L(\boldsymbol{r}_K, \boldsymbol{A}) = \exp\left[-\frac{1}{N_o}\sum_{i=1}^{K}|r_i - S_i(\boldsymbol{A})|^2\right]. \tag{A.10}$$

From Parseval's theorem,

$$\sum_{i=1}^{K}|r_i - S_i(\boldsymbol{A})|^2 = \int_{T_{obs}}|r_K(t) - s_K(t, \boldsymbol{A})|^2 dt$$

and so

$$\sum_{i=1}^{K}|R_i - S_i(\boldsymbol{A})|^2 = \int_{T_{obs}}|R_K(t) - s_K(t, \boldsymbol{A})|^2 dt.$$

Taking the limit in the mean as $K \to \infty$, yields

$$\begin{aligned}\underset{K\to\infty}{\text{l.i.m.}}\sum_{i=1}^{K}|R_i - S_i(\boldsymbol{A})|^2 &= \underset{K\to\infty}{\text{l.i.m.}}\int_{T_{obs}}|R_K(t) - s_K(t, \boldsymbol{A})|^2 dt \\ &= \int_{T_{obs}}|R(t) - s(t, \boldsymbol{A})|^2 dt.\end{aligned}$$

In terms of sample processes, we can write (A.5) in the required time continuos form. Namely

$$L(r(t), \boldsymbol{A}) = \exp\left[-\frac{1}{N_o}\int_{T_{obs}}|r(t) - s(t, \boldsymbol{A})|^2 dt\right]. \tag{A.11}$$

Appendix B

Derivation of Equation (2.18) for General M

The starting point of this derivation is equation (2.17), found by setting the derivative of the log-likelihood function to zero and substituting the approximations of the hyperbolic functions. The equation is repeated below:

$$\sum_{k=l}^{l+K-1}\sum_{u=0}^{M/2-1}\left[\frac{\left(\frac{2C_2}{N_o}\Re[e^{-j\widehat{\Delta\theta}}e^{-ju2\pi/M}z_k]\right)}{1!}+\frac{\left(\frac{2C_2}{N_o}\Re[e^{-j\widehat{\Delta\theta}}e^{-ju2\pi/M}z_k]\right)^3}{3!}\right.$$

$$\left.+\frac{\left(\frac{2C_2}{N_o}\Re[e^{-j\widehat{\Delta\theta}}e^{-ju2\pi/M}z_k]\right)^5}{5!}+\ldots\right]\left[\frac{2C_2}{N_o}\Im[e^{-j\widehat{\Delta\theta}}e^{-ju2\pi/M}z_k]\right]=0. \qquad \text{(B.1)}$$

The solution of the above equation can be found for all M.

BPSK - $M = 2$: Substituting $M = 2$ into (B.1), and using only the first term in the infinite sum,

$$\sum_{k=l}^{l+K-1}[\frac{2C_2}{N_o}\Re[e^{-j\widehat{\Delta\theta}}z_k]][\frac{2C_2}{N_o}\Im[e^{-j\widehat{\Delta\theta}}z_k]] = 0$$

$$\sum_{k=l}^{l+K-1}\left[(\frac{2C_2}{N_o})^2\Re[e^{-j\widehat{\Delta\theta}}z_k]\Im[e^{-j\widehat{\Delta\theta}}z_k]\right] = 0.$$

Define $u_k \stackrel{def}{=} e^{-j\widehat{\Delta\theta}} z_k \stackrel{def}{=} a_k + jb_k$. Therefore,

$$\sum_{k=l}^{l+K-1} a_k b_k = 0.$$

By expanding u_k^2,

$$u_k^2 = a_k^2 - b_k^2 + 2ja_k b_k,$$

we note that

$$a_k b_k = \frac{\Im[u_k^2]}{2}.$$

Applying this result,

$$\begin{aligned}
\sum_{k=l}^{l+K-1} \frac{\Im[u_k^2]}{2} &= 0 \\
\sum_{k=l}^{l+K-1} \Im[e^{-j2\widehat{\Delta\theta}} {z_k}^2] &= 0 \\
\Im\left[e^{-j2\widehat{\Delta\theta}} \sum_{k=l}^{l+K-1} [{z_k}^2]\right] &= 0 \\
\cos(2\widehat{\Delta\theta}) \sum_{k=l}^{l+K-1} \Im[{z_k}^2] - \sin(2\widehat{\Delta\theta}) \sum_{k=l}^{l+K-1} \Re[{z_k}^2] &= 0.
\end{aligned}$$

Solving for $\widehat{\Delta\theta}$,

$$\widehat{\Delta\theta} = \frac{1}{2} \arctan\left[\frac{\sum_{k=l}^{l+K-1} \Im[{z_k}^2]}{\sum_{k=l}^{l+K-1} \Re[{z_k}^2]}\right]. \tag{B.2}$$

QPSK - $M = 4$: Equation (B.1) reduces to

$$\sum_{k=l}^{l+K-1} \sum_{u=0}^{1} \left[\left(\frac{2C_2}{N_o} \Re[e^{-j\widehat{\Delta\theta}} e^{-ju2\pi/4} z_k]\right) + \frac{\left(\frac{2C_2}{N_o} \Re[e^{-j\widehat{\Delta\theta}} e^{-ju2\pi/4} z_k]\right)^3}{3!}\right] \bullet$$
$$\left[\frac{2C_2}{N_o} \Im[e^{-j\widehat{\Delta\theta}} e^{-ju2\pi/4} z_k]\right] = 0 \quad .$$

Therefore,

$$\begin{aligned}
&\sum_{k=l}^{l+K-1} \left[\frac{2C_2}{N_o} \Re[e^{-j\widehat{\Delta\theta}} z_k] + \left(\frac{2C_2}{N_o}\right)^3 \frac{1}{6} \Re^3[e^{-j\widehat{\Delta\theta}} z_k]\right] \left[\frac{2C_2}{N_o} \Im[e^{-j\widehat{\Delta\theta}} z_k]\right] - \\
&\sum_{k=l}^{l+K-1} \left[\frac{2C_2}{N_o} \Im[e^{-j\widehat{\Delta\theta}} z_k] + \left(\frac{2C_2}{N_o}\right)^3 \frac{1}{6} \Im^3[e^{-j\widehat{\Delta\theta}} z_k]\right] \left[\frac{2C_2}{N_o} \Re[e^{-j\widehat{\Delta\theta}} z_k]\right] = 0
\end{aligned}$$

$$\sum_{k=l}^{l+K-1}\left[\frac{2C_2}{N_o}a_k+\left(\frac{2C_2}{N_o}\right)^3\frac{1}{6}a_k^3\right]\left[\frac{2C_2}{N_o}b_k\right] - \sum_{k=l}^{l+K-1}\left[\frac{2C_2}{N_o}b_k+\left(\frac{2C_2}{N_o}\right)^3\frac{1}{6}b_k^3\right]\left[\frac{2C_2}{N_o}a_k\right] = 0.$$

After multiplication and some reduction, we are left with

$$\sum_{k=l}^{l+K-1} a_k b_k(a_k^2-b_k^2)=0.$$

Consider u_k^4,

$$\begin{aligned} u_k^4 &= u_k^2 u_k^2 \\ &= (a_k^2-b_k^2+2ja_kb_k)(a_k^2-b_k^2+2ja_kb_k) \\ &= (a_k^2-b_k^2)^2-4a_k^2b_k^2+j4a_kb_k(a_k^2-b_k^2). \end{aligned}$$

Therefore,

$$a_kb_k(a_k^2-b_k^2)=\frac{\Im[u_k^4]}{4}$$

and

$$\sum_{k=l}^{l+K-1}\Im[u_k^4]=0.$$

Replacing u_k by $e^{-j\widehat{\Delta\theta}}z_k$ and solving for $\widehat{\Delta\theta}$ results in

$$\widehat{\Delta\theta}=\frac{1}{4}\arctan\left[\frac{\sum_{k=l}^{l+K-1}\Im[z_k{}^4]}{\sum_{k=l}^{l+K-1}\Re[z_k{}^4]}\right]. \tag{B.3}$$

General M: A similar result is obtained for $M=8$ and for $M=16$, and so by induction, equations (B.2) and (B.3) can be extended for all M. The result is

$$\widehat{\Delta\theta}=\frac{1}{M}\arctan\left[\frac{\sum_{k=l}^{l+K-1}\Im[z_k{}^M]}{\sum_{k=l}^{l+K-1}\Re[z_k{}^M]}\right]. \tag{B.4}$$

Appendix C

Derivation of the moments of ξ and η for NPE/$\bar{\text{M}}$, NPE/$\bar{\text{M}}\bar{\text{F}}$, and NFE

The moments for these random variables must be calculated for three estimators:

1. NPE/$\bar{\text{M}}$
2. NPE/$\bar{\text{M}}\bar{\text{F}}$
3. NFE.

NPE/$\bar{\text{M}}$: For this estimator,

$$\begin{aligned}
\xi &= \frac{1}{K}\sum_{k=l}^{l+K-1} p_1(\rho_k)\sin\left(2\pi\Delta f T_S(k-l-N)M + M\epsilon_k\right) \\
&\stackrel{def}{=} \frac{1}{K}\sum_{k=l}^{l+K-1} A(k) \qquad \text{(C.1)} \\
\eta &= \frac{1}{K}\sum_{k=l}^{l+K-1} p_1(\rho_k)\cos\left(2\pi\Delta f T_S(k-l-N)M + M\epsilon_k\right) \\
&\stackrel{def}{=} \frac{1}{K}\sum_{k=l}^{l+K-1} B(k). \qquad \text{(C.2)}
\end{aligned}$$

The moments of $A(k)$ and $B(k)$ are shown below.

$$\begin{aligned}\mu_A(k) = \mathrm{E}[A(k)] &= \mathrm{E}[p_1(\rho_k)\sin(2\pi\Delta f T_S(k-l-N)M + M\epsilon_k)] \\ &= \mathrm{E}[p_1(\rho_k)\sin(2\pi\Delta f T_S(k-l-N)M)\cos(M\epsilon_k) \\ &\quad + p_1(\rho_k)\cos(2\pi\Delta f T_S(k-l-N)M)\sin(M\epsilon_k)] \\ &= \sin(2\pi\Delta f T_S(k-l-N)M)\mathrm{E}[p_1(\rho_k)\cos(M\epsilon_k)] \\ &\quad + \cos(2\pi\Delta f T_S(k-l-N)M)\mathrm{E}[p_1(\rho_k)\sin(M\epsilon_k)]. \quad \text{(C.3)}\end{aligned}$$

Owing to the independence of the random variables, we can drop the subscript k in the expectations (this will be done for all expectations in this appendix). In addition, $\mathrm{E}[p_1(\rho_k)\sin(M\epsilon_k)]$ evaluates to zero. In fact, for general nonlinearity $g(\rho)$ and even R,

$$\begin{aligned}\mathrm{E}[g(\rho)\sin(R\epsilon)] &= \int_0^\infty\int_{-\pi}^{\pi} g(\rho)\sin(R\epsilon) f_{\rho,\epsilon}(\rho,\epsilon)\,d\epsilon\,d\rho \\ &= \int_0^\infty\int_{-\pi}^{\pi} g(\rho)\sin(R\epsilon)\frac{\rho}{\pi N_o}\exp\left[-\frac{\rho^2}{N_o} + \frac{\sqrt{\gamma}\rho\cos\epsilon}{\sqrt{N_o/2}} - \frac{\gamma}{2}\right]d\epsilon\,d\rho \\ &= \int_0^\infty g(\rho)\frac{\rho}{\pi N_o}\exp\left[-\frac{\rho^2}{N_o} - \frac{\gamma}{2}\right]\cdot \\ &\quad \int_{-\pi}^{\pi}\sin(R\epsilon)\exp\left[\frac{\sqrt{\gamma}\rho\cos\epsilon}{\sqrt{N_o/2}}\right]d\epsilon\,d\rho \\ &= 0\,.\end{aligned}$$

The last equality holds since

$$\sin(R\epsilon)e^{\sqrt{\gamma}\rho\cos\epsilon/\sqrt{N_o/2}} = -\sin(-R\epsilon)e^{\sqrt{\gamma}\rho\cos(-\epsilon)/\sqrt{N_o/2}}.$$

Using this result in (C.3) yields

$$\mu_A(k) = \sin(2\pi\Delta f T_S(k-l-N)M)\mathrm{E}[p_1(\rho)\cos(M\epsilon)] \quad \text{(C.4)}$$

Similarly,

$$\sigma_A^2(k) = \mathrm{E}[A^2(k)] - \mathrm{E}^2[A(k)]$$

$$
\begin{aligned}
&= \mathrm{E}[{p_1}^2(\rho_k)\sin^2(2\pi\Delta f T_S(k-l-N)M + M\epsilon_k)] \\
&\quad -\mathrm{E}^2[A(k)] \\
&= \frac{\mathrm{E}[{p_1}^2(\rho_k)]}{2} - \frac{\mathrm{E}[{p_1}^2(\rho_k)\cos(4\pi\Delta f T_S(k-l-N)M + 2M\epsilon_k)]}{2} \\
&\quad -\mathrm{E}^2[A(k)] \\
&= \frac{\mathrm{E}[{p_1}^2(\rho)]}{2} - \frac{\mathrm{E}[{p_1}^2(\rho)\cos(2M\epsilon)]\cos(4\pi\Delta f T_S(k-l-N)M)}{2} \\
&\quad -\sin^2(2\pi\Delta f T_S(k-l-N)M)\mathrm{E}^2[p_1(\rho)\cos(M\epsilon)] \qquad \text{(C.5)}
\end{aligned}
$$

and

$$
\begin{aligned}
\mu_B(k) &= \mathrm{E}[B(k)] \\
&= \mathrm{E}[p_1(\rho_k)\cos(2\pi\Delta f T_S(k-l-N)M + M\epsilon_k)] \\
&= \mathrm{E}[p_1(\rho)\cos(M\epsilon)]\cos(2\pi\Delta f T_S(k-l-N)M) \qquad \text{(C.6)} \\
\sigma_B^2(k) &= \mathrm{E}[{p_1}^2(\rho_k)\cos^2(2\pi\Delta f T_S(k-l-N)M + M\epsilon_k)] - \mathrm{E}^2[B(k)] \\
&= \frac{\mathrm{E}[{p_1}^2(\rho)]}{2} + \frac{\mathrm{E}[{p_1}^2(\rho)\cos(2M\epsilon)]\cos(4\pi\Delta f T_S(k-l-N)M)}{2} \\
&\quad -\cos^2(2\pi\Delta f T_S(k-l-N)M)\mathrm{E}^2[p_1(\rho)\cos(M\epsilon)] \qquad \text{(C.7)} \\
\mathrm{E}[A(k),B(k)] &= \mathrm{E}[p_1(\rho_k)\sin(2\pi\Delta f T_S(k-l-N)M + M\epsilon_k) \\
&\quad p_1(\rho_k)\cos(2\pi\Delta f T_S(k-l-N)M + M\epsilon_k)] \\
&= \frac{\mathrm{E}[{p_1}^2(\rho_k)\sin(4\pi\Delta f T_S(k-l-N)M + 2M\epsilon_k)]}{2} \\
&= \frac{\mathrm{E}[{p_1}^2(\rho)\cos(2M\epsilon)]}{2}\sin(4\pi\Delta f T_S(k-l-N)M). \qquad \text{(C.8)}
\end{aligned}
$$

If we note that all samples for k and j are independent, then the moments of ξ and η can be easily determined.

$$
\begin{aligned}
\mu_\xi = \mathrm{E}[\xi] &= \frac{1}{K}\sum_{k=l}^{l+K-1}\mu_A(k) \\
&= \frac{\mathrm{E}[p_1(\rho)\cos(M\epsilon)]}{K}\sum_{k=l}^{l+K-1}\sin(2\pi\Delta f T_S(k-l-N)M) \\
&= 0 \qquad \text{(C.9)}
\end{aligned}
$$

$$
\sigma_\xi^2 = \mathrm{E}[\xi^2] = \frac{1}{K^2}\mathrm{E}\left[\sum_{k=l}^{l+K-1}A(k)\sum_{j=l}^{l+K-1}A(j)\right]
$$

$$
\begin{aligned}
&= \frac{1}{K^2}\sum_{k=l}^{l+K-1}\sum_{j=l}^{l+K-1}\mathrm{E}[A(k)A(j)] \\
&= \frac{1}{K^2}\sum_{k=l}^{l+K-1}\left[\mathrm{E}[A^2(k)]+\mathrm{E}[A(k)]\sum_{\substack{j=l\\ j\neq k}}^{l+K-1}\mathrm{E}[A(j)]\right] \\
&= \frac{1}{K^2}\sum_{k=l}^{l+K-1}\left[\mathrm{E}[A^2(k)]+\mathrm{E}[A(k)]\sum_{j=l}^{l+K-1}\mathrm{E}[A(j)]-\mathrm{E}^2[A(k)]\right] \\
&= \frac{1}{K^2}\sum_{k=l}^{l+K-1}\sigma_A^2(k) \\
&= \frac{\mathrm{E}[{p_1}^2(\rho)]}{2K}-\frac{\mathrm{E}[{p_1}^2(\rho)\cos(2M\epsilon)]}{2K^2}\sum_{k=l}^{l+K-1}\cos(4\pi\Delta f T_S(k-l-N)M) \\
&\quad -\frac{\mathrm{E}^2[p_1(\rho)\cos(M\epsilon)]}{2K}-\frac{\mathrm{E}^2[p_1(\rho)\cos(M\epsilon)]}{2K^2}\bullet \\
&\quad \sum_{k=l}^{l+K-1}\cos(4\pi\Delta f T_S(k-l-N)M)\,. \qquad \text{(C.10)}
\end{aligned}
$$

The finite summation can be evaluated using equation (1.342.1) in [32], and the result is shown below.

$$
\begin{aligned}
\sum_{k=l}^{l+K-1}\cos(4\pi\Delta f T_S(k-l-N)M) &= \frac{\sin(2K\pi\Delta f T_S M)}{\sin(2\pi\Delta f T_S M)} \\
&\stackrel{def}{=} K S_K(2M\Delta f T_S)\,. \qquad \text{(C.11)}
\end{aligned}
$$

The final expression for σ_ξ^2 is given by

$$
\begin{aligned}
\sigma_\xi^2 &= \frac{\mathrm{E}[{p_1}^2(\rho)]}{2K}-\frac{\mathrm{E}[{p_1}^2(\rho)\cos(2M\epsilon)]}{2K}S_K(2M\Delta f T_S)- \\
&\quad \frac{\mathrm{E}^2[p_1(\rho)\cos(M\epsilon)]}{2K}[1-S_K(2M\Delta f T_S)]\,. \qquad \text{(C.12)}
\end{aligned}
$$

In a similar manner,

$$
\begin{aligned}
\mu_\eta = \mathrm{E}[\eta] &= \frac{1}{K}\sum_{k=l}^{l+K-1}\mu_B(k) \\
&= \frac{\mathrm{E}[p_1(\rho)\cos(M\epsilon)]}{K}\sum_{k=l}^{l+K-1}\cos(2\pi\Delta f T_S(k-l-N)M)
\end{aligned}
$$

$$= \mathrm{E}[p_1(\rho)\cos(M\epsilon)]S_K(M\Delta fT_S) \tag{C.13}$$

$$\begin{aligned}
\sigma_\eta^2 &= \mathrm{E}[(\eta-\mu_\eta)^2] \\
&= \mathrm{E}\left[\frac{1}{K}\sum_{k=l}^{l+K-1}(B(k)-\mu_B(k))\frac{1}{K}\sum_{j=l}^{l+K-1}(B(j)-\mu_B(j))\right] \\
&= \frac{1}{K^2}\sum_{k=l}^{l+K-1}\Big[\mathrm{E}[(B(k)-\mu_B(k))^2]+\mathrm{E}[B(k)-\mu_B(k)]\bullet \\
&\qquad \sum_{\substack{j=l \\ j\neq k}}^{l+K-1}\mathrm{E}[B(j)-\mu_B(j)]\Big] \\
&= \frac{1}{K^2}\sum_{k=l}^{l+K-1}\sigma_B^2(k) \\
&= \frac{\mathrm{E}[p_1{}^2(\rho)]}{2K}+\frac{\mathrm{E}[p_1{}^2(\rho)\cos(2M\epsilon)]}{2K}S_K(2M\Delta fT_S)- \\
&\qquad \frac{\mathrm{E}^2[p_1(\rho)\cos(M\epsilon)]}{2K}[1+S_K(2M\Delta fT_S)]
\end{aligned} \tag{C.14}$$

$$\begin{aligned}
\mathrm{COV}[\eta,\xi] &= \mathrm{E}\left[\frac{1}{K}\sum_{k=l}^{l+K-1}(B(k)-\mu_B(k))\frac{1}{K}\sum_{j=l}^{l+K-1}(A(j)-\mu_A(j))\right] \\
&= \frac{1}{K^2}\sum_{k=l}^{l+K-1}[\mathrm{E}[(B(k)-\mu_B(k))(A(k)-\mu_A(k))]+\mathrm{E}[B(k)-\mu_B(k)]\bullet \\
&\qquad \sum_{j=l}^{l+K-1}\mathrm{E}[A(j)-\mu_B(j)]-\mathrm{E}[B(k)-\mu_B(k)]\mathrm{E}[A(k)-\mu A(k)]\Big] \\
&= \frac{1}{K^2}\sum_{k=l}^{l+K-1}[\mathrm{E}[B(k)A(k)]-\mu_B(k)\mu_A(k)] \\
&= \frac{1}{K^2}\left[\frac{\mathrm{E}[p_1{}^2(\rho)\cos(2M\epsilon)]}{2}-\frac{\mathrm{E}^2[p_1(\rho)\cos(M\epsilon)]}{2}\right]\bullet \\
&\qquad \sum_{k=l}^{l+K-1}\sin(4\pi\Delta fT_S(k-l-N)M) \\
&= 0
\end{aligned} \tag{C.15}$$

This last result implies that ξ and η are uncorrelated. This fact also establishes their independence, which was required for the application of the CLT.

NPE/$\bar{\text{M}}\bar{\text{F}}$: For the nonlinear phase estimator with modulation and frequency error removal,

$$\begin{aligned}\xi &= \frac{1}{N+1}\sum_{r=0}^{N} p_2(\rho_{l+r})p_2(\rho_{l+K-r-1})\sin\left(M\epsilon_{l+r}+M\epsilon_{l+K-r-1}\right)\\ &= \frac{1}{N+1}\sum_{r=0}^{N} A(r) \qquad (C.16)\\ \eta &= \frac{1}{N+1}\sum_{r=0}^{N} p_2(\rho_{l+r})p_2(\rho_{l+K-r-1})\cos\left(M\epsilon_{l+r}+M\epsilon_{l+K-r-1}\right)\\ &= \frac{1}{N+1}\sum_{r=0}^{N} B(r). \qquad (C.17)\end{aligned}$$

For this estimator, special consideration is given for the $r = N$ term in the sums (the middle symbol of the observation window). All $A(r)$ and $B(r)$ ($r \neq N$), are a function of four random variables – $\rho_{l+r}, \rho_{l+K-r-1}, \epsilon_{l+r}, \epsilon_{l+K-r-1}$. However, the term in question is a function of only two, ρ_N, ϵ_N, and consequently this affects the derivation of the moments. The moments of $A(r)$ and $B(r)$ are given below.

$$\mu_A(r) = \begin{cases} 0 & r \neq N \\ 0 & r = N \end{cases}$$

$$\sigma_A^2(r) = \begin{cases} \dfrac{\mathrm{E}^2[p_2{}^2(\rho)]}{2} - \dfrac{\mathrm{E}^2[p_2{}^2(\rho)\cos(2M\epsilon)]}{2} & r \neq N \\ \dfrac{\mathrm{E}[p_2{}^4(\rho)]}{2} - \dfrac{\mathrm{E}[p_2{}^4(\rho)\cos(4M\epsilon)]}{2} & r = N \end{cases}$$

$$\mu_B(r) = \begin{cases} \mathrm{E}^2[p_2(\rho)\cos(M\epsilon)] & r \neq N \\ \mathrm{E}[p_2{}^2(\rho)\cos(2M\epsilon)] & r = N \end{cases}$$

$$\sigma_B^2(r) = \begin{cases} \dfrac{\mathrm{E}^2[p_2{}^2(\rho)]}{2} + \dfrac{\mathrm{E}^2[p_2{}^2(\rho)\cos(2M\epsilon)]}{2} - \mathrm{E}^4[p_2(\rho)\cos(M\epsilon)] & r \neq N \\ \dfrac{\mathrm{E}[p_2{}^4(\rho)]}{2} + \dfrac{\mathrm{E}[p_2{}^4(\rho)\cos(4M\epsilon)]}{2} - \mathrm{E}^2[p_2{}^2(\rho)\cos(2M\epsilon)] & r = N \end{cases}$$

The moments of ξ and η are determined to be,

$$\mu_\xi = 0 \qquad (C.18)$$

$$\sigma_\xi^2 = \frac{N\mathrm{E}^2[p_2{}^2(\rho)] - N\mathrm{E}^2[p_2{}^2(\rho)\cos(2M\epsilon)] + \mathrm{E}[p_2{}^4(\rho)]}{2(N+1)^2} - \frac{\mathrm{E}[p_2{}^4(\rho)\cos(4M\epsilon)]}{2(N+1)^2} \quad \text{(C.19)}$$

$$\mu_\eta = \frac{N\mathrm{E}^2[p_2(\rho)\cos(M\epsilon)] + \mathrm{E}[p_2{}^2(\rho)\cos(2M\epsilon)]}{(N+1)} \quad \text{(C.20)}$$

$$\sigma_\eta^2 = \frac{N\mathrm{E}^2[p_2{}^2(\rho)] + N\mathrm{E}^2[p_2{}^2(\rho)\cos(2M\epsilon)] - 2N\mathrm{E}^4[p_2(\rho)\cos(M\epsilon)]}{2(N+1)^2} + \frac{\mathrm{E}[p_2{}^4(\rho)] + \mathrm{E}[p_2{}^4(\rho)\cos(4M\epsilon)] - 2\mathrm{E}^2[p_2{}^2(\rho)\cos(2M\epsilon)]}{2(N+1)^2} \quad \text{(C.21)}$$

$$\mathrm{COV}[\eta,\xi] = 0\,.$$

NFE: For the nonlinear frequency estimator, η and ξ are as defined below:

$$\xi = \frac{1}{N}\sum_{r=0}^{N-1} p_3(\rho_{l+2r})p_3(\rho_{l+2r+1})\sin(M\epsilon_{l+2r+1} - M\epsilon_{l+2r}) = \frac{1}{N}\sum_{r=0}^{N-1} A(r) \quad \text{(C.22)}$$

$$\eta = \frac{1}{N}\sum_{r=0}^{N-1} p_3(\rho_{l+2r})p_3(\rho_{l+2r+1})\cos(M\epsilon_{l+2r+1} - M\epsilon_{l+2r}) = \frac{1}{N}\sum_{r=0}^{N-1} B(r). \quad \text{(C.23)}$$

The moments of $A(r)$ and $B(r)$ are given below:

$$\mu_A(r) = 0$$
$$\sigma_A^2(r) = \frac{\mathrm{E}^2[p_3{}^2(\rho)]}{2} - \frac{\mathrm{E}^2[p_3{}^2(\rho)\cos(2M\epsilon)]}{2}$$
$$\mu_B(r) = \mathrm{E}^2[p_3(\rho)\cos(M\epsilon)]$$
$$\sigma_B^2(r) = \frac{\mathrm{E}^2[p_3{}^2(\rho)]}{2} + \frac{\mathrm{E}^2[p_3{}^2(\rho)\cos(2M\epsilon)]}{2} - \mathrm{E}^4[p_3(\rho)\cos(M\epsilon)].$$

The moments of ξ and η are shown below:

$$\mu_\xi = 0 \quad \text{(C.24)}$$

$$\sigma_\xi^2 = \frac{\mathrm{E}^2[p_3{}^2(\rho)]}{2N} - \frac{\mathrm{E}^2[p_3{}^2(\rho)\cos(2M\epsilon)]}{2N} \quad \text{(C.25)}$$

$$\mu_\eta = \mathrm{E}^2[p_3(\rho)\cos(M\epsilon)] \tag{C.26}$$

$$\sigma_\eta^2 = \frac{\mathrm{E}^2[{p_3}^2(\rho)]}{2N} + \frac{\mathrm{E}^2[{p_3}^2(\rho)\cos(2M\epsilon)]}{2N} - \frac{\mathrm{E}^4[p_3(\rho)\cos(M\epsilon)]}{N} \tag{C.27}$$

$$\mathrm{COV}[\eta,\xi] = 0. \tag{C.28}$$

Appendix D

Probability Density Function of the Degradation for NPE/$\bar{\text{M}}$

Although this analysis is presented for the NPE/$\bar{\text{M}}$, it can be easily extended to the two other nonlinear estimators. To do so, merely change the value of M to $2M$ for the NPE/$\bar{\text{M}}\bar{\text{F}}$, and to $2\pi M$ for the NFE. In addition, use the definitions of μ_η, σ_η^2, and σ_ξ^2 which apply to the correct estimator.

For the NPE/$\bar{\text{M}}$, we know that η and ξ are independent Gaussian random variables with moments μ_η, σ_η^2, μ_ξ, and σ_ξ^2. Their joint pdf can be written as

$$f_{\eta,\xi}(\eta,\xi) = \frac{1}{2\pi\sigma_\eta\sigma_\xi}\exp\left[-\frac{(\eta-\mu_\eta)^2}{2\sigma_\eta^2} - \frac{\xi^2}{2\sigma_\xi^2}\right] \tag{D.1}$$

where we have made the substitution $\mu_\xi = 0$. We can now apply the following transformation

$$\begin{aligned} Z_1 &= \frac{1}{M}\arctan\left[\frac{\xi}{\eta}\right] \\ Z_2^2 &= \xi^2+\eta^2. \end{aligned}$$

Solving for η and ξ (sample values) in terms of z_1 and z_2,

$$\xi = z_2\sin(Mz_1) \tag{D.2}$$

$$\eta = z_2\cos(Mz_1). \tag{D.3}$$

The joint pdf of Z_1 and Z_2 is given from [29]

$$f_{Z_1,Z_2}(z_1,z_2) = |\mathcal{J}| f_{\eta,\xi}(\eta = z_2\cos(Mz_1), \xi = z_2\sin(Mz_1)) \tag{D.4}$$

where

$$\mathcal{J} = \det\begin{bmatrix} \frac{\partial\eta}{\partial z_1} & \frac{\partial\eta}{\partial z_2} \\ \frac{\partial\xi}{\partial z_1} & \frac{\partial\xi}{\partial z_2} \end{bmatrix}$$

and therefore $|\mathcal{J}| = Mz_2$. Using (D.2) and (D.3) in (D.4) results in

$$f_{Z_1,Z_2}(z_1,z_2) = \frac{Mz_2}{2\pi\sigma_\eta\sigma_\xi}\exp\left[-\frac{(z_2\cos(Mz_1)-\mu_\eta)^2}{2\sigma_\eta^2} - \frac{(z_2\sin(Mz_1))^2}{2\sigma_\xi^2}\right]$$
$$= \frac{Me^{-\mu_\eta{}^2/2\sigma_\eta^2}}{2\pi\sigma_\eta\sigma_\xi} z_2 \exp\left[-z_2^2\left(\frac{\cos^2(Mz_1)}{2\sigma_\eta^2}+\frac{\sin^2(Mz_1)}{2\sigma_\xi^2}\right) + z_2\frac{\mu_\eta\cos(Mz_1)}{\sigma_\eta^2}\right].$$

We need the marginal distribution of Z_1.

$$f_{Z_1}(z_1) = \int_0^\infty f_{Z_1,Z_2}(z_1,z_2)dz_2$$
$$= \frac{Me^{-\mu_\eta{}^2/2\sigma_\eta^2}}{2\pi\sigma_\eta\sigma_\xi}\int_0^\infty z_2\exp\left[-z_2^2\left(\frac{\cos^2(Mz_1)}{2\sigma_\eta^2}+\frac{\sin^2(Mz_1)}{2\sigma_\xi^2}\right) + z_2\frac{\mu_\eta\cos(Mz_1)}{\sigma_\eta^2}\right]dz_2.$$

To solve this integral, we use the result

$$\int_0^\infty z_2\exp[-z_2^2a + z_2b]dz_2 =$$
$$\frac{1}{2a}\left\{1+\frac{b}{2\sqrt{a}}\sqrt{\pi}\exp\left(\frac{b^2}{4a}\right)\left[1+\mathrm{erf}\left(\frac{b}{2\sqrt{a}}\right)\right]\right\}.$$

Substituting the correct values of a and b,

$$f_{Z_1}(z_1) = \frac{Me^{-\mu_\eta{}^2/2\sigma_\eta^2}}{2\pi}\frac{\sigma_\eta\sigma_\xi}{\sigma_\eta^2\sin^2(Mz_1)+\sigma_\xi^2\cos^2(Mz_1)}\left\{1+\frac{\mu_\eta}{\sqrt{2}\sigma_\eta}\sqrt{\pi}\sqrt{\frac{\sigma_\xi^2\cos^2(Mz_1)}{\sigma_\eta^2\sin^2(Mz_1)+\sigma_\xi^2\cos^2(Mz_1)}}\right.$$
$$\left.\exp\left[\frac{\mu_\eta{}^2}{2\sigma_\eta^2}\frac{\sigma_\xi^2\cos^2(Mz_1)}{\sigma_\eta^2\sin^2(Mz_1)+\sigma_\xi^2\cos^2(Mz_1)}\right]\left[1+\mathrm{erf}\left(\frac{\mu_\eta}{\sqrt{2}\sigma_\eta}\sqrt{\frac{\sigma_\xi^2\cos^2(Mz_1)}{\sigma_\eta^2\sin^2(Mz_1)+\sigma_\xi^2\cos^2(Mz_1)}}\right)\right]\right\}$$
$$-\pi/M \le z_1 < \pi/M \tag{D.5}$$

The desired pdf is obtained by noting that $f_\delta(\delta) = f_{Z_2}(\delta)|_{Z_2=\delta}$.

Appendix E

Derivation of P_{ARE} for NPE/$\bar{\mathrm{M}}$

We will define the following three events, possible for every symbol:

C: $-\pi/M \leq \epsilon_k < \pi/M$ – symbol does not produce a region error

E_1: $\pi/M \leq \epsilon_k < 3\pi/M$ – symbol produces a region error

E_2: $-3\pi/M \leq \epsilon_k < -\pi/M$ – symbol produces a region error

The event of a particular region error (E_1 or E_2) is independent from symbol to symbol and given by,

$$p_r = p_{e_1} = p_{e_2} = \int_{\pi/M}^{3\pi/M} f_{\epsilon_k}(\epsilon_k) d\epsilon_k \ . \tag{E.1}$$

Since $f_{\epsilon_k}(\epsilon_k)$ is known (3.38), p_r can be found from numerical integration.

Each transmitted symbol produces as an outcome, one of these three events. Event C occurs n_c times, event E_1 occurs n_{e1} times, and event E_2 occurs n_{e2} times. The probability of such a set of L received symbols is given by,

$$\Pr[\text{events C, E}_1\text{, and E}_2 \text{ occur } n_c, n_{e1}, \text{ and } n_{e2} \text{ times respectively}] = \frac{L!}{n_c! n_{e1}! n_{e2}!}(1-2p_r)^{n_c} {p_r}^{n_{e1}} {p_r}^{n_{e2}} \ , \tag{E.2}$$

where the term $L!/(n_c! n_{e1}! n_{e2}!)$ represents the total number of ways that events C, E_1 and E_2 can occur n_c, n_{e1}, and n_{e2} times, respectively [33].

Using Maximum Likelihood principles, it can be shown that a correct decision is made if $n_c > n_{e1}$ and $n_c > n_{e2}$. That is,

$$n_c > \max(n_{e1}, n_{e2}) \,. \tag{E.3}$$

Consequently to find P_{ARE}, we sum over all the mutually exclusive events such that $n_c \leq \max(n_{e1}, n_{e2})$. Therefore,

$$P_{ARE} = \sum_{\forall n_c \leq \max(n_{e1}, n_{e2})} \frac{L!}{n_c! n_{e1}! n_{e2}!} {p_r}^{n_{e1}+n_{e2}} (1-2p_r)^{n_c}. \tag{E.4}$$